INFORMATION TO USERS

This reproduction was made from a copy of a manuscript sent to us for publication and microfilming. While the most advanced technology has been used to photograph and reproduce this manuscript, the quality of the reproduction is heavily dependent upon the quality of the material submitted. Pages in any manuscript may have indistinct print. In all cases the best available copy has been filmed.

The following explanation of techniques is provided to help clarify notations which may appear on this reproduction.

1. Manuscripts may not always be complete. When it is not possible to obtain missing pages, a note appears to indicate this.

2. When copyrighted materials are removed from the manuscript, a note appears to indicate this.

3. Oversize materials (maps, drawings, and charts) are photographed by sectioning the original, beginning at the upper left hand corner and continuing from left to right in equal sections with small overlaps. Each oversize page is also filmed as one exposure and is available, for an additional charge, as a standard 35mm slide or in black and white paper format.*

4. Most photographs reproduce acceptably on positive microfilm or microfiche but lack clarity on xerographic copies made from the microfilm. For an additional charge, all photographs are available in black and white standard 35mm slide format.*

***For more information about black and white slides or enlarged paper reproductions, please contact the Dissertations Customer Services Department.**

U·M·I Dissertation Information Service

University Microfilms International
A Bell & Howell Information Company
300 N. Zeeb Road, Ann Arbor, Michigan 48106

Nolan, Robert Patrick

INTERACTION OF QUARTZ WITH BIOLOGICAL MEMBRANES

City University of New York PH.D. 1986

PLEASE NOTE:

In all cases this material has been filmed in the best possible way from the available copy. Problems encountered with this document have been identified here with a check mark ✓.

1. Glossy photographs or pages ✓
2. Colored illustrations, paper or print _____
3. Photographs with dark background _____
4. Illustrations are poor copy _____
5. Pages with black marks, not original copy ✓
6. Print shows through as there is text on both sides of page _____
7. Indistinct, broken or small print on several pages _____
8. Print exceeds margin requirements _____
9. Tightly bound copy with print lost in spine _____
10. Computer printout pages with indistinct print _____
11. Page(s) _____ lacking when material received, and not available from school or author.
12. Page(s) _____ seem to be missing in numbering only as text follows.
13. Two pages numbered _____. Text follows.
14. Curling and wrinkled pages _____
15. Dissertation contains pages with print at a slant, filmed as received _____
16. Other _____

University
Microfilms
International

Interaction of Quartz with Biological Membranes

By

Robert Patrick Nolan

A dissertation submitted to the Graduate Faculty in Chemistry in partial fulfillment of the requirements for the degree of Doctor of Philosophy, The City University of New York.

1986

This manuscript has been read and accepted for the Graduate Faculty in Chemistry in satisfaction of the dissertation requirement for the degree of Doctor of Philosophy.

May 30, 1986
Date

Chairman of Examining Committee

June 5, 1986
Date

Executive Officer

Supervisory Committee

The City University of New York

ABSTRACT

The interaction of quartz with the macrophage membrane plays a central role in the pathogenesis of silicosis. The erythrocyte has been used as a model to study mineral/membrane interaction. Many pathogenic minerals, including quartz, have the ability to alter the permeability of the erythrocyte membrane. The hemaglobin released by this membranolytic action can be easily quantitated by optical spectroscopy. The variation in membranolytic activity of quartz was studied with respect to surface structure, particle size, and quartz variety. Quartz membranolytic activity can, depending on its surface structure, vary from a level indistinguishable from background lysis to one of potent hemolytic effect. The ratio of the change in hemolytic index closely follows the ratio of the change in surface area. The quartz variety was the least important of the three variables. For a quartz specimen which was shown to be membranolytically active, the contribution of the chemical functionalities on the surface were determined. The two major functional groups on the quartz surface are the silanol group which can undergo hydrogen bonding and the ionized silanol group which impart negative surface charge. The membranolytic activity of quartz has long been attributed to the surface silanol groups. The experimental evidence which supports this hypothesis is the inhibition of membranolytic activity by hydrogen bonding polymers. Blocking the quartz surface charge with metal cations also

inhibits the membranolytic effects. To further understand the role of quartz surface charge, experiments were done to identify a receptor on the erythrocyte membrane. When the anion transport receptor, which binds the negative quartz surface charge, was blocked by inhibitor known to complex with it, hemolysis is antagonized. The principles which control quartz membranolytic activity were also found to be applicable to the titanium dioxide polymorphs, rutile and anatase.

PREFACE

I would like to acknowledge the following for their scientific contribution to this thesis: A.M. Langer, J.S. Harington, Gerald Oster, K.W. Foster, J.A. Hamilton, and G.B. Herson. I would also like to thank the members of my committee for their participation. Carol Shiroky needs to be acknowledged for her excellent work in typing the thesis, and Valerie Josephson and Rupert Fuller for the graphics.

This thesis was made possible by support from the National Institute of Environmental Health Sciences ES00928, Mobile Foundation, National Institute for Occupational Safety and Health OH01905, Societe Nationale de l'Amiante, Canada, and the Stony Wold-Herbert Fund, Inc.

This thesis is dedicated

to

the memory of

the late

PROFESSOR AL STEYERMARK

TABLE OF CONTENTS

Page

LIST OF TABLES

LIST OF ILLUSTRATIONS

CHAPTER I

Introduction

The Hemolytic Model

Although hemolysis of erythrocytes plays no part in the pathogenesis of silicosis, the technique provides a simple and rapid way of studying the effects of inorganic dust (and mineral fibers) on biological membranes. The erythrocyte membrane is not typical, yet the *in vitro* technique of hemolysis has proved to be a simple and rapid way of attempting to find possible correlations between cytotoxicity and hemolytic activity. Numerous investigators have considered that this simple membrane model may be used as a measure of a mineral's cytotoxicity. The mature erythrocyte has been used as such a model since the early part of this century, and it appeared more recently with Goldie (1938) and Dogmon and Simonot (1951).

Citations exist in the literature concerning the importance of the erythrocyte membrane in studying effects of specific mineral dusts (see e.g., Harley and Margolis, 1961; Stalder and Stober 1965; Allison et al., 1966; Nash et al., 1966; Macnab and Harington, 1967; Heppleston and Styles, 1967; Schlipkoter, 1968; Secchi and Rezzonico, 1968; Gabor and Anca, 1974; Hobza and Hurych, 1978). The use of the erythrocyte membrane specifically for the study of the actions of silica was the focus of several early investigations (Landsteiner and Jagic, 1904; Harley and Margolis, 1961; Kessel et al., 1963). Since these early investigations, numerous workers have found that there may exist several broad relationships between the cytotoxicity of a mineral species and its hemolytic activity (see e.g.,

Koshi et al., 1968; Schnitzer and Pundsack, 1970; Harington et al. 1971a).

The hemolytic activity of various forms of silica has been reviewed by Harington et al. (1975). There are at least two types of such hemolysis: direct hemolysis initiated by contact of the erythrocytes with silica, as a powder or, in certain circumstances, as a solution and indirect hemolysis in which colloidal silicic acid and certain soluble silicate polymers sensitize the erythrocyte to lysis by complement (Harington et al., 1971b).

Apart from occasional studies, for instance by Harington et al. (1971a), the mechanism of indirect hemolysis has been almost totally neglected and merits further analysis. By the same token, the effect of monomeric and polymeric silicic acid offers advantages to studies on mechanisms of hemolytic actions by silica compounds (see Iler, 1978). In addition, particle size of silica is important (Harley and Margolis, 1961), as is the likelihood that the hemolytic action of silica is basically an osmotic lysis which can in turn be prevented osmotically by polyvinylpyridine-N-Oxide (PVPNO) (Harington, et al. 1971b).

Informative comparative investigations of the hemolytic activities of silica and various forms of asbestos fibers (Macnab and Harington, 1967; Harington et al. 1971b) and specific studies of the mechanisms of hemolysis by silica (Summerton et al., 1977; Iler 1978) have greatly clarified the manner in which the silica surface interacts with

biological membranes.

The Surface of Quartz

The surface of quartz readily hydrates in the presence of water because of both geometrical and energetic considerations. This hydration process forms surface silanol groups (-SiOH) which, depending on pH, results in the presence of partially ionized silanol groups ($-SiO^-$). The ratio of $-SiO^-$ to -SiOH proton is pH dependent (Iler, 1978). The nonionized silanol groups is a hydrogen donor functionality which has been implicated in the biological activity of quartz. As proposed by Nash et al. (1966), surface silanol groups (polymeric silicic acid) act as proton-donor groups and may break structures of biological macromolecules (similar to actions of urea in the denaturation process of proteins). This hypothesis was further considered by Allison (1968) who suggested that most biological macromolecules are "hydrogen acceptors," and that those few compounds which are hydrogen donors are toxic. These same conclusions were reached by Stober and Brieger (1968), as well as by others. This general model of interaction, with a focus on the hydrogen-donor quality of the silanol group, has been accepted by most investigators on a number of experimental and theoretical grounds.

The non-ionized silanol groups occupying the surface of the quartz particles are essentially neutral so that the net surface charge is imparted by the ionized silanol groups. Under almost all physiological conditions, quartz remains

essentially negative in surface charge (see e.g. Mehrishi and Seaman, 1966; Bergman and Langrish, 1972; Iler, 1978). Even disruption of the crystalline character of the quartz surface and the creation of a Beilby layer does not appear to alter the negative surface character significantly. It has been broadly noted that a reduction in the measurable surface charges brings about a reduction in the cytotoxic character of quartz (see e.g., Bergman and Langrish, 1972). It has been presumed that the reduction of negative character merely reflected greater silanol group formation at the expense of the ionized form. Its acceptance appears odd in that these experiments, involving reduction of surface charge, were carried out under buffered pH conditions. The surface charge can be reduced by cations under these conditions as long as the cations are not H^+.

A number of investigators have shown that the alterations of surface charge of quartz (reduction in negative charge) through bonding of trace metals markedly decrease its cytotoxicity (Stalder and Stober, 1965; Macnab and Harington, 1967; Policard et al., 1971; Bergman and Langrish, 1972; Beck et al., 1973). Yet, in these investigations, the effects of trace metal adsorption was never studied in relation to its effect on silanol groups disruption. The observation remained, however, that reduction of available ionized silanol groups markedly reduced cytotoxicity.

As an offshoot of the importance of surface charge, there is a school which supports the hypothesis that

electron transfer effects ("semiconductor activity") may also be an important mechanism of activity. There has recently been a spate of studies focusing on the production of free electrons on the surface of quartz, as related to its cytotoxicity. The availability of these electrons (from both subsurface defects and those made available from conduction bands) appears to correlate with membrane activity. This thesis states that membrane damage is brought about by reduction of membrane macromolecules (see e.g., Robock and Klosterkotter, 1975; Beck et al., 1973; Kriegseis et al, 1976; Hobza and Hurych, 1978). Interestingly, there are two observations which appear to challenge this hypothesis: first, electron transfer effects are related to trace metal substitution within the quartz structure, suggesting that electron transfer is following another, more important, characteristic (see Beck et al., 1973), and second, conduction of electrons under physiological conditions is largely unknown, and may not be reflected by in vitro experimental conditions.

In addition to the surface silanol group (ionized and nonionized) and electron transfer characteristics of the surface, it should be noted that the reports which exist in the literature suggests that the state of the silica, in terms of crystallinity, may be a determinant of its pathogenicity (see discussion in Langer, 1978). Differences in biological activity have implicated the polymeric state of silica (see e.g., Harley and Margolis, 1961) which apparently produces differences in bond character (Iler,

1978).

Silicosis and Silica

Silicosis is a disease of the lung cause by the inhalation of one or more of the several silica polymorphs. The pathological condition is marked by the development of fibrosis, which may occur in the lung parenchyma in any lobe. Peribronchiolar and perivascular lesions are common, and interstitial involvement may occur as well. The classical lesion (the silicotic nodule) is composed of concentric, laminated masses of acellular collagenous tissue. These scar lesions are frequently accompanied by a decrease in pulmonary function, occasionally with findings of obstructive airway disease. Numerous other complications may also ensue, e.g., tuberculosis as well as a number of systemic effects (see e.g., Holt, 1957; Schepers, 1960; Zaidi, 1969; Kleinerman, 1974; Zuskind et al., 1976; Langer, 1978).

Silica is an oxide of silicon and may occur in a number of polymorphic forms (see Frondel, 1962). It is well known that these polymorphs, forms to which humans are exposed in the workplace, possess different biological potentials. There has developed an enormous literature in this area, some of it recently reviewed in Bergman and Langrish (1972) and Langer (1978). Of the silica polymorphs, quartz is the most important: it is one of the most common minerals in the earth's crust, occurring as common rock former, as a common host substance for ore deposition, and therefore also as a

common gangue mineral. The result is that large numbers of workers are exposed to quartz dust occupationally. Its ubiquitous nature underscores its importance biologically (see Langer, 1980).

It has been observed that even the single mineral quartz may possess a range of biological activities. Occurring in different geological localities, its physical-chemical properties may vary markedly and appear to impart different biological potentials. This feature has been discussed in a number of recent papers (Bergman and Langrish, 1972; Weiss et al., 1973; Robock and Klosterkötter, 1975; Langer, 1978). It has been shown, for example, that quartz occurring with measurable concentrations of iron or aluminum has a blunted activity; that quartz of small particle size (0.5-2.0um) tends to be more hazardous to workers than coarse, respirable dust; that mechanical methods to size-reduce quartz may produce noncrystalline layers on the surface, thereby blunting its activity; and the mechanical activities which produce shattered crystalline surfaces tend to enhance activity (see review in Langer, 1978). Many of these observations support the hypothesis that the nature of the quartz surface and differences in physical-chemical properties are clearly first order determinants of biological activity.

The Biological Action of Quartz

There is general consensus among most investigators that the action of quartz follows a "well-developed

sequelae"; the inhalation of quartz is generally restricted "to respirable particles," on the order of less than 3um in mean aerodynamic diameter; the nature of pulverized quartz is such that its surface easily hydrates, binding water either from the atmosphere or in the alveolar wall space (disposition of particles may occur in either the small airways or in the alveolar spaces themselves; once within the human host, the hydrated particles may be become coated with proteins, surfactants, or other substances normally available in these tissues; the presence of the dust elicits a response within the host (a chemotactic factor) which marshalls alveolar macrophages; quartz particles are phagocytosed (endocytosed) by the alveolar macrophages according to normal processes; the dust particles are encapsulated within a phagosomal vacuole which then fuses with primary lysosome organelles (containing lysosomal enzymes); lysosomal (hydrolytic) enzymes are discharged into the phagosomal vesicle forming a secondary lysosome (bounded by a lysosome-phagosome membrane wall) containing particles and enzymes; the enzymes digest organic molecules on the surface, "cleansing" the quartz surface; quartz particles with "clean" surfaces interact with the secondary lysosome membrane, causing it to either "leak" or disintegrate; lysosomal enzymes and undigested particles are released into the macrophage host, whereupon the cell undergoes autolysis and dies; at a time prior to, during, or after the macrophage death, substances are released ("collagen-stimulating factors") which stimulate fibroblasts to greatly

increase collagen synthesis; and repeated macrophage death, fibroblast stimulation, and collagen synthesis produce the silicotic condition.

Within the above sequelae, there are some areas in which consensus is still lacking. For example, there are differences observed in rapid and delayed effects, in the exact nature of the factor which stimulates fibroblasts, etc. And even the final product, collagen, has been studied in terms of its own synthesis (see Stalder and Stober, 1965; Nash et al., 1966; Allison et al., 1966; Heppleston and Styles, 1967; Allison, 1968, 1971, 1978; Miller and Harington, 1972; Harington et al., 1973; Harington, 1974; Chvapil, 1974, 1977; Gabor and Anca, 1974; Kriegseis et al., 1976; Summerton et al., 1977; Depasse, 1978; Hobza and Hurych, 1978; Miller, 1979; Miller et al., 1980).

All current theories of silicosis generally agree on two points: the alveolar macrophage must be compromised or damaged, and the mechanism of damage involves either the phagosome-lysosome membrane or the plasma membrane. The mechanism by which the membrane is damaged, resulting in release of the vesicle contents (including particles) into the cytoplasm, has been the focus of discussion. Although all theories agree that this important vesicle membrane is damaged, disagreement exists over the general biological events concerning the specific target of interaction (membrane components) and the extent and the nature of the damage (frank rupture, creation of osmotic channels, geometrical redistribution of membrane components, etc.).

These may be summarized as follows:

- Catalytic peroxidation of membrane lipids (see e.g., Marasas and Harington, 1960; Gabor and Anca, 1974; Chvapil and Peng, 1975; Chvapil et al., 1976; Chvapil, 1977). Although this effect has been observed in a number of experimental systems, its reproducibility has not been uniform (see e.g., Kilroe-Smith, 1974). Those investigators reluctant to accept this mechanism have observed that superoxides are generated after membrane damage has taken place.
- Damage and/or rupture of membrane through particle interaction with phosphate ester groups on phospholipids (see e.g., Brown, 1957; Stalder and Stober, 1965; Nash et al., 1966; Allison, 1971, 1978; DeKorosy and Taboch, 1973). The mechanism of interaction remains attractive on the basis of experimental evidence.
- Damage and/or rupture of the membrane through particle interaction with secondary amide groups on proteins (see e.g., Scheel, 1955; Harley and Margolis, 1961; Scheel et al., 1964; Desai et al., 1975; Summerton et al., 1977; Desai and Richards, 1978). As with the lipoprotein model, much evidence exists to support this. Support for the protein model of interaction is suggested by the presence of altered proteins, which are in part denatured and are "seen" as antigens by the host. This initiates

within the host a form of autoimmune disease (see e.g., Vigliani and Pernis, 1963).

It is of interest to note that the material used in the experimental studies differed as to their state of crystallinity, particle size, and geological origin. Some of the variations in experimental results may in part be explained by these differences (see e.g., Iler, 1979, and discussion of bonding differences observed for silica in the different polymeric states).

After membrane damage, the dying and/or dead macrophage, through a released factor, stimulates the fibroblast in the production of collagen. The process and form of cell communication have been reviewed in a number of recent publications (Chvapil, 1977; Chvapil et al., 1976; Heppleston, 1978).

CHAPTER II

Methodology for the Determination of the Membranolytic Activity of Quartz

INTRODUCTION

It is often stated that the fibrogenicity and carcinogenicity of a mineral dust may be measured by its cytotoxic potency (Harington et al., 1975). The hemolytic assay had been used to gauge mineral cytotoxicity. Quartz and many other fibrogenic minerals have the ability to interact with erythrocyte membrane and alter its permeability so that the hemoglobin contained within the cell is released. If the above stated relationship is true, then one may study the details of the hemolysis assay, the nature of the materials being tested and gain insights which may lead to an understanding of fibrogenic and carcinogenic potential of certain minerals.

Therefore, to gain an understanding of the action of mineral dust on cell membranes, the hemolysis assay represents a rapid and inexpensive model. A defined hemolytic assay has been developed which has sufficient precision and accuracy to differentiate a range of physicochemical states for a single mineral type. The variables which must be controlled for to have a reproducible hemolytic assay are described in this chapter.

The Hemolysis Assay as an Index of Cytotoxicity

Erythrocyte damage induced by mineral dust, and the accompanying quantitative measurement of the hemoglobin released on membrane failure, has developed into a rapid

technique for gauging mineral cytotoxicity (Nolan et al., 1981). However, a wide range of hemolytic indices can be found in the literature for a single mineral species. These values, often expressed as mass of mineral required to lyse 50% of the erythrocytes in a stock suspension, vary so greatly that interstudy comparisons are impossible. Consequently, it has been observed that perhaps the hemolytic assay cannot be relied on for mineral dust evaluation, especially for measuring small differences in membrane activity for a single mineral species.

Scrutiny of the variously reported assay systems, where sufficient details are given, suggests that technical factors play a major role in producing disparate results. Among the variables in study design are animal species from which the erythrocytes are obtained; age of the cells outside the intact animal (often not given); cell concentration in the standard erythrocyte suspension, which range from 10^5-10^8 cells/ml; different test mass concentrations of the same mineral species; determination of hemolytic activity along different portions of the dose response curve; time of interaction between the erythrocytes and the mineral dust, which range from 15 to 120 minutes; different spectrophotometric criteria for the measurement of lysate absorbance (530-541nm); different cell media and uncharacterized mineral specimens. On the basis of these methodological variations, it may be anticipated that measureably different cytotoxicity values would be produced even for the same mineral species.

MATERIALS AND METHODS

The Hemolytic Assay

The hemolytic assay described here is modified after Schnitzer and Pundsack (1970), who based their protocol on Macnab and Harington (1967) and Secchi and Rezzonico (1968). The hemolysis experiments were performed using packed erythrocytes which were suspended at approximately 4% concentration in Veronal buffered saline (VBS). A 0.25ml aliquot of the 4% erythrocyte suspension was diluted to 5ml with distilled water. If the absorbance at 530nm was not 0.300±0.010 absorbance units (A) the volume (V) was adjusted using the following relationship:

$$V_f \times A_f = V_i \times A_i$$

Where V_f if the final volume, A_f is the final absorbance, V_i is the initial volume, and A_i is the initial absorbance. The A_f should be 0.300A, then it follows that:

$$V_f \times 0.300 = V_i \times A_i$$

It is experimentally desirable to prepare a greater than 4% erythrocyte suspension and then dilute to obtain a standard concentration, because it is easier to dilute than concentrate. The stock suspension of erythrocytes contains approximately 3.6×10^8 cells/ml.

The quartz was introduced into glass tubes from a stock suspension in VBS prepared on the day of the experiment. The volume was then adjusted to 4ml with VBS. The erythrocyte suspension was never added to dry quartz; the hemolysis experiments were always carried out in buffered suspension

maintained in standard 16 x 125mm flint disposable culture tubes. After addition of VBS, 4ml of stock erythrocyte suspension was added to the tubes containing the quartz and buffer. The addition made the final concentration of erythrocytes 1.8 x 10^8 cells/ml with a final volume of 8ml.

The positive control used in the experiment was 4ml of stock erythrocyte suspension added to 4ml of distilled water, which yielded total lysis; the negative control was 4ml of VBS added to 4ml of stock erythrocyte suspension, which gave background absorbance. This latter value reflected mechanical lysis or leaking from the cells.

The erythrocyte/quartz suspensions were placed in a temperature bath set at 37^{o}C for a period of two hours. The tubes were inverted every 30 minutes by hand to resuspend the settled cells and quartz. In adddition, the suspension was generally maintained as the tubes were constantly moved by gyratory motion. At the end of two hours, the content of all the tubes were centrifuged (800xg) and the absorbance of the clear supernatant, cell and particle free, was determined at 530nm.

The absorbance of 100% should be ten times the A_f value from the standardization of the erythrocyte suspensions. Once the absorbance of the sample (A_s) has been determined, the percentage hemolysis (%H) can be calculated from the relationship:

$$\%H = \frac{A_s}{A_f \times 10} \times 100$$

Determination of the Hemolytic Reference Point, HC50

The hemolytic activity of a mineral is defined as the mass of mineral required to release 50% of hemoglobin (HC50, mg/ml) contained in the standard erythrocyte suspension. The HC50 value was obtained through extrapolation of multiple (usually 4 points in duplicate) data points defining the linear portion of the dose-response curve. Further, as a function of the optical system used to measure absorbance, the direct, onscale measurement of the hemolytic activity was always less than HC33. The rationale for this was based on our experimental observation that at about 50% hemolysis the linear dose-response begins to alter, producing a marked change in line slope (dose-response variation).

Estimation of Variance

The degree of hemolysis is a dose-response function, related to the mass concentration of the mineral dust in the system. On the basis of several data points, the linear regression lines (best estimates) were calculated. The coefficient of determination (r^2) yielded proportion of total variance explained. With measured challenges, we computed the standard error of the estimate for each experiment (the observed hemolytic value [y] and the predicted hemolytic value [y']). When several experiments were carried out in a single system, F values were computed for related scattergrams to determine their measure of difference.

Powder Preparations

Quartz specimens were prepared and characterized in the manner described by Nolan, et al. (1981). For this study, the primary focus was on those quartz varieties that were visibly colored (e.g., rose quartz) or obtained from a non-industrial source (e.g., Gauley Bridge, West Virginia). (A description of these specimens, including their localities, is given in Table II.5.) Specimens obtained as quartz crystal were pulverized in a carborundum mortar and pestle, and then examined by both polarized light microscopy and powder x-ray diffraction. Most were found to be of high purity. Occasionally a few fragments of mica and feldspar were observed by polarized light microscopy but mineral impurity appeared to account for less than by 1 part in 1000 by volume. For all specimens but one, these mineral contaminants were not detectable by the powder x-ray method. Microsize quartz fragments appeared colorless and indistinguishable as particulates when examined by polarized light microscopy. The specimen from Gauley Bridge, however, contained measurable amounts of mineral contaminants. The quartz, in this case derived from a quartzite formation in the southern Appalachian Mountains, appeared coated with limonite minerals and occurred with fibrous micas (sericite), rutile needles, and feldspar. These contaminant minerals appeared to acount for the high HC50 of this specimen.

Powder x-ray diffractometry produced patterns in excellent agreement with the standard powder x-ray diffraction

file data card ASTM 5-0490. Of the 14 characteristic reflections from 20^{o} to 65^{o} two theta, all were resolved, indexed, and their interplanar spacings measured. Those reflections that remained on scale (for the full-scale setting at 2000 cps) were within $\pm$ 0.002A of their reported values. Those reflections that were "off scale" -- in which the peak center was estimated -- were within $\pm$ 0.006A of the reported d-spacing values. All the quartz specimens yielded x-ray data in excellent agreement with the published standard.

Particle Size Distribution

The hemolytic index of a single mineral species was measured for a number of different particle size fractions. In addition to size reduction, the comminution of quartz produces several related changes, that is, an increase both in particle number and surface area. The fractionation of the quartz size classes by Stokes' settling formula idealized particles as unit spheres to facilitate computation. The reduction of a unit sphere's diameter by one-half, corresponding to a halving of its radius, produces an eightfold increase in "spherical" particle number (for each cycle) accompanied by a two-fold increase in surface area. Quartz, however, behaves physically as an "irregular" particle, with most planes of failure not well crystallographically controlled. These computed ideal relationships are therefore never achieved during comminution.

Stokes' law relates particle size to settling velocity.

Considering resistance to settling (R), which impedes fall, it was determined that:

$$R = 6\pi r\eta v$$

Where r = radius of particle (cm)

η = viscosity of the fluid in which particle fails

v = settling velocity of particle (cm/sec)

Counter forces of gravity and buoyancy also act on falling particles and, when equal to total resistance, the following condition is met:

$$6\pi r\eta v = 4/3\pi r^3 (d_1 - d_2)g$$

Where d_1 = density of particle with volume $4/3\pi r^3$

d_2 = density of fluid

g = acceleration due to gravity ($980 cm/sec^2$)

Solving for velocity in cm/sec, the equation yields:

$$V = \frac{2(d_1 - d_2)gr^2}{9\eta}$$

Substituting values of water for the fluid, with the temperature set at $24^{\circ}C$, quartz with a specific gravity of $2.65 g/cm^3$, the desired constant, C, is 3.57×10^4. Therefore,

$$V = Cr^2$$

for quartz in water.

We note that this model is simplified and is based on a number of assumptions; nevertheless, reasonable size fractions may be extracted.

One of the silica specimens used in this experiment was "industrial silica flour" (quartz). To effect a uniform separation, the small particles (1 and 2um Stokes'diameter)

were removed by decantation after allowing all the larger ones to settle out in water. The small particles were concentrated by centrifugation and the process repeated until all the supernatant that could have contained particles of 1 and 2um Stokes' diameter appeared clear.

Velocity of Fall by Time

Particle Diameter	Fall Height				
(um)	(cm)	(hrs)	(min)	(sec)	ΣSec
20	20		9	17	557
15	15		12	22	742
10	10		18	34	1,114
5	10	1	14	4	4,444
2	10	7	43	48	27,828
1	10	30	55	48	111,348

The 5, 10, 15 and 20 micrometer size particles were removed in 10ml fractions. The process was repeated until the desired amounts of each of the size fractions were collected.

Size-Fractionated Materials

Each of the size-fractionated splits of the silica was examined in a similar fashion as the parent powder. Polarized light micropscopic examination of all size splits indicated that the rarely appearing associated feldspar was not confined to any single size class of particle. X-ray diffraction patterns obtained on the size splits were almost

indistinguishable, with no line-broadening effects discernible. This observation is in keeping with diffraction theory. The process by which the quartz specimens were pulverized appears to have produced little surface artifact (Beilby layer). Minor intensity changes were noted for some reflections in the ≤5um Stokes' diameter fractions, likely to be due to orientation effects.

The Stokes' diameter fractions represent mixtures of sizes (Table II.1). The original material examined by polarized light microscopy was observed to comprise heterogeneous mixtures of all size ranges. The coarse 20um Stokes' diameter fraction was noted to consist of many large fragments in matrices of smaller particles (Table II.1). The finer 5um Stokes' diameter fraction contained large particles but smaller particles were present in qreater abundance than in the coarse splits. Even the finest fraction contained rare residual 5um grains within the fine matrix.

Two Stokes' diameters are included for comparison: the 20um fraction is skewed toward the larger particle size range, whereas the 5um fraction is skewed in the opposite direction. Approximately 18% of the 20um Stokes' diameter fraction is greater than 15um in size, compared with a 0.5% content of similar particles in the 5um fraction. Conversely, approximately 31% of the 5um fraction is less than 5um in size, compared to a content of only some 5% of similar particles in the 20um fraction. Interestingly, both materials possess the 5.1 to 10.0um size range as their modal

class. As to mean particle size, each split was shown to be different (see Table II.1). The heterogeneity of the different size classes is a function of the initial size distribution of the particles in the sedimentation cylinder.

EXPERIMENTAL RESULTS

Hemolysis as Related to Erythrocyte Age

Ten and thirteen days old mature sheep erythrocytes were prepared for hemolysis as described in the Materials and Methods. Age of the cells was based on the number of days out of the animal (reported to us by the invoice accompanying receipt of each batch). These cells were challenged with unfractionated industrial silica flour. The results of these hemolytic experiments are shown in Table II.2 and Figure II.1.

Best estimate analysis of these data sets shows a slight increase in standard error about the best fit regression lines in progressively older cells. The 50% hemolytic concentration (HC50) range for all 24 data points is 6 parts in 133 (or just under 5%). All the best estimate lines are statistically indistinguishable by the F-test. The HC50 ranges from 12.67mg/ml to 13.78mg/ml. The high values were obtained on the more aged cells.

Sheep erythrocytes may be used for at least two weeks after leaving the animal host with no major introduction of age artifact. Some increase in scatter is evident, but it is not of sufficient magnitude to cause a statistically

significant difference in hemolytic activity.

Hemolysis With Higher Particle Content

Lysates with absorbances greater than 1 may be in the nonlinear portion of the dose-response curve, and, therefore, direct measurement of the HCs greater than 33% may produce an incorrect value. To obtain accurate readings on such a concentrated particulate system or on minerals of potent activity the lysates must be quantitatively diluted. This allows the absorbance to be measured within the linear portion of the absorption curve.

Standard erythrocyte suspensions were challenged with quartz dust above and below this critical lysis range. The suspensions were appropriately diluted so that the measure of absorbance could accurately be made, and the results of these experiments are shown in Table II.3 and Figure II.2.

The observed HC50, calculated from the best estimate line for the eight points measured for dust concentrations equal to or greater than 8.84mg/ml, is greater than the value calculated for the lower 12 particulate concentrations (less than 6.47mg/ml; Table II.3). The differences in these values is approximately 2.4mg/ml, which corresponds to a mass of quartz capable of hemolyzing almost 10% of the cell population present in the test suspension (see Table II.2).

Dilutions even at a silica concentration above 14mg/ml yield hemolytic activities in the linear range when diluted back onto scale (Figure II.2). When concentrations of dust produce activities greater than 50% the slope dramatically

flattens out (see Figure II.2). This region is statistically different as evidenced by the F values. At or near the 50% hemolysis point there is a dramatic change in the slope of the dose-response curve. This flattening out of the curve gives higher values for the HC50 than if the points below 33% hemolysis are used and the HC50 is extrapolated.

This slope effect may be related to a number of factors. For example, the cellular debris, i.e. hemoglobin, released after hemolysis may possibly be binding to the particulate surface, thereby blocking its active functionality. This has been previously suggested by Desai and Richards (1978). Another point is that the particulates may be so concentrated that they are settling out of the cell suspension rapidly, so that the effective amount of particulate in contact with the cells is proportionately less or not linearly proportional to its concentration. Also, dilution itself introduces an error into the system.

If particle adsorption of protein is the predominant factor in change of slope, then mineral species of high adsorptive capacity, e.g. chrysotile, would produce even greater variation at similar or lower concentrations. These data support the conclusion that hemolysis may be more accurately measured when small amounts of dust are used to challenge high concentrations of erythrocytes.

Hemolysis With Time

It has been reported in the literature that there is an initial rapidly hemolytic period after which cell contact

with the mineral particulate produces negligible additional effect. The cited time period for this varies, and it is unclear whether this is related to mineral species or to some feature of the experimental system.

Utilizing industrial silica flour, we have determined the hemolytic concentration, HC25, to be approximately 6.5mg/ml. This single dose of quartz was used to challenge sheep erythrocytes in time increments of 30 minutes for as long as three hours. (The results of this experiment are given in Table II.4 and Figure II.3.) As with previous reports in the literature, the first 30 minutes of mineral/erythrocyte contact results in rapid hemolysis; over 85% of the total hemolysis occurs here. The first plateau is not reached until one hour after particle contact. An additional 30 minutes produces a leveling of activity and a further 30 minutes produces a slight increase of activity within statistical limit ($\pm 1\sigma$). For quartz, a measure of hemolytic activity is achieved with 120 minutes of cell contact. Different mineral species must be tested before detailed experimentation to determine the optimum time for maximum hemolysis.

Hemolysis of Quartz Specimens From Different Geological Localities

On an epidemiological basis, quartz minerals from different geological localities appear to possess different biological activities (Langer, 1978). To this end, we compared hemolytic activity of four varieties of natural quartz

minerals with our standard industrial silica flour. Quartz crystals obtained from a number of geological localities were comminuted and passed through a 325 mesh ASTM sieve collecting particles less than 45um in size. These powders were tested with sheep erythrocytes and their results compared with silica flour. The results are given in Table II.5.

The difference in erythrocyte membrane activity among these five quartz specimens is of almost two orders of magnitude. A likely cause is difference in size distribution of the specimens, which was observed when examined by optical microscopy. Another is impurity: specimen #4 (quartzite), representing a crushed quartz-rich rock (greater than 90% quartz content by weight) is contaminated by trace substances, including iron oxide minerals. Microscopic examination of the crushed powder revealed limonite-like mineral on the quartz fragments. Iron compounds are well-known suppressors of silica activity. Rose quartz, specimen, is reddish in color, suggesting the presence of both mineral impurities and trace metals. Both specimens contain agents that act to blunt activity.

Hemolysis and Particle Size

The different size fractions, obtained from industrial silica flour specimens by sedimentation techniques, were examined separately. The results of the experiments are given in Table II.6 and Figure II.4. The HC50 varies from the large size particle fractions down to that of the 2um

Stokes' diameter in a progressively decreasing order. At the 5um Stokes' diameter, the r^2 value for the coefficient of determination dropped markedly, and scatter about the linear regression line increased dramatically, indicating an increase in unexplained variance. The coefficient similarly is low at the 2um Stokes' diameter and the scatter appears to increase as well.

From the 20um Stokes' diameter down to smaller sizes there is a corresponding increase in particle number (by almost two orders of magnitude) and an increase in surface area by several fold. The HC50's correspondingly decrease approximately two-fold. The hemolytic activity appears to be surface area related in that increase in the number of active functionalities, e.g., doubling of surface area, correlates with increased membrane activity (one-half the quartz required to lyse 50% of the erythrocytes).

The decrease in the r^2 value, increase in "scatter" and reduction in biological activity of 1um Stokes' diameter was likely an effect of small particle clumping.

DISCUSSION AND CONCLUSIONS

To determine reproducible hemolytic activities for mineral dusts, it is important that the test system be well characterized. Erythrocyte concentration, method of lysate measurement, e.g. particle size distribution and presence of contaminants, must be known variables if the hemolytic phenomenon is to be understood.

The use of aged sheep cells that have been out of the animal for up to two weeks does not influence the HC50 value for quartz in a two-hour determination. Standard error about the linear regression line is small and the HC50 values are within 5%. The older cells show more scatter about the best-estimate line, which may reflect slightly greater membrane fragility. Still, the scatter shows only a 0.5% variation between observed and computed hemolytic values -- not a significant variation. The F-test clearly shows the dose-response curves to be statistically identical.

Theoretically, utilizing a 2% sheep erythrocyte suspension, a full-scale spectrophotometric absorbance (up to 1.0) would be produced by 33% hemolysis. Any value above this hemolytic point necessitates dilution to provide an absorbance within the linear range of the spectrophotometer. This also avoids the considerable flattening of the response curve that occurs at high mineral concentration. As to hemolysis with respect to time, hemolysis in the quartz/sheep erythrocyte model is almost entirely complete after two hours. However, this may not be the case for other kinds of minerals and other cell systems.

The HC50 values can vary over two orders of magnitude depending on the geological localities from which the quartz is obtained. This may be a function of trace metal content, mineral contaminants or even differing size distributions for the different comminuted specimens. In terms of the latter, variation in the membranolytic activity may be ob-

served with a single specimen.

Once a single quartz dust was size-fractionated into widely disparate Stokes' diameters, computation of particle number and surface area showed that the hemolytic activity more closely follows surface area. This is in keeping with the findings that the surface functionalities on quartz are responsible for the mineral's membrane-damaging effects. On size reduction, increase in surface area produces a progressively more active dust per unit mass of challenge.

It has been observed that size fractionation of mineral dust may occur as it is manipulated or handled in a canister. Such physical manipulation may produce different size fractions within a single specimen and thereby produce different hemolytic responses. Characterization of multiple aliquots may be required, and optical microscopy may be useful in characterizing such splits.

The hemolytic activity of mineral dusts may be measured with good reproducibility if the test system is thoroughly described. Minerals of different species may be compared in a single system only if particle number and surface area are equivalent. Equal mass challenges may be misleading if these two physical characteristics do not match. When such parameters are controlled, then relative cytotoxicity may be compared between two populations of particles. It is only on this level that accuracy of the test system will be achieved and meaningful mineral comparisons made possible.

If the hemolytic test system can be used to measure cytotoxicity and fibrogenicity, we conclude the following:

there may be no absolute value of fibrogenicity for a single mineral species. Unlike classical toxicological principles for organic compounds, mineral dust "toxicity" may be more closely related to particle size than total mass delivered to the biological test. If a mineral dust is not metabolized, then the existing surface area and resultant functionalities represent the interaction potential. Host processes may have limited effects on changing biological potential. The physical characteristics of quartz dust control, in large measure, its fibrogenic potential.

Table II.1 -- Particle-size distribution in representative splits

Size (um)	20um Stoke's Diameter N	20um Stoke's Diameter %	5um Stoke's Diameter N	5um Stoke's Diameter %
2	0	0.00	27	6.77
2.1- 5	21	5.34	96	24.06
5.1-10	200	50.89	242	60.65
10.1-15	100	25.45	32	8.02
15.1-20	46	11.70	2	0.50
20	26	6.62	0	0.00
	X size = 10.5um		X size = 6.3um	

Means calculated on basis of particle class centroids.

Table II.2 -- Hemolytic response of sheep red blood cells of different ages to Industrial Silica Flour (ISF)

As Received ISF (mg/ml)	(%H)[a]	10 days old ISF (mg/ml)	(%H)	13 days old ISF (mg/ml)	(%H)
1.21	5.31	0.93	4.83	1.68	7.64
1.50	6.15	1.16	5.85	1.95	9.20
2.36	9.10	1.49	8.10	3.36	13.72
3.03	11.31	2.06	9.56	3.54	14.62
3.51	12.90	2.15	10.14	3.82	14.74
3.70	13.72	3.35	14.69	4.54	18.79
4.55	16.95	3.54	15.37	4.76	18.79
4.85	18.91	3.88	16.05	7.40	27.55

Computed HC50s

As received: 13.42 mg/ml

10 days old: 12.67 mg/ml

13 days old: 13.78 mg/ml

All (X 24): 13.29 $\pm$ 0.6 mg/ml

$\pm$ 4.7% HC50 value

Table II.2 -- Hemolytic response of sheep red blood cells of different ages to Industrial Silica Flour (ISF) (cont)

Best estimate and coefficient of determination

As received: %H = 3.40 X mg/ml ISF + 0.33

r^2 = 0.9944: SE^b = 0.38

10 days old: %H = 3.81 X mg/ml ISF + 1.73

r^2 = 0.9918; SE = 0.44

13 days old: %H = 3.47 X mg/ml + 2.17

r^2 = 0.9943; SE = 0.52

[a]Values given to second decimal place; consider accurate to first,

r^2 = coefficient determination.

[b]Standard error of Y. Note that estimating equation is expressed as mg/ml quartz.

Table II.3 -- Hemolytic response of sheep erythrocyte cells to Industrial Silica Flour in a range of concentrations

ISF mg/ml	%H (y)	SE(y')
1.86	8.83	7.73
2.38	12.59	0.15
2.55	11.42	4.00
3.22	15.08	0.01
3.48	16.40	0.29
3.61	14.79	1.99
3.66	15.17	1.28
4.18	16.75	0.88
5.15	21.45	1.48
6.16	22.78	0.01
6.36	24.61	1.46
6.47	25.34	2.89
8.84	30.76	9.73
11.11	37.16	2.59
11.43	41.80	5.48
12.81	41.59	0.72
14.22	49.59	16.81
16.63	51.74	1.10
19.28	55.52	0.82
23.98	64.98	2.52

HC50 values less than 30%: HC50 = 14.07 mg/ml; %H = 3.29X + 3.72

$r^2 = 0.9746$

HC50 vlaues larger than 30% HC50 = 16.35 mg/ml; %H = 2.16X + 14.77

$r^2 = 0.9532$

Table II.4 -- Change in hemolysis with time

Time (min)	Percentage Hemolysis[a]	Change in Hemolysis[b]	Change in Percentage Hemolysis[c]
30	25.76	0.00	0.00
60	27.49	+1.73	+6.79
90	27.53	+1.77	+6.87
120	29.17	+3.40	+13.20
150	29.23	+3.46	+13.43
180	29.76	+3.99	+15.49

[a]Based on three determinations (average)

[b]Thirty-minute interval used as the reference point

[c]Percentage change as compared to the reference percentage measured at 30 minutes

Table II.5 -- Hemolytic response of sheep erythrocytes to quartz specimens obtained from different geological localities[a]

Specimens	HC50 mg/ml	Best Estimate Coefficient of Determination
Smokey quartz[b]	7.85	%H = 6.30X + 0.56; r_2^2 = 0.99
Hydrothermal quartz[c]	6.44	%H = 7.79X + 0.13; r_2^2 = 0.98
Rose quartz[d]	138.51	%H = 0.35X + 1.52; r_2^2 = 0.93
Quartzite (90% + Qu)[e]	56.59	%H = 0.88X + 0.20; r_2^2 = 0.98
Quartz Min-U-Sil 15[f]	2.72	%H = 15.37X + 8.25; r^2 = 0.98

[a]Specimens were hand-ground in a mortar and pestle and passed through a sieve. Splits less than 45 um in size were used in these experiments.

[b]Smokey quartz, prepared from a single crystal. Origin: Bancroft, Ontario, Canada.

[c]Hydrothermal crystal of quartz. Euhedral, clear and transparent. Origin: Mount Ida, Montgomery County, Arkansas.

[d]Rose quartz, prepared from a massive, anhedral specimen. Origin: Texas Creek, Fremont, Colorado.

[e]Quartzite. Massive. Hand specimen of rock type. Origin: Gauley Bridge, West Virginia.

[f]Quartz, industrial-grade Min-U-Sil 15. Used in work of Nolan et al. (1981). Origin: Pennsylvania Glass and Sand Company. The Min-U-Sil 15 hemolysis experiments were done with human erythrocytes.

Table II.6 -- Hemolytic activity of Industrial Silica Flour -- Influence of particle size on hemolysis

Material	mg/ml	Best Estimate Coefficient of Determination
As received	11.46	$\%H = 4.25X + 1.27;\ r^2 = 0.9930$
1um Stokes' Diameter	6.12	$\%H = 7.38X + 4.79;\ r^2 = 0.9519$
2um Stokes' Diameter	4.90	$\%H = 9.68X + 2.53;\ r^2 = 0.8460$
5um Stokes' Diameter	10.35	$\%H = 4.24X + 6.12;\ r^2 = 0.8061$
10um Stokes' Diameter	12.70	$\%H = 3.77X + 2.08;\ r^2 = 0.9975$
15um Stokes' Diameter	13.51	$\%H = 3.54X + 2.18;\ r^2 = 0.9982$
20um Stokes' Diameter	14.35	$\%H = 3.20X + 4.07;\ r^2 = 0.9941$

Figure II.1 -- Hemolytic response of sheep red blood cells to Industrial Silica Flour (quartz) as a function of age of cell outside the donor animal. Estimating equations, determined for each of the data sets, are statistically indistinguishable by F-test.

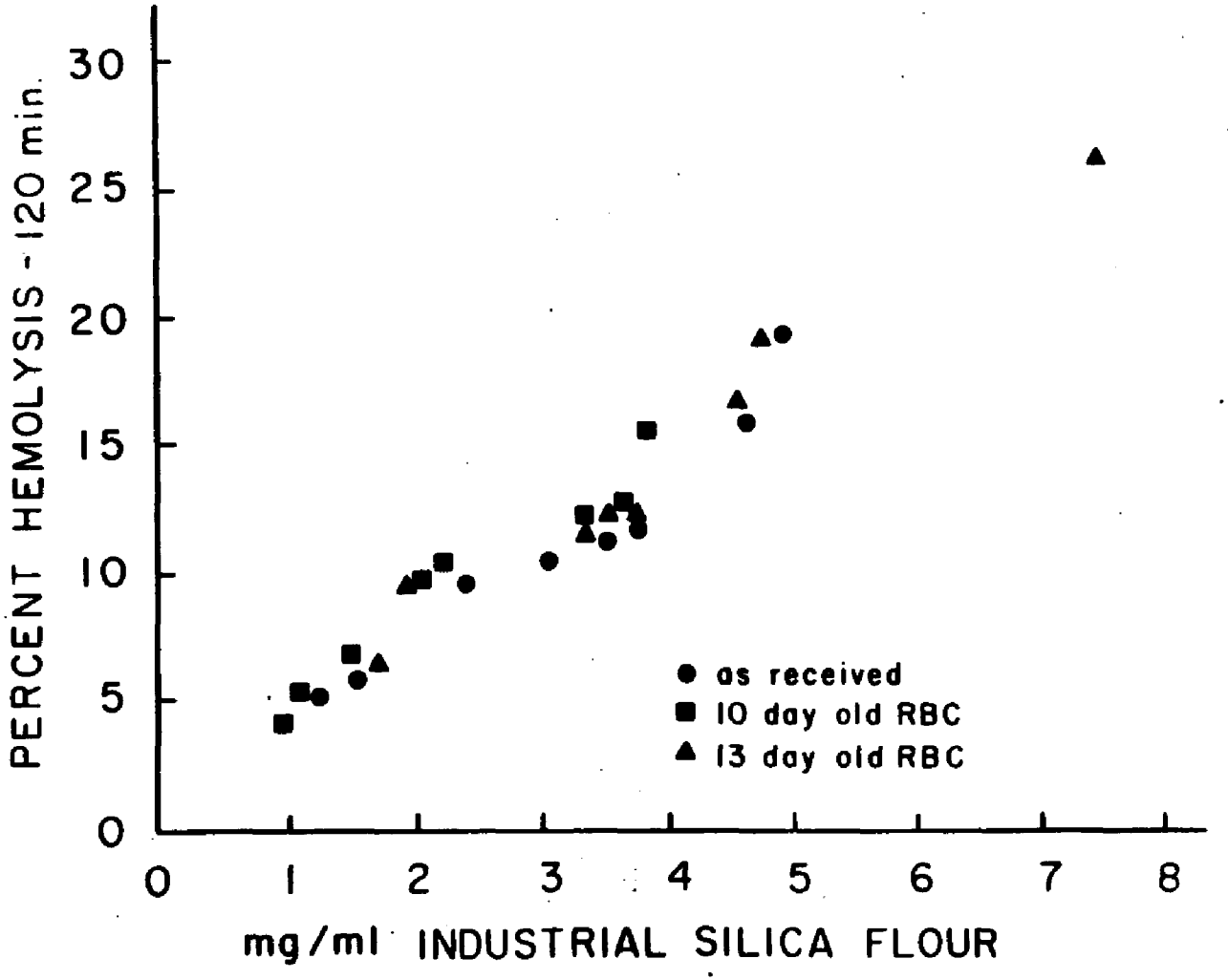
PERCENT HEMOLYSIS - 120 min.
30
25
20
15
10
5
0
0
1
2
3
4
5
6
7
8
mg/ml INDUSTRIAL SILICA FLOUR
os received
10 day old RBC
13 day old RBC

Figure II.2 -- Hemolytic response of sheep erythrocyte cells to Industrial Silica Flour (quartz) as a function of mineral dust concentration. Dashed line is at the 30% hemolytic response, approximately at the point absorbance = 1. Note that the three points, defined by the silica concentration greater than 15.0 mg/ml, produce a change in slope and a corresponding change in the estimated equation. Table II.3 gives an equation based on all data points above the HC30, thereby representing the change in the high particle concentration range.

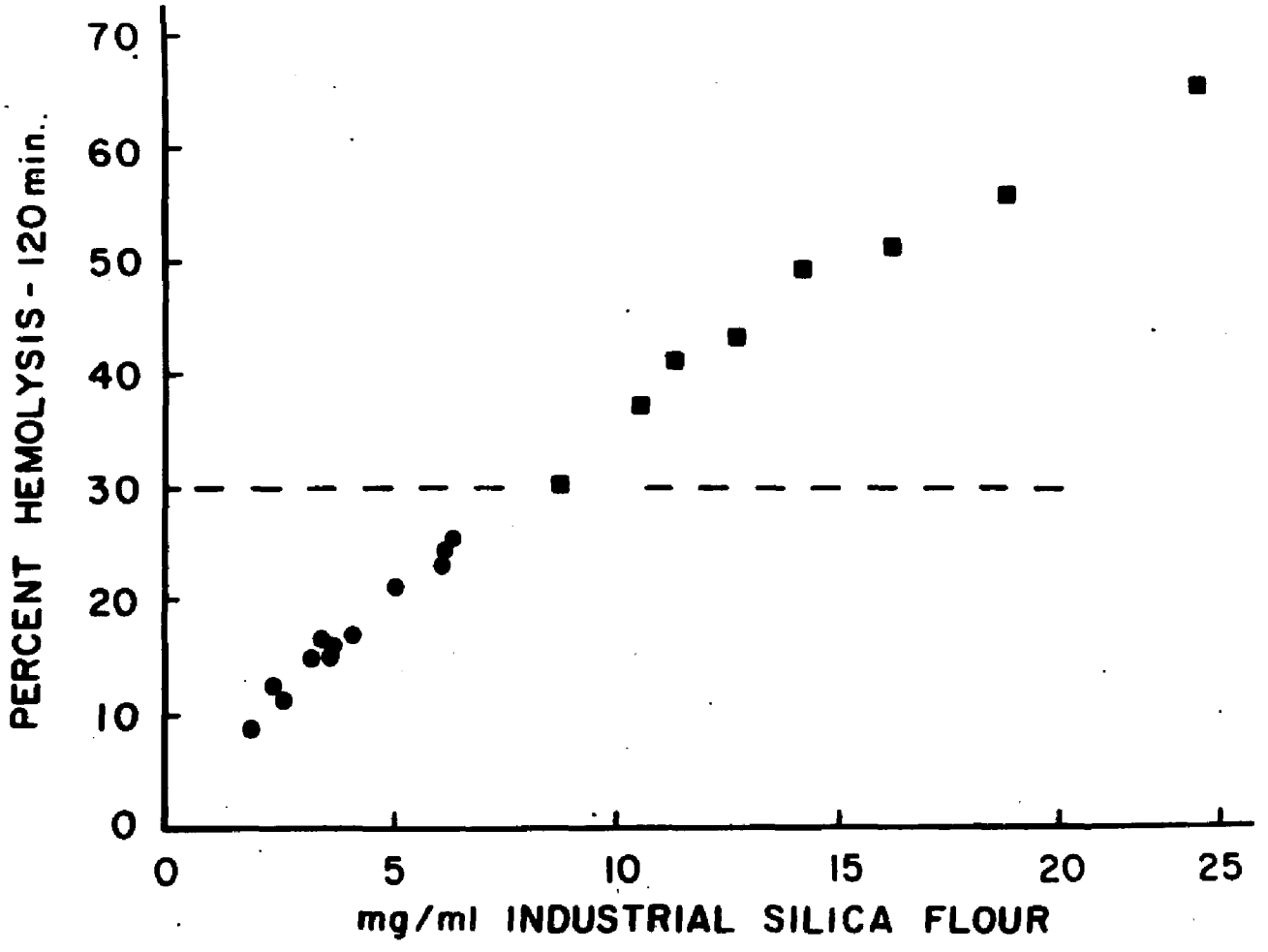
PERCENT HEMOLYSIS - 120 min.
70
60
50
40
30
20
10
0
0
5
10
15
20
25
mg/ml INDUSTRIAL SILICA FLOUR

Figure II.3 -- Hemolytic response of sheep erythrocytes to 6.5mg/ml of Industrial Silica Flour (quartz) as a function of time. Each data point represents an average of three determinations. Measured variation above 120 minutes is within the limits of a standard deviation (1 sigma).

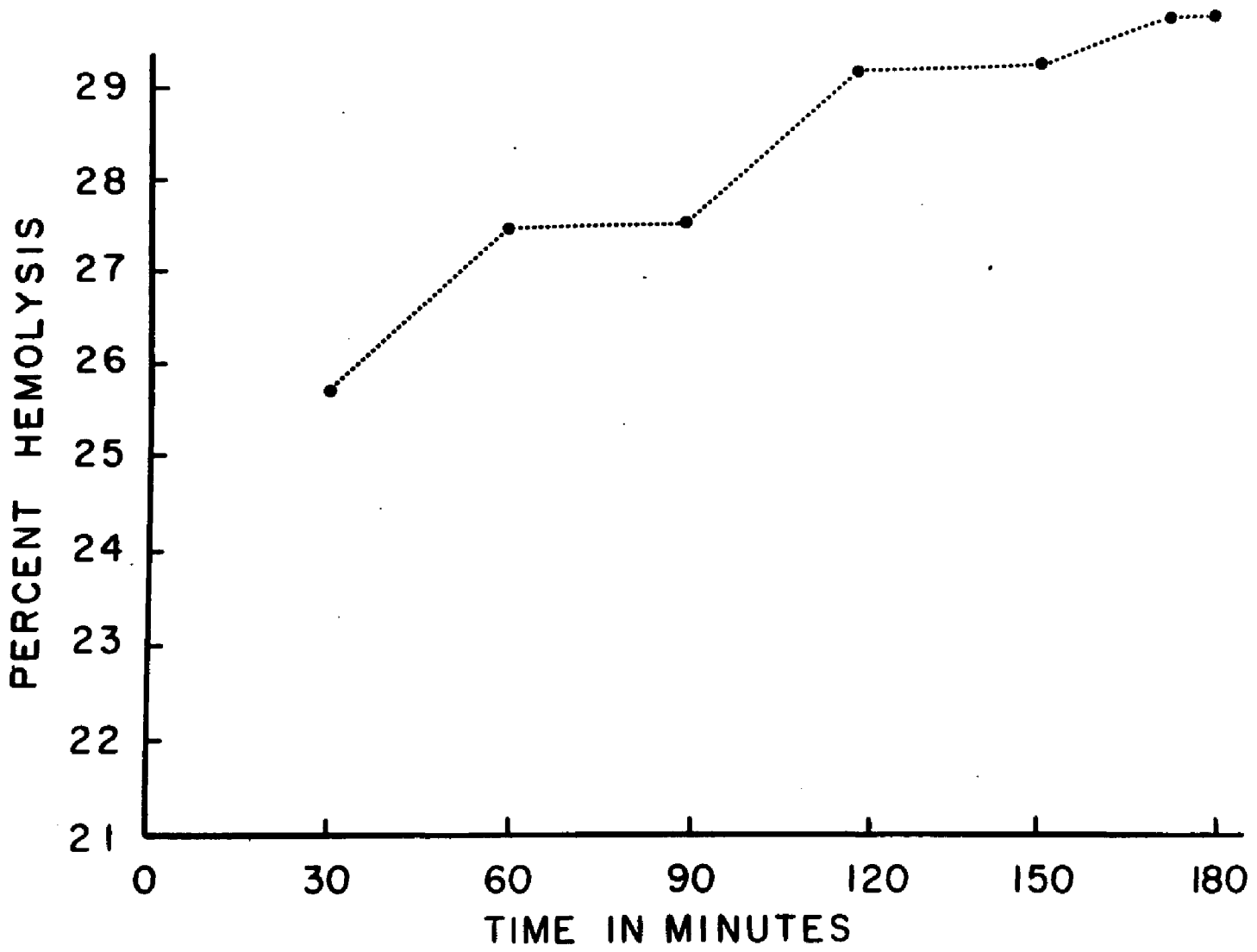
PERCENT HEMOLYSIS
29
28
27
26
25
24
23
22
21
0
30
60
90
120
150
180
TIME IN MINUTES

Figure II.4 -- Hemolytic response of sheep red blood cells to Industrial Silica Flour (ISF) and size fractions extracted from a representative bulk sample of ISF. Specimen as received (ISF), 20um, 15um, 10um particle splits fall about a line that is statistically identical for one estimating equation. The steepest line is defined by data points obtained when 2um and 1um Stoke's diameter particles challenged SRBCs. These extremes are significantly different on a statistical basis (by F-test).

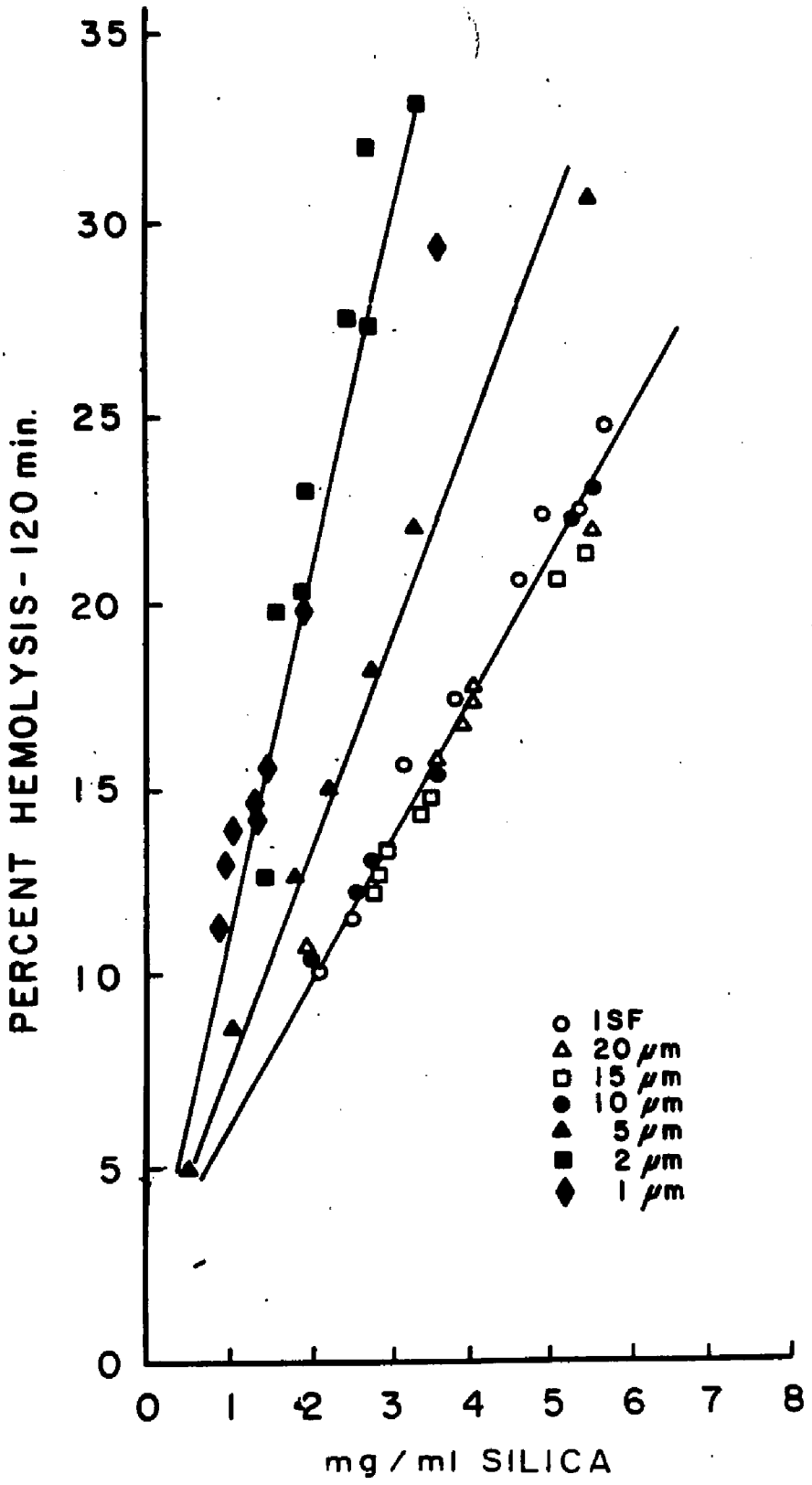
PERCENT HEMOLYSIS - 120 min.
35
30
25
20
15
10
5
0
0
1
2
3
4
5
6
7
8
mg / ml SILICA
ISF
20 μm
15 μm
10 μm
5 μm
2 μm
1 μm

Chapter III

Variability in the Membranolytic Activity of Quartz

INTRODUCTION

The particle size of mineral dust capable of producing pneumoconiosis in man has long been recognized as one of the important factors imparting biological activity. Investigators have traditionally considered particle size in terms of inhalation potential, particle disposition in the lung, and the host's ability to effectively clear the material from the pulmonary tissue. In the earliest experimental studies, particle size was frequently correlated with magnitude of the tissue response elicited by the dust. For the silica polymorphs, reduction in particle size frequently produced more extensive silicotic lesions, a more rapid tissue response, greater systemic effect, and some variation in the location and nature of the lesions. Although it appeared that surface area and particle number were important variables controlling host response, very few subsequent _in vivo_, and virtually no _in vitro_, studies provided strict controls for these variables (Reiser and Last, 1979).

The importance of such oversights have had profound pragmatic effects. Gravimetric-based standards for dust control are average values and may be of limited usefulness in some circumstances, especially where fine dust are generated in the work environment (NIOSH/OSHA, 1980). Dusts of small particle size may be many times more fibrogenic than identical masses of dust made up of larger size particles. Comparative studies of mineral dusts cannot be made on a mass basis; study of biological responses to

mineral dust requires knowledge of its state of aggregation.

In order to determine the range of biological activity of a single mineral, as many of its varietal types should be examined and as many variables as possible should be controlled for in the experimental protocol. If one accepts the hypothesis that the interactions of a mineral dust with the cellular components of an intact host is centered on mineral surface-cell membrane reaction, then particle size and surface properties are crucial variables. The surface properties of quartz were modified by treatment of the quartz specimens with acid, bases, water, and heat. In order to determine the contribution of the surface properties, the particle size must be held constant. Therefore, for the same unit mass of dust challenge, in any experimental system, narrow-size fractions are the most desirable to study. Additionally, the study of varieties of a single mineral provides data which concern the role of trace metals, and of compositional and crystallographic variation.

MATERIALS AND METHODS

Quartz Specimens

Min-U-Sil 15, a commercially available crystalline silica distributed by Pennsylvania Glass and Sand Company, 3 Penn Center, Pittsburgh, PA 15235. PGS Company reports that 95% of the specimen is less than 15um in size. Nine hundred eighty-four particles were sized by direct measure-

ment on light microscopy photographs: 11% possessed greatest dimension between 5 and 20um, 22% between 2 and 4.9um, and 67% at or below 1.9um (see Nolan et al., 1981).

Sigma Amorphous Silica, No. S-5031, Sigma Chemical Company, St. Louis, MO, was obtained as a pulverized, fine, industrial powder. Sigma reports 95% of the particles range between 0.5 and 20um and 80% between 1 and 5um. Sigma Amorphous Silica is a finer-sized quartz than Min-U-Sil 15. Sigma refers to their specimen as "amorphous" although it is crystalline with the quartz structure (see Characterization of Quartz below and Discussion of Davies, 1981).

Five naturally occuring specimens were obtained from Ward's National Science Establishment Inc., Rochester, NY, as both massive anhedral minerals and as large euhedral crystal:

Rock Crystal Quartz, large single crystal, Hot Springs, Arkansas;

Rose Quartz, massive, Antsirabe, Madagascar;

Rose Quartz, massive, Custer, South Dakota;

Amethyst, large single crystals, Rio Grande do Sul, Brazil;

Milky Quartz, massive, Grafton, New Hampshire.

Preparation of Quartz Specimens

Size reduction

The large single crystals were pulverized in the dry state by grinding in a carborundum mortar and pestle until all the particles passed through a 45um wire mesh opening

(USA Standard Testing Sieve No. 325, Fisher Scientific Company).

Size fractionation

Each quartz specimen was size fractionated on the basis of particle settling velocity in water by means of the Andreasen pipette technique (Nolan and Langer, 1983). The particles were suspended by agitation in a cylinder filled with distilled water. Size fractions were withdrawn from the cylinder at depths and times corresponding to Stokes' diameter of 1, 2, 5, 10, 15, and 20um according to a published protocol (Nolan and Langer, 1983). Before use, each size fraction was dried at 110°C for 24 hours.

Characterization of Quartz

X-Ray diffraction

Quartz specimens were examined for homogeneity by polarized light microscopy and continuous-scan x-ray diffraction. The ≤45um bulk specimen and each size fraction were scanned between 5 and 80 degrees 2 theta. Any peak three times greater than background (by visual inspection) was examined for position and relative intensity and then compared with two standard alpha quartz patterns (Frondel, 1962). Twenty-four reflections from 4.225A $(31\bar{4}0)$ match within $\pm$ 0.002 A. For 2 theta above 45°, d-spacings match within $\pm$ 0.001A. All of the specimens were found to be high purity (≥99.5%) alpha quartz as indicated by both analytical techniques.

Size distribution measurements

To determine size distribution, each size fraction of Stokes' diameter from 5 to 20um were photographed by light microscopy. A stage micrometer was photographed to provide calibration. Final enlargements yielding magnifications of 500x-700x were used. Size fractions of Stokes' diameters 1.0 and 2.0um were photographed by transmission electron microscopy at 2000x direct magnification with a photographic enlargement of 2.5 (final enlargement, 5000x). In all cases, the greatest dimension was taken as the measure of particle size. The results are, therefore, skewed toward larger particle size values.

Surface area calculations

For each of the quartz size fractions, the surface area per particle and the particle number per unit mass differ. The quartz particles are irregular in shape and for this analysis, both particle shape and size distribution are approximated. It is assumed that all of the particles are cubic within each size class. Surface area/particle and particle number/mg were calculated for cubes of the following side lengths: 0.5, 1, 2, 5, 10, and 20um (see Table III.1). The particle number per mg was calculated assuming the density of quartz to be 2.65gm/cm^3.

Hemolytic model

The lysis of erythrocytes by quartz is a useful quantitative assay (Nolan et al., 1981). A standard suspension of washed human erythrocytes, at a final concentration of 1.8 x 10^8 cells/ml, was incubated with various concentrations of

quartz at 37°C for 120 minutes. The intact erythrocytes, quartz, and cell stroma were then centrifuged and the absorbance of the supernatant (proportional to the released hemoglobin) was measured at 530nm (Nolan et al., 1981). The absorbances were normalized to 100% release of hemoglobin from osmotically lysed suspensions of erythrocytes.

The hemolytic activity of each quartz specimen as a function of particle size was determined. Each size fraction was suspended in veronal buffered saline and sonicated to form a uniform dispersion. Sonication was particularly important to disperse the aggregated particles with Stokes' diameter of 1 and 2um. The stock suspensions of quartz were diluted to four concentrations in duplicate and challenged with standard suspensions of erythrocytes. After the quartz and erythrocyte suspensions were incubated at 37°C for 120 minutes, the percentage hemolysis (%H) was spectrophotometrically measured. Min-U-Sil 15 was included in each experiment as a control for differences in erythrocytes. The observed linear relationship between (%H) and quartz concentration (mg/ml SiO_2) was measured between 0-40% and quantitatively defined by linear regression analysis. The membranolytic activity is reported as the concentration of quartz required to lyse 50% of the cells (HC50, mg/ml) (Nolan et al., 1981). From the duplicate experiments the %H at each concentration was averaged and shown with their standard deviations. The variance observed in replicate runs is small (less than several percent of the calculated mean value).

EXPERIMENTAL RESULTS

Membrolytic Activity as a Function of Particle Size

Specimens obtained as fine industrial powder

Both the Min-U-Sil 15 and the Sigma Amorphous Silica were obtained as fine industrial powder. The membranolytic activity of the size fractionated Min-U-Sil 15 was determined as a function of Stokes' diameter (see Figure III.1 and Table III.2). The HC50 for the Min-U-Sil 15 ranged from 0.3 $\pm$ 0.0mg/ml for the 1um to 12.2 $\pm$ 1.8mg/ml for the 20um fraction. The HC50 for the Min-U-Sil 15 was determined using three different erythrocyte donors. The HC50s with standard deviation are shown in Table III.2. The membranolytic activity of the Sigma Amorphous Silica specimen, which was obtained as a fine powder, was determined as a function of Stokes' diameter. The HC50 range for the Sigma was 0.29 $\pm$ 0.09mg/ml for the 1um fraction to 7.20 $\pm$ 0.58mg/ml for the 20um fraction (see Figure III.2). The HC50 of each size was determined using several different erythrocyte donors. The HC50s and the standard deviations are shown in Table III.3, along with the particle size distribution.

Different Quartz Varieties Obtained as Massive Anhedral Specimens and Single Crystals

The rock crystal, rose quartz (Madagascar), rose quartz (South Dakota), amethyst (Brazil), and milky quartz (New Hampshire) were pulverized in a dry state to less than

45um. The membranolytic activity was measured before size fractionation and the resulting HC50 values are shown in Table III.4. After fractionation in water, the activity of all the size fractions were markedly reduced. As an example, see activity of specific size fractions of rock crystal quartz and rose quartz (Madagascar) in Tables III.5A and III.5B.

Study of Non-Membranolytic Specimens

To test whether an impurity was binding to the surface of the size fractionated quartz specimen, thereby blocking its active surface sites, aliquots of the 20um rock crystal quartz were refluxed for one hour in aqua regia or 25% potassium hydroxide. Also, a residue aliquot of the size fractionated rock crystal was treated with hydrofluoric acid. Whereas none of these treatments increased the membranolytic activity of the minerals, hydrofluoric acid treatment of the Min-U-Sil 15 control reduced its membranolytic activity markedly (Nolan et al., 1985).

Although the size-fractionated rock crystal and rose quartz were found to have reduced membranolytic activity, the erythrocytes and particles were still able to adhere to each other in the test system. The erythrocytes and quartz form complexes and settle out of suspension, a feature readily observed by eye. As a further test of adherence, erythrocyte suspensions were preincubated with various concentrations of 1um non-membranolytic rock crystal or rose quartz and then challenged with known membranolytically

active Min-U-Sil 15. The hemolytic activity of Min-U-Sil 15 (1.5mg/ml) was inhibited by about 50% (21%H to 11%H) by 300ug/ml of 1um rock crystal or rose quartz. Saturation of the inhibitory effects of 1um rock crystal or rose quartz occurred at approximately the HC50 value of the membranolytically active 1um quartz. Size-fractionated quartz specimens which have reduced membranolytic activity are apparently capable of adhering to the cell surface, and in doing so prevent attachment of other active particles to cells and thereby inhibit lysis. Mineral antagonism has been previously reported, but for asbestos (Harington, Personal Communication).

To determine whether hydrogen bonding of the different quartz specimens varied, the ability of the particles with the same Stokes' diameter to bind 2-poly(vinylpyridine-N-oxide) was determined. The 20um size fraction of Min-U-Sil 15, Sigma Amorphous Silica, rock crystal, and rose quartz were compared (see Figure III.3). The order of binding of 2-PVPNO was: Sigma Amorphous Silica > Min-U-Sil 15 > rose quartz > rock crystal quartz. This order of binding is consistent with the order of hemolytic activity for the 20um size fraction of these specimens (Tables III.5 and III.7).

The loss of membranolytic activity on hydration must be related to the quartz surface chemistry and structure. The effect of heating on the membranolytic activity of the size-fractionated rock crystal and rose quartz was studied. The 1um size fractions of rock crystal and Sigma Amorphous Silica were heated to approximately 600^{o}C for five hours.

The heating increased the membranolytic activity of the 1um rock crystal from a negligible level to that of 1um Sigma Amorphous Silica. Heating increased the membranolytic activity of the Sigma Amorphous Silica only slightly (Figure III.4). Each of the specimens which had been size-reduced from large single crystals and fractionated in water by sedimentation lost membranolytic activity on hydration. Each of these size specimens were heated to 400-500°C for six hours, and the membranolytic activity was then restored and found comparable with the size-fractionated Min-U-Sil 15 and Sigma Amorphous Silica (see Tables III.6 and III.7) (Nolan et al., 1985). Although the surface properties responsible for the membranolytic activity were restored by heating, the precise nature of the induced change is unknown.

Membranolytic Activity of Surface Modified Quartz

Potassium Hydroxide Modification -- Seven and one-half grams of Min-U-Sil 15 was added to 100ml of 10% potassium hydroxide solution (w/v), and the suspension was stirred at room temperature for two hours. After two hours, the suspension was centrifuged and repeatedly washed with distilled water. The potassium hydroxide-modified quartz was then dried at 110°C for 12 hours. After drying, the specimen was divided into equal samples, one of which was heated to 400-500°C for five to six hours. The membranolytic activity of each of the two KOH-modified quartz specimens and the control (a size-matched Min-U-Sil 15) was

determined (see Figure III.5 and Table III.8).

Hydrofluoric Acid Modification -- Fifteen grams of Min-U-Sil 15 were added to 50ml of 20% hydrofluoric acid (v/v) for three minutes, then diluted with distilled water to 100ml, centrifuged and washed repeatedly with distilled water. The HF-modified specimen was then divided in half and one-half was heated to 400-600^{o}C for six hours. The membranolytic activity of the HF-modified specimens and the size-matched Min-U-Sil 15 were then determined (see Figure III.6 and Table III.8).

Dimethylchlorosilane Modification -- To investigate the possible effects of hydrophobicity on hemolysis, 25ml of dimethylchlorosilane was added to 10 grams of Min-U-Sil 15 and stirred in an open flask overnight. The dimethylchlorosilane evaporated by morning, and the dry quartz powder was washed with distilled water and dried at 110^{o}C for 12 hours. The membranolytic activity of the dimethylchlorosilane-modified quartz was determined and compared to the particle size matched control (see Figure III.7 and Table III.3).

Binding of 2-poly(vinylpyridine-N-oxide) to Surface Modified Quartz -- Various concentrations of quartz were added to 5ml of 50ug/ml 2-PVPNO solution. The quartz and 2-PVPNO were allowed to stand at room temperature for 60 minutes. The suspensions were vortexed occasionally to resuspend the quartz. After an hour, the 2-PVPNO bound to the quartz surface was separated from the free 2-PVPNO by centrifugation. The concentration of 2-PVPNO in the clear supernatant was determined by the absorbance of the polymer

at 260nm. This procedure allows the amount of 2-PVPNO bound to a given concentration of quartz to be determined (see Figures III.8, III.9, III.10 and Table III.9).

DISCUSSION AND CONCLUSIONS

The ability of quartz to alter the permeability of the erythrocyte membrane to hemoglobin, i.e., induce erythrocyte lysis, depends largely on two mineral variables: particle size (and therefore surface area) and surface properties. After all, it is the quartz surface which interacts with the cell membrane.

The amount of surface area per unit mass of any quartz specimen will vary with its particle size distribution. In order to define the concentration of quartz required to lyse 50% of the cells in suspension containing a given number of erythrocytes, the particle size distribution must be specified. For example, the two fine industrial powders Min-U-Sil 15 and Sigma Amorphous Silica can be fractionated on the basis of their Stokes' diameter into several narrow size fractions. Size fractions of 1, 2, 5, 10, 15 and 20um Stokes' diameter were collected, and the concentration of quartz required to lyse 50% of the cells -- the HC50 (mg/ml SiO_2) -- was determined for each of those size fractions. As the Stokes' diameter decreased from 20 to 1um, the membranolytic activity of Min-U-Sil 15 and Sigma Amorphous Silica increased by a factor of 40 and 25, respectfully.

The Stokes' diameter represents idealized particles.

For calculating the Stokes' settling velocities, the assumption is made that the quartz particles are spherical. They are not spherical, however, and the actual size distribution within each Stokes' fraction must therefore be measured directly. Each Stokes' diameter contained a distribution of particle sizes. It is important to note that these size-fractionated materials have significantly narrowed size distributions as compared to the initial bulk powder, i.e., the measured size distributions of the 1 and 2um fractions differed significantly from the 5, 10, 15, and 20um fractions. The HC50s of these fractions show differences and similarities that reflect size distribution. For example, 10, 15, and 20um Stokes' diameters have almost the same size distribution and therefore the same HC50s. Experimentalists may acquire narrow size-range minerals through sedimentation fractionation, but particle size determinations requires direct measurement.

The ratio of the surface area of a gram of quartz composed of 20um as compared to a gram of 0.5um particles is about 1:45 (see TableIII.1). Considering the approximations, the difference in HC50s for the particle size fractionation of Min-U-Sil 15 is about 40-fold, and the calculated change in surface area and the HC50 are therefore in reasonably good agreement (Nolan et al., 1985).

The five specimens of quartz were obtained as euhedral crystals and massive anhedral specimens weighing approximately 400 grams each. They were selected for study because they possessed the following properties: each was a high-

purity quartz; the specimens could be pulverized by the same method of size reduction; the different quartz varieties were acceptable for comparative studies. Milky quartz, amethyst, rock crystal, and rose quartz (the last from two different geological locations) represent the different quartz varieties. These were identified by the color of the bulk specimens, although once reduced to a fine powder, the color differences were no longer discernible (Nolan and Langer, 1983). Large specimens are necessary for long-term study in multiple model systems. Varieties of the same mineral are important for ascertainment of secondary properties, e.g., role of trace metal impurities such as aluminum and iron.

The five specimens were pulverized by hand in a carborundum mortar and pestle to a particle size of less than 45um. The average HC50 of the five specimens was 6.41$\pm$1.20mg/ml, while the average of the Min-U-Sil 15 control was 2.97$\pm$0.10mg/ml. The <45um milky quartz was found to be the most hemolytic. This specimen was observed to be the most brittle and the easiest to pulverize during grinding (Table III.4). These specimens were then size-fractionated in water by sedimentation, and the membranolytic activity of the 1, 2, 5, 10, 15, and 20um diameter fractions were determined separately. The membranolytic activity of each size fraction of many specimens was markedly reduced. This reduction occurred in those specimens that had been size-reduced in a carborundum mortar and pestle and not in specimens that had been obtained

commercially as fine powders (Table III.5) (Nolan et al., 1985). Manipulation of mineral dusts in the laboratory may alter their membranolytic activity.

Although the powders derived from the massive quartz specimens lost their membranolytic activity upon hydration, they were still able to adhere to the erythrocyte membrane. The hydrogen bonding of 2-poly(vinylpyridine-N-oxide) to the quartz surface was determined quantitatively on two quartz samples obtained as fine industrial powders and two size-reduced from massive specimens. For each specimen, the 20um Stokes' diameter fraction obtained by water fractionation was studied. With surface area held constant, the non-membranolytic specimens were unable to hydrogen bond as much 2-poly(vinylpyridine-N-oxide) as compared to the two membranolytic quartz specimens. Increased hydrogen bonding ability therefore appeared to correlate with the increased membranolytic activity.

But further study of surface modified quartz has shown, however, that hydrogen bonding of 2-poly(vinylpyridine-N-oxide) need not always correlate with the membranolytic activity (see Table III.9 and Nolan et al., 1985). The specimens which lost membranolytic activity on hydration were found to recover that ability after heating. The membranolytic activities of these heat-reactivated specimens were comparable to other quartz specimens of similar size distribution. Heating had very little effect on the fine industrial powders which lost no activity on hydration (see Figure III.4). The HC50 ratio of the 20 to 1um Stokes'

diameter for the five specimens average 30 $\pm$ 15.

Chemically induced modification of the surface properties of quartz have a significant effect on the mineral's membranolytic activity. The surface properties of a standard quartz specimen were modified by treatment, singularly, with potassium hydroxide, hydrofluoric acid, and dimethylchlorosilane. These surface modified specimens have similar particle size distributions and by continuous scan x-ray diffraction are indistinguishable from each other and a high purity alpha-quartz control. Yet the membranolytic activity of several of the specimens, as measured by their hemolytic index, differed markedly.

Potassium hydroxide-modified quartz increased in membranolytic activity by approximately 20% while quartz modified with hydrofluoric acid was markedly less active (a reduction of almost 450%). The activity of the hydrofluoric acid-modified quartz was restored to a value within 25% of its unmodified control by heating to 400-600^{o}C for six hours. Recrystallization of a surface-disrupted layer is thought to be the mechanism of reactivation. Quartz rendered hydrophobic by reaction with dimethylchlorosilane was over 600% less active than its untreated control. The variation in the membranolytic activity of the different quartz specimens could not be correlated with the ability of the different specimens to hydrogen bond 2-poly(vinylpyridine-N-oxide). Some data suggest that an increased hydrogen bonding ability may actually reduce activity (see Table III.9). The size distribution of the quartz alone is

not sufficient information to predict the membranolytic activity of an untested dust; characteristic(s) of the quartz surface properties must be specified.

Variation in surface properties created by hydration, the method of size reduction and treatment with hydrofluoric acid caused the largest differences in membranolytic activity. The quartz specimens which lost activity on hydration or hydrofluoric acid treatment, as well as those that were later heat-reactivated, were indistinguishable by the standard x-ray crystallographic and optical methods. The particle size difference was the second most important variable in determining the membranolytic activity. The differences in activity attributed to quartz variety emerged as the least important factor.

Table III.1 -- Relationship between particle size and surface area with constant shape

Stoke's Diameter	No. of particles/mg	Surface Area (um^2)/particle	Surface Area (um^2/mg)
0.50um	$\sim 3x10^9$	1.5	$45x10^8$
1.00um	$\sim 4x10^8$	6.0	$24x10^8$
2.00um	$\sim 4x10^7$	24.0	$9.6x10^8$
5.00um	$\sim 3x10^6$	150.0	$4.5x10^8$
10.00um	$\sim 3x10^5$	600.0	$1.8x10^8$
20.00um	$\sim 4x10^4$	2400.0	$1.0x10^8$

Table III.2 -- Particle size distribution and membranolytic activity of size fractionated Min-U-Sil 15

Stoke's Diameter	No. of Particles Sized	<1.0um	1.0-5.0um	5.1-10.0um	10.1-15.0um	>15.0um	HC50 mg/ml
1um	605	81.0%	19.0%	0.0%	0.0%	0.0%	0.3±0.0
2um	448	13.2%	73.9%	12.9%	0.0%	0.0%	1.8±0.2
5um	555	2.7%	69.0%	22.3%	5.2%	0.8%	7.3±0.6
10um	700	0.0%	27.0%	43.3%	21.9%	7.8%	11.7±1.8
15um	751	0.0%	12.3%	31.7%	37.4%	18.6%	11.9±2.0
20um	680	0.0%	22.9%	34.7%	26.8%	15.6%	12.2±1.8
Unfractionated Min-U-Sil 15							2.8±0.3

Table III.3 -- Particle size distribution and membranolytic activity of size fractionated sigma amorphous silica

Stoke's Diameter (um)	No. of Particles Sized	<1.0um	1.1-5.0um	5.1-10.0um	10.1-15.0um	>15.0um	HC50 mg/ml
1um	586	93.2%	6.8%	0.0%	0.0%	0.0%	0.29±0.09
2um	417	3.6%	92.6%	3.8%	0.0%	0.0%	3.14±0.13
5um	598	0.0%	62.9%	36.3%	0.8%	0.0%	5.85±0.35
10um	619	0.0%	70.3%	29.7%	0.0%	0.0%	6.74±0.09
15um	683	0.0%	61.2%	38.2%	0.6%	0.0%	6.67±0.01
20um	629	0.0%	68.8%	30.9%	0.3%	0.0%	7.20±0.58
Unfractionated Min-U-Sil 15							2.86±0.23

Table III.4 -- HC50s of the unfractionated <45um quartz specimens

	HC50 mg/ml	Unfractionated Min-U-Sil 15 HC50, mg/ml
Rock Crystals, Hot Springs, Arkansas	6.44	2.86
Rose Quartz, Antsirabie, Madagascar	5.68	2.85
Rose Quartz, Custer, South Dakota	7.58	3.06
Amethyst, Rio Grande do Sul, Brazil	7.58	3.06
Milky Quartz, Grafton, New Hampshire	4.81	3.00

Table III.5 -- Membranolytic activity of the water fractionated quartz specimens

Stokes' Diameter	A. Rock Crystal Hot Springs, AK Quartz mg/ml	%H	B. Rose Quartz Antsirabe, Madag. Quartz mg/ml	%H
1.0um	0.0625	2.1±0.1		1.0±0.0
	0.1250	2.9±0.1		0.9±0.0
	0.1875	3.9±0.0		0.9±0.0
	0.2500	1.8±0.0		0.8±0.0
2.0um	0.175	2.3±0.1		1.0±0.0
	0.375	2.4±0.2		0.9±0.1
	0.525	2.1±0.0		0.9±0.1
	0.700	2.7±0.3		0.9±0.1
5um	0.625	2.2±0.0		1.2±0.0
	1.250	2.5±0.0		1.3±0.0
	1.875	2.4±0.0		1.3±0.0
10um	0.875	2.4±0.0		1.2±0.0
	1.750	2.6±0.1		1.4±0.2
	2.625	3.0±0.1		1.5±0.1
	3.50	3.4±0.0		1.5±0.0

Controls Unfractionated Min-U-Sil 15

A. mg/ml	%H
0.375	7.4
0.750	14.8
1.125	21.6
1.500	27.4

B. mg/ml	%H
0.375	6.1
0.750	13.1
1.125	19.4
1.50	25.0

Table III.5 -- Membranolytic activity of the water fractionated quartz specimens (cont)

Stokes' Diameter	A. Rock Crystal Hot Springs, AK Quartz mg/ml	%H	B. Rose Quartz Antsirabe, Madag. Quartz mg/ml	%H	Controls Unfractionated Min-U-Sil 15
15um	0.750	2.7±0.3	0.875	1.3±0.0	
	1.500	3.0±0.2	1.750	1.4±0.0	
	2.250	3.4±0.1	2.625	1.6±0.0	
	3.000	3.4±0.0	3.500	1.8±0.01	
20um	0.750	2.4±0.1	0.875	1.3±0.1	
	1.500	3.1±0.1	1.750	1.5±0.1	
	2.250	3.9±0.2	2.625	1.7±0.0	
	3.000	4.7±0.1	3.50	1.8±0.1	

Table III.6 -- Size distribution of quartz specimens size-reduced from large single crystals and massive specimens

Rock Crystal Quartz, Arkansas

Stoke's Diameter	No. of Particles Sized	<1.0um	1.0-5.0um	5.1-10.0um	10.1-15.0um	>15.0um
1um	667	66.1%	33.9%	0.0%	0.0%	0.0%
2um	246	4.9%	71.5%	23.6%	0.0%	0.0%
5um	659	4.6%	53.0%	34.4%	6.7%	1.3%
10um	547	5.3%	31.3%	39.5%	17.0%	6.9%
15um	586	2.5%	31.1%	45.9%	12.8%	7.7%
20um	602	0.0%	26.1%	38.4%	18.9%	18.6%

Rose Quartz, Madagascar

Stoke's Diameter	No. of Particles Sized	<1.0um	1.0-5.0um	5.1-10.0um	10.1-15.0um	>15.0um
1um	479	78.7%	21.3%	0.0%	0.0%	0.0%
2um	211	2.4%	73.0%	24.6%	0.0%	0.0%
5um	652	5.2%	42.5%	31.3%	18.2%	2.8%
10um	845	5.7%	23.3%	47.2%	14.9%	8.9%
15um	575	0.4%	22.6%	41.9%	18.4%	16.7%
20um	422	0.0%	28.4%	38.9%	18.5%	14.2%

Table III.6 -- Size distribution of quartz specimens size-reduced from large single crystals and massive specimens (cont)

Rose Quartz, South Dakota

Stoke's Diameter	No. of Particles Sized	<1.0um	1.0-5.0um	5.1-10.0um	10.1-15.0um	>15.0um
1um	805	85.7%	13.3%	1.0%	0.0%	0.0%
2um	346	34.0%	52.6%	28.7%	0.0%	0.0%
5um	507	0.0%	48.5%	42.0%	6.7%	2.8%
10um	506	0.0%	36.4%	35.9%	13.1%	14.6%
15um	226	0.0%	33.5%	31.2%	16.2%	19.2%
20um	494	0.0%	29.8%	30.0%	18.8%	21.3%

Amethyst, Rio Grande do Sul, Brazil

Stoke's Diameter	No. of Particles Sized	<1.0um	1.0-5.0um	5.1-10.0um	10.1-15.0um	>15.0um
1um	193	86.8%	13.2%	0.0%	0.0%	0.0%
2um	209	34.0%	37.3%	28.7%	0.0%	0.0%
5um	601	0.0%	35.8%	55.7%	7.7%	0.8%
10um	497	0.0%	47.7%	26.3%	18.3%	6.7%
15um	673	0.0%	73.4%	21.4%	2.8%	2.4%
20um	633	0.0%	41.6%	24.8%	17.8%	15.8%

Table III.6 -- Size distribution of quartz specimens size-reduced from large single crystals and massive specimens (cont)

Milky Quartz, New Hampshire

Stoke's Diameter	No. of Particles Sized	<1.0um	1.0-5.0um	5.1-10.0um	10.1-15.0um	>15.0um
1um	1009	87.5%	12.2%	0.3%	0.0%	0.0%
2um	306	32.7%	42.2%	25.2%	0.0%	0.0%
5um	501	0.0%	27.3%	52.9%	16.6%	3.2%
10um	736	0.0%	42.0%	27.0%	16.4%	14.5%
15um	578	0.0%	30.0%	56.6%	10.9%	2.5%
20um	745	0.0%	33.6%	39.9%	14.4%	12.2%

Table III.7 -- Membranolytic activity after heating of the quartz specimens size-reduced from large crystallites

Stoke's Diameter	Rock Crystal Quartz HC50 (mg/ml)	Rose Quartz Madagascar HC50 (mg/ml)	Rose Quartz South Dakota HC50 (mg/ml)	Amethyst Brazil HC50 (mg/ml)	Milky Quartz Grafton, NH HC50 (mg/ml)
1um	0.61	1.26	0.34	1.22	1.06
2um	3.21	3.72	2.17	3.25	6.28
5um	8.42	6.74	7.04	8.57	7.51
10um	15.65	12.12	11.28	11.92	15.11
15um	17.04	17.10	14.77	15.29	17.19
20um	19.40	38.86	18.31	17.84	21.82
Unfractionated Min-U-Sil 15	3.86	2.91	3.48	2.85	2.82

Table III.8 -- Size distribution of surface-modified Min-U-Sil 15

Modification	No. of Particles Sized	1-5.0um	5.1-10um	10.1-15.0um	>15.0um
Unmodified	684	57.0	22.4	12.6	8.0
KOH	1061	51.5	28.5	15.3	3.7
KOH & Heat	1347	56.9	27.0	14.0	2.1
HF	1092	56.1	23.5	14.9	5.5
HF & Heat	772	52.5	19.8	13.3	14.4
$(CH_3)_2SiCl_2$	1034	49.5	31.6	14.1	4.8

Table III.9 -- Variation in the amount of poly(2-vinylpyridine-N-oxide) which bound to 50mg/ml of each of the surface modified Min-U-Sil 15's

	ug/ml of 2-PVPNO bound to 50mg/ml Quartz	HC50, mg/ml
Unmodified Min-U-Sil 15	70.2±0.2	2.72
KOH	44.9±0.1	2.13
KOH & Heat	37.3±0.1	2.58
HF	62.0±0.5	12.28
HF & Heat	40.0±0.4	2.98
$(CH_3)_2SiCl_2$	19.1±0.3	21.74

Figure III.1 -- Membranolytic activity of the size fractionated Min-U-Sil 15.

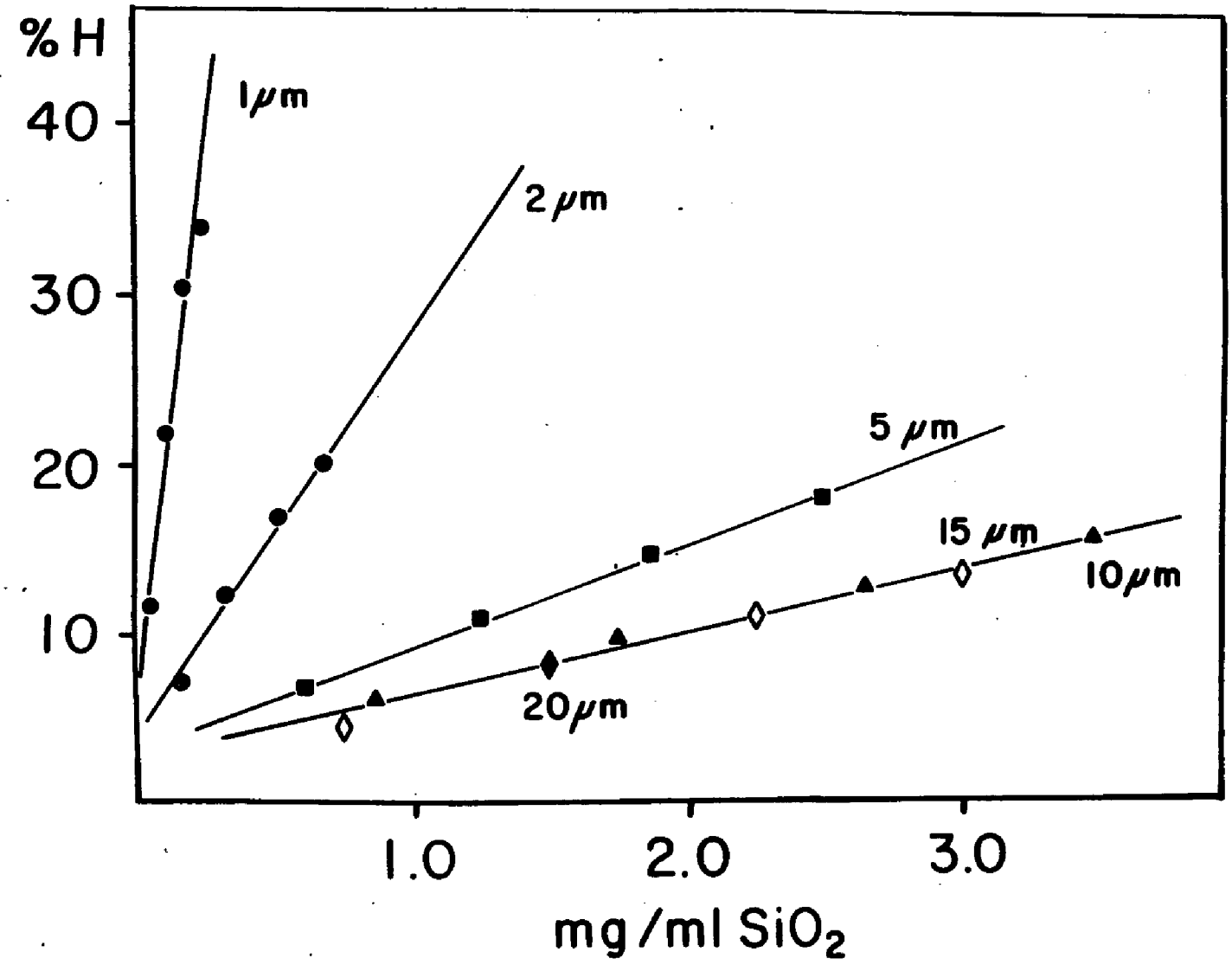
%H
40
30
20
10
1μm
2μm
5μm
15μm
10μm
20μm
1.0
2.0
3.0
mg/ml SiO2

Figure III.2 -- Membranolytic activity of size fractionated sigma "amorphous" silica as a function of Stokes' diameter.

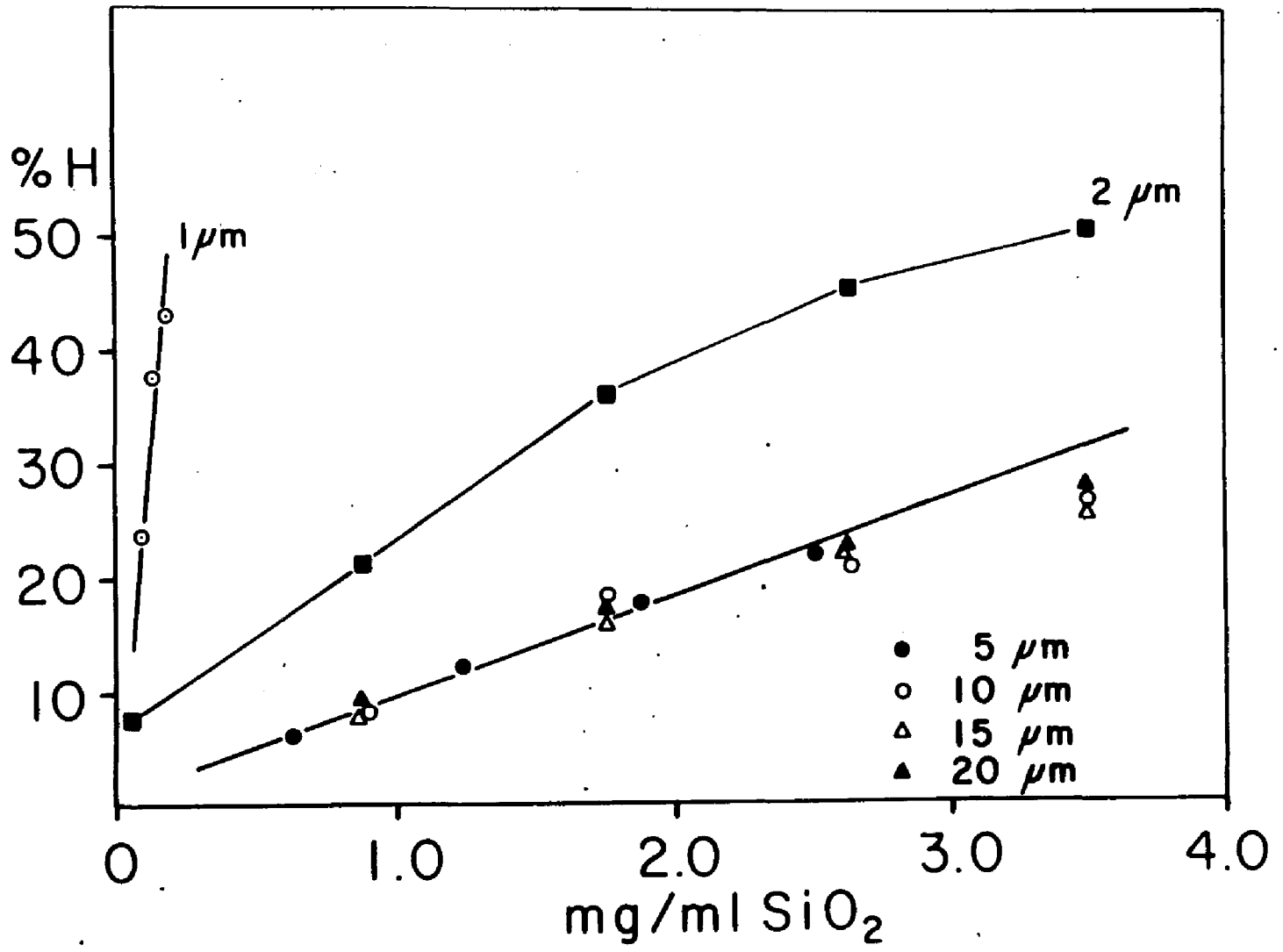
% H
50
40
30
20
10
1 μm
2 μm
5 μm
10 μm
15 μm
20 μm
0
1.0
2.0
3.0
4.0
mg/ml SiO2

Figure III.3 -- Comparison of the hydrogen bonding ability of four size-matched quartz specimens.

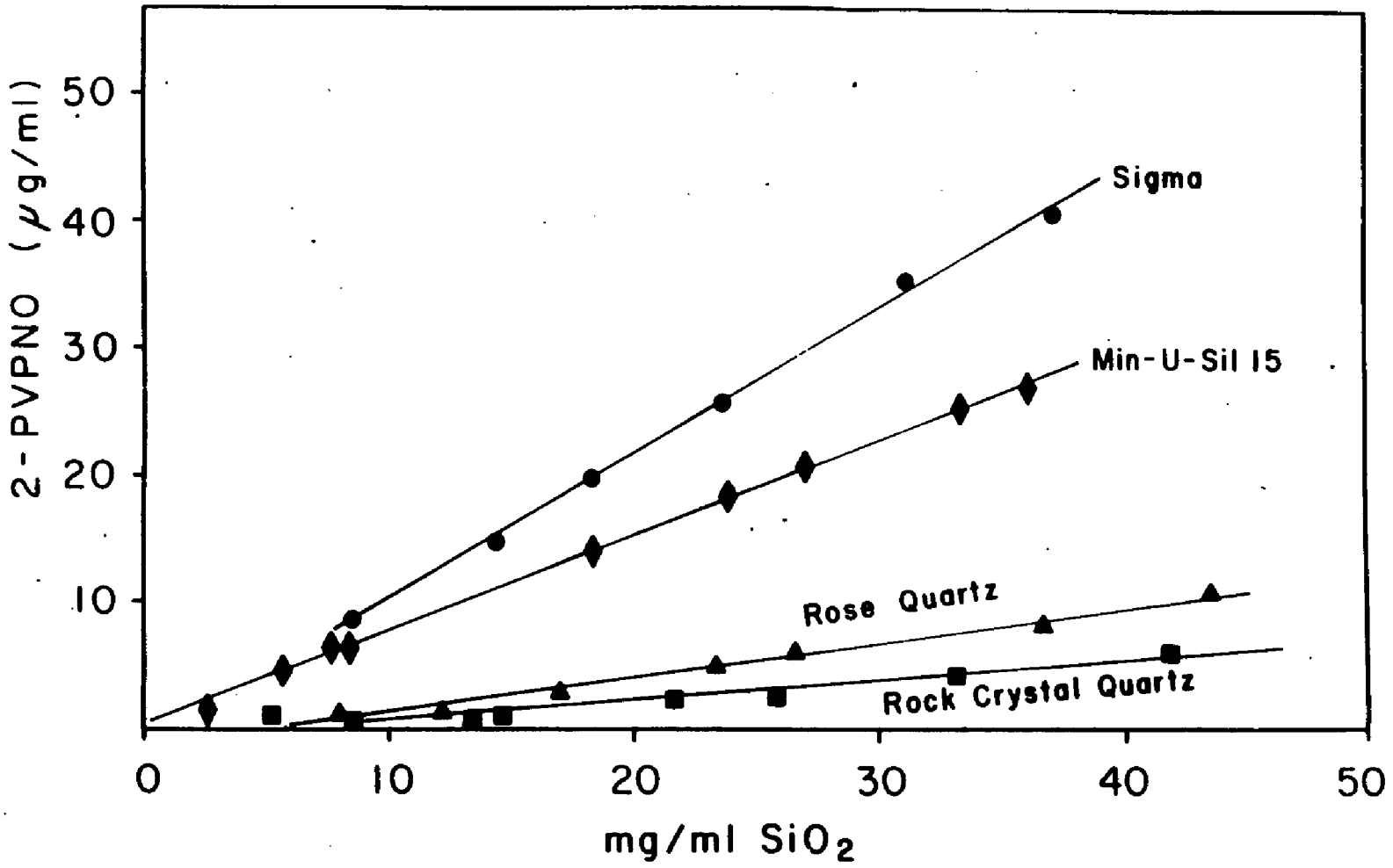
2-PVPNO (μg/ml)
50
40
30
20
10
0
10
20
30
40
50
mg/ml SiO_2
Sigma
Min-U-Sil 15
Rose Quartz
Rock Crystal Quartz

Figure III.4 -- Effects of heating on the membranolytic activity of two size-matched quartz specimens.

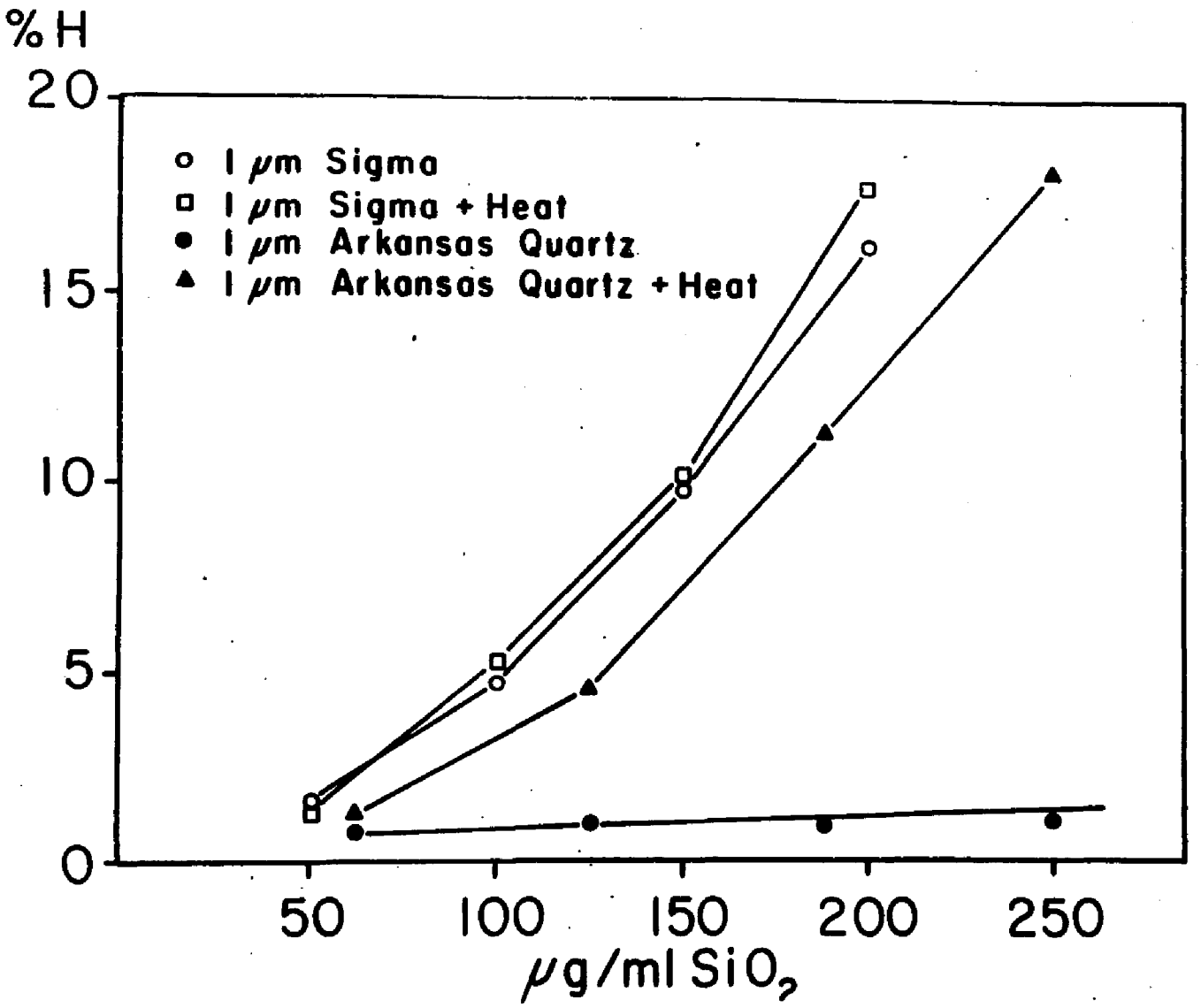
%H
20
15
10
5
0
1 μm Sigma
1 μm Sigma + Heat
1 μm Arkansas Quartz
1 μm Arkansas Quartz + Heat
50
100
150
200
250
μg/ml SiO2

Figure III.5 -- Membranolytic activity of KOH-modified quartz.

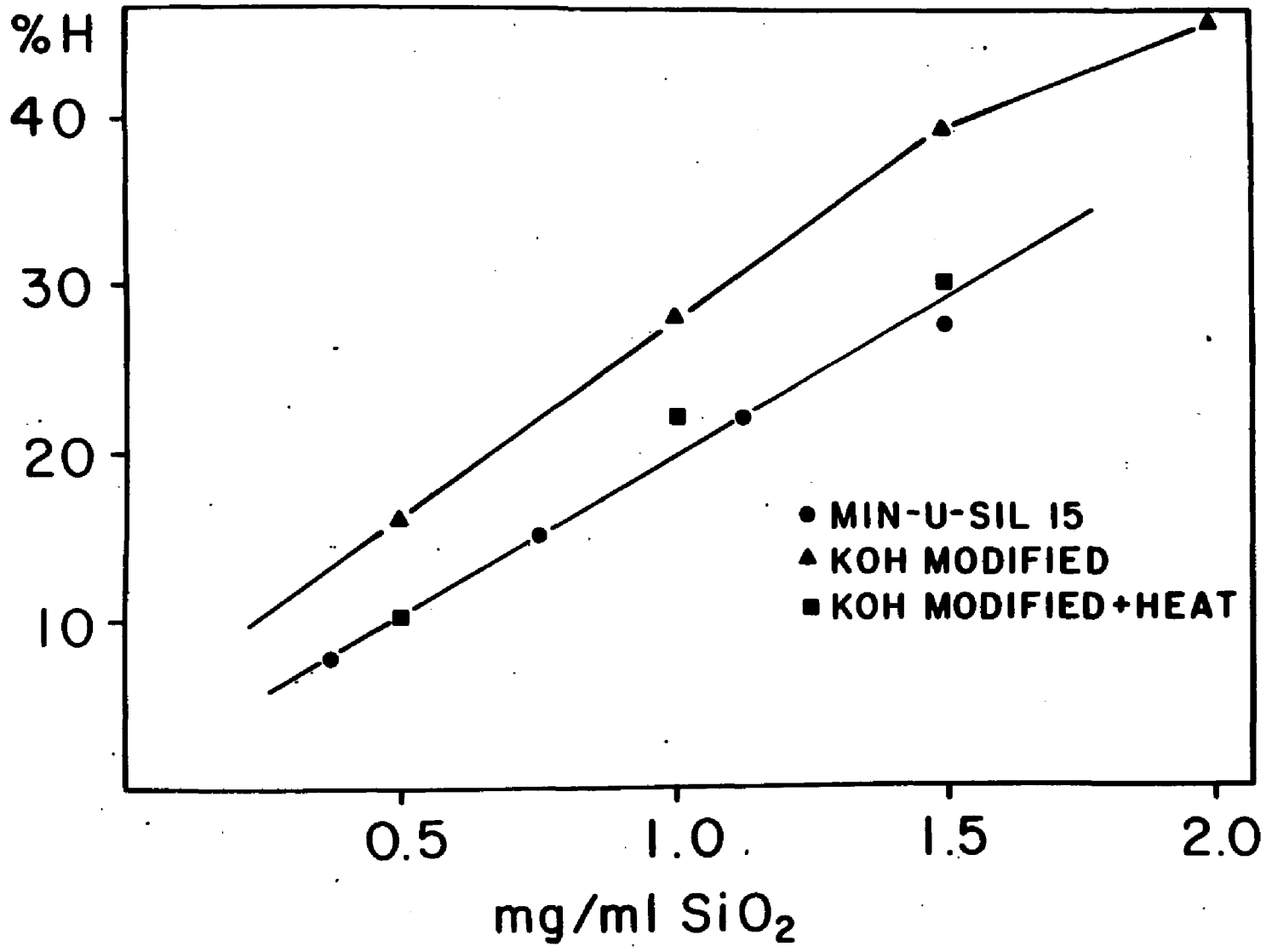
%H
40
30
20
10
0.5
1.0
1.5
2.0
mg/ml SiO_2
● MIN-U-SIL 15
▲ KOH MODIFIED
■ KOH MODIFIED+HEAT

Figure III.6 -- Membranolytic activity of HF-modified quartz.

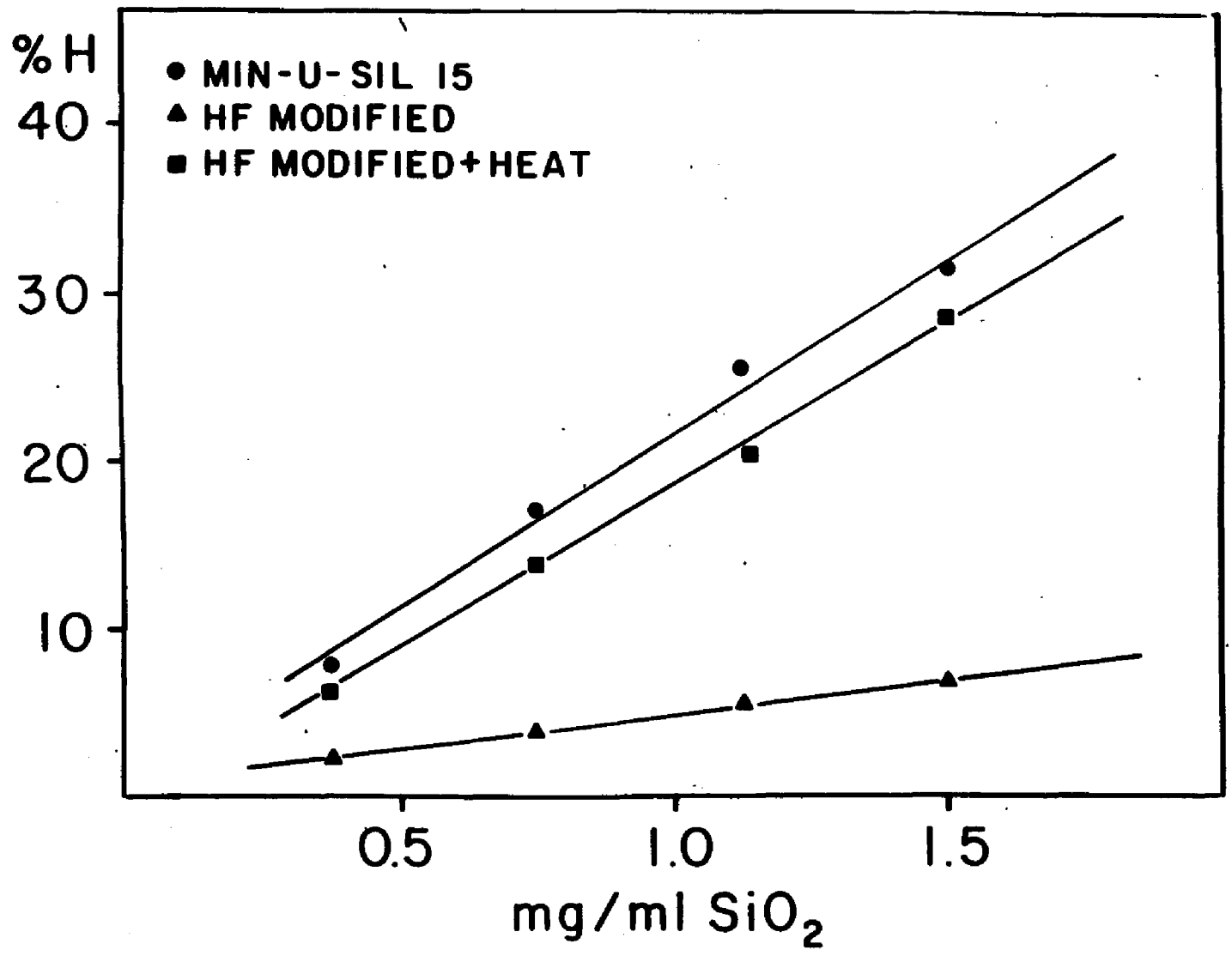
%H
40
30
20
10
● MIN-U-SIL 15
▲ HF MODIFIED
■ HF MODIFIED+HEAT
0.5
1.0
1.5
mg/ml SiO_2

Figure III.7 -- Membranolytic activity of dimethylchlorosilane-modified quartz.

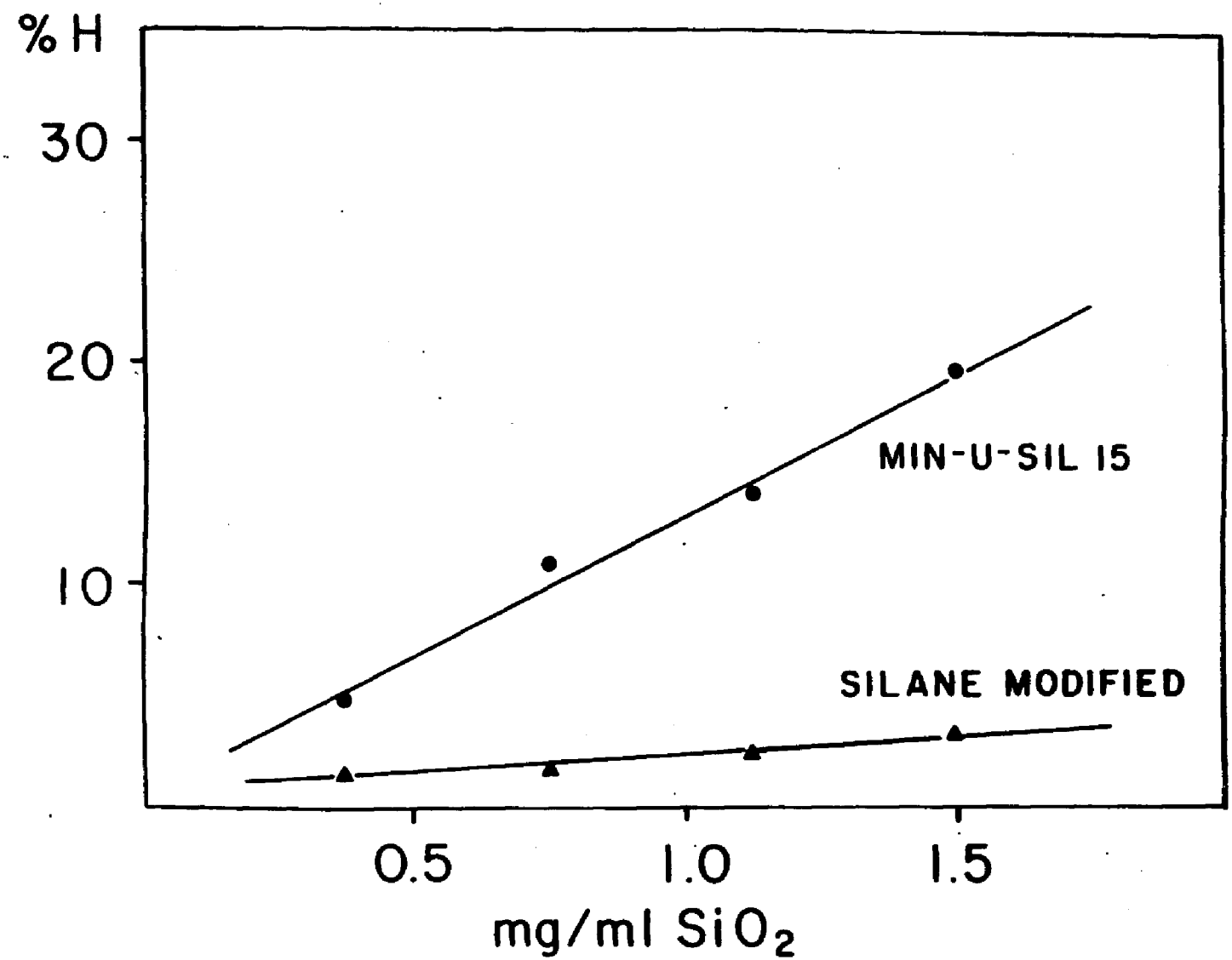
%H
30
20
10
MIN-U-SIL 15
SILANE MODIFIED
0.5
1.0
1.5
mg/ml SiO_2

Figure III.8 -- Binding of 2-PVPNO to KOH-modified quartz and KOH modified quartz which was heated.

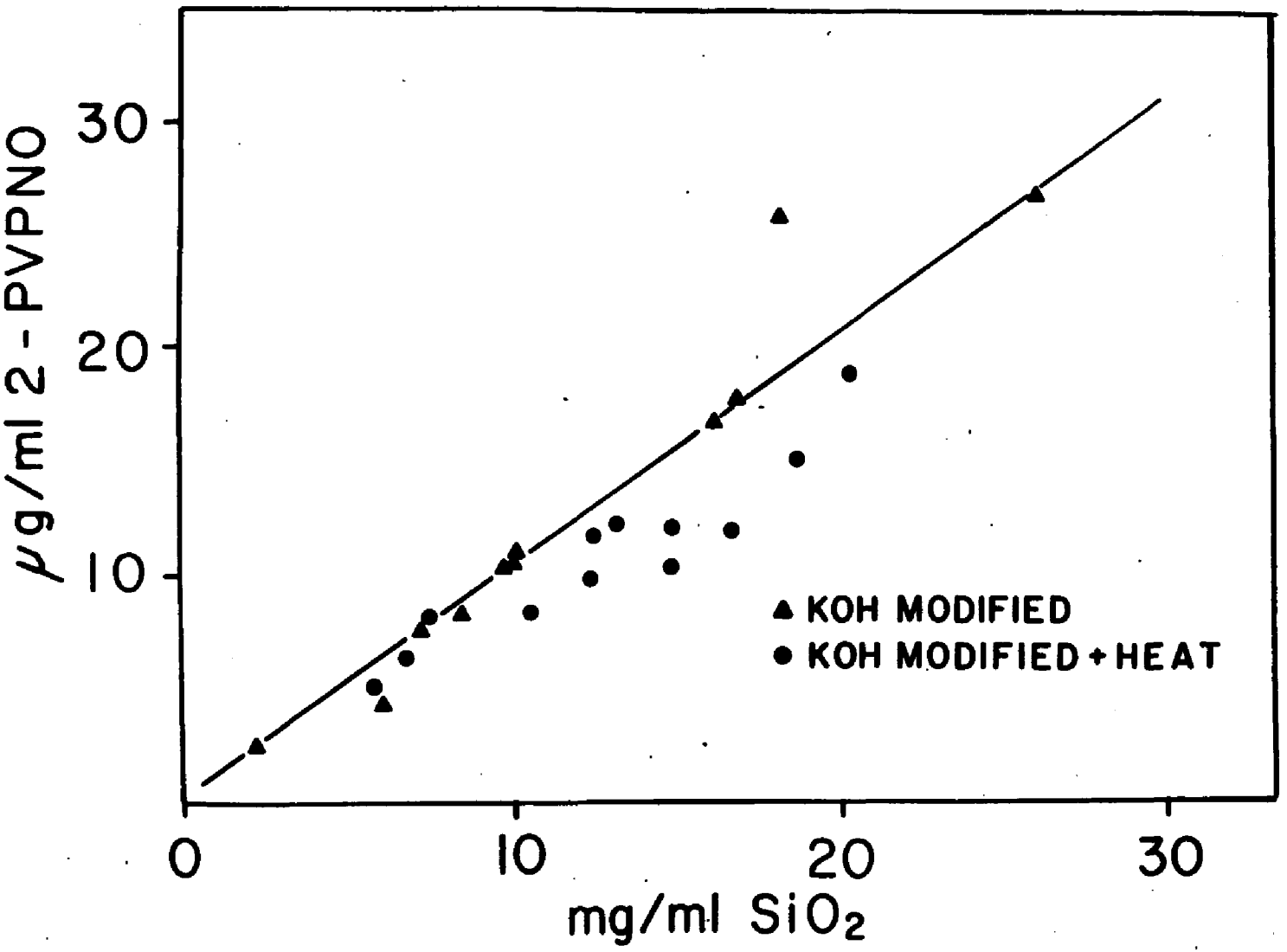
μg/ml 2-PVPNO
30
20
10
0
10
20
30
mg/ml SiO2
▲ KOH MODIFIED
● KOH MODIFIED + HEAT

Figure III.9 -- Binding of 2-PVPNO to HF-modified quartz and HF modified quartz which was heated.

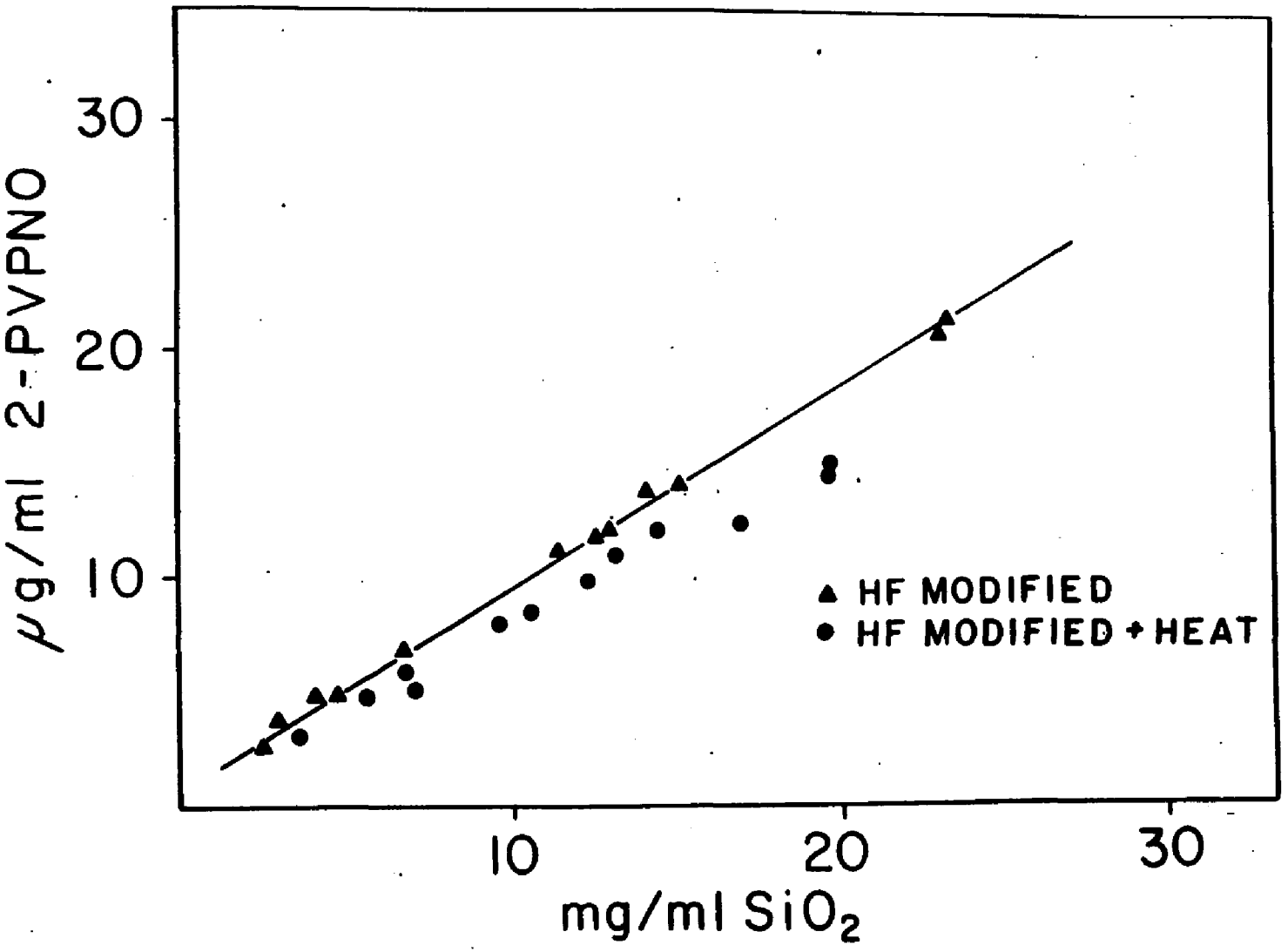
30
20
10
μg/ml 2-PVPNO
10
20
30
mg/ml SiO2
▲ HF MODIFIED
● HF MODIFIED + HEAT

Figure III.10 -- Binding of 2-PVPNO to dimethylchlorosilane-modified quartz.

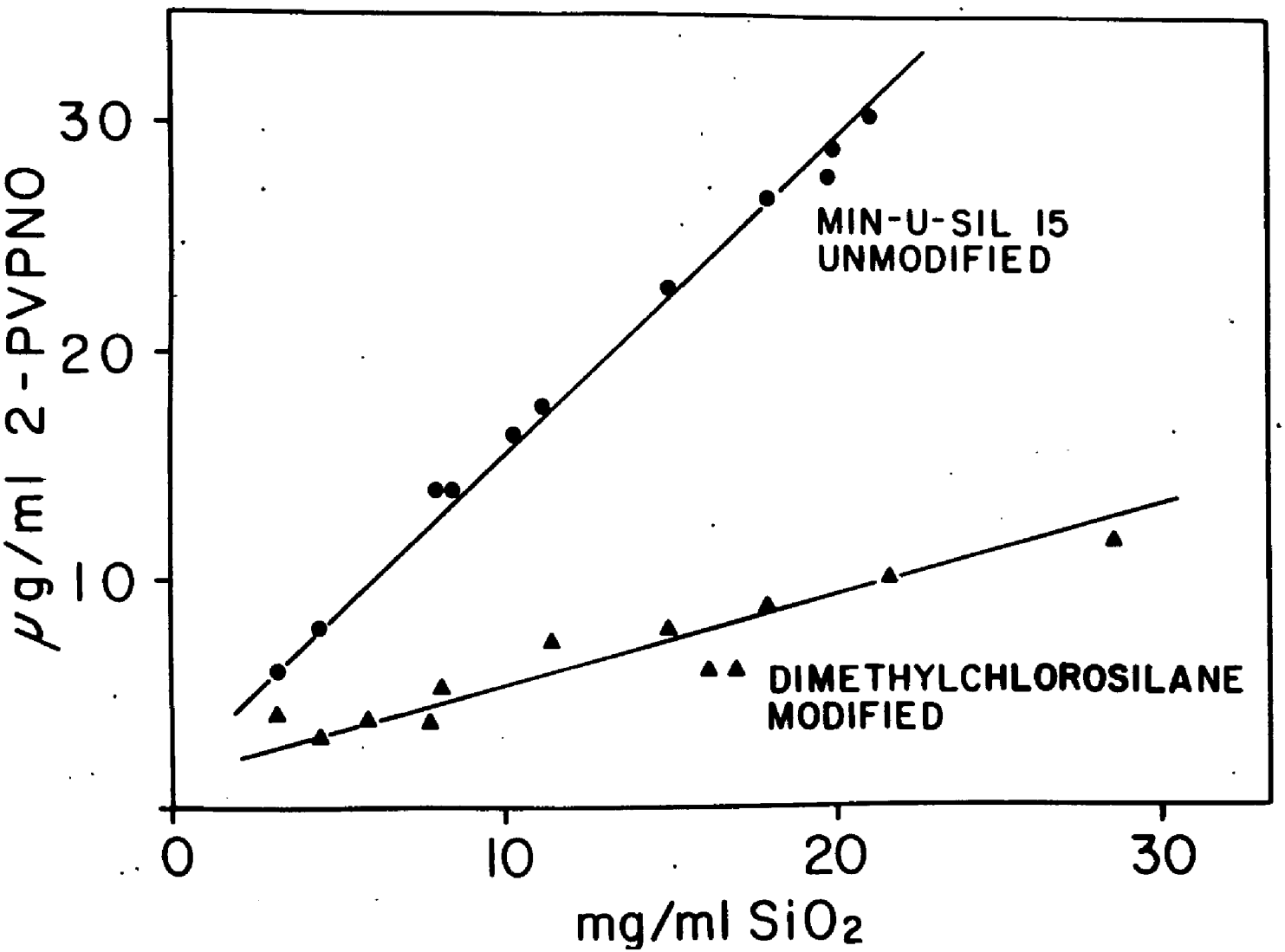
30
20
10
μg/ml 2-PVPNO
MIN-U-SIL 15
UNMODIFIED
DIMETHYLCHLOROSILANE
MODIFIED
0
10
20
30
mg/ml SiO2

CHAPTER IV

Quartz Membranolytic Activity as Related to Its Surface Functionalities

INTRODUCTION

The surface of quartz readily hydrates in the presence of water. This hydration process forms surface silanol groups (-SiOH) which, depending on pH, result in the presence of ionized silanol groups (SiO^-).* The ratio of $-SiO^-$ to SiOH is pH dependent (Iler, 1978). The nonionized silanol group is a hydrogen donor functionality which has been implicated in the biological activity of quartz. As proposed by Nash et al (1966), surface silanol groups (polymeric silicic acid) act as proton donor groups and may break down biological macromolecules (similar to the action of urea and the denaturation of proteins). This hypothesis was further considered by Allison (1968), who suggested that most biological macromolecules are "hydrogen acceptors," and that those few which are hydrogen donors are toxic. These same conclusions were reached by Stober and Brieger (1968), as well as by others. The general model of interaction, with a focus on the hydrogen-donor quality of the silanol group, has been accepted by most investigators on a number of experimental and theoretical grounds.

The contribution of the negative surface change of hydrated quartz to its activity is considered in the following experiments.

*In the following discussion when SiOH is shown, it should be understood that it is on the silica surface and is linked through three siloxanes, SiOSi, to three adjacent silica atoms.

MATERIALS AND METHODS

The silica used in this experiment was a commercially available crystalline quartz, trade name Min-U-Sil 15. Min-U-Sil 15, a pulverized Oriskany sandstone, was obtained from the Pennsylvania Glass and Sand Company, Pittsburgh, PA. "15" connotes that all particles are less than 15um. The received specimen was examined by polarized light microscopy and found to consist of fine powder, almost entirely composed of particles with optical properties consistent with alpha quartz. When immersed in an oil (n=1.548), most of the particles "disappeared" because of low relief, an effect consistent with a randomly oriented aggregate of particles with refractive indices closely matched to that of the immersion oil (quartz, N_Z = 1.553; N_X = 1.544). It was visually estimated that 99% of the specimen, by volume, was quartz. Other mineral impurities were noted, by relief and birefringence characteristics, but no attempt was made at a definitive identification. Traces of feldspar were among these phases.

Nearly all the mineral fragments in the specimen lay well below the 15um size range (Figure IV.1). Size measurements determined on photomicrographs (obtained by light microscopy) of a disperse aliquot indicated that only some 11% of the particles possessed greatest dimensions between 5 and 20um, 22% between 2 and 4.9um, and 67% at or below 1.9um (n=110, 214, and 660, respectively). The same material was to be used for all manipulations, and therefore it was

considered unnecessary to size-fractionate the specimen.

The Min-U-Sil 15 specimen was examined by a powder diffraction technique using a Philip x-ray diffractometer. The specimen was examined by continuous-scan x-ray diffraction analysis using standard diffractometry methods. The x-ray diffraction analysis was performed in the following manner: copper target; 45kV/20mA; curved crystal graphite monochrometer; scintillation counter (1020V dc); scan 1^{o} 2θ/minutes; 2000 counts per second, full scan; time constant, 1 second.

In the scan from 5 to 85^{o} 2θ, almost all the characteristic quartz reflections were observed. Those which escaped detection are listed on the standard powder diffraction data card (5-0490) with the intensities of less than 1. However, of the 22 reflections in this region with intensities greater than 1, all were observed to be present in the spectrum. Of these, 13 reflections agreed with the powder standard to the third place ($\pm$0.000A), and those which were "at variance" with these values were within $\pm$0.002A. The comparison was excellent.

Biological Systems, Inhibitors, and Physical Measurements

The cells used were human erythrocytes or red blood cells (RBCs) obtained from volunteers by venopuncture. The buffy coat and white cells were removed in the standard manner and the erythrocytes were washed three times with veronal buffered saline (VBS). The hemolytic inhibitors used to antagonize membrane lysis were of two varieties: a

hydrogen-bonding polymer, i.e., poly-(2-vinylpyridine-N-oxide) (PVPNO) was obtained from Polyscience, Inc., Warington, PA 18976), and several metal salts whose cations are often observed as contaminants of quartz varieties, i.e., iron (as ferric chloride, $FeCl_3:6H_2O$), aluminum (as aluminum chloride, $AlCl_3:6H_2O$), and zinc (as zinc chloride, $ZnCl_2$). The cationic salts are reagent-grade chemicals available from Fisher Scientific, Springfield, NJ.

The ultraviolet spectra used to measure PVPNO hydrogen bonding onto quartz particles were recorded at 260nm on a Beckman Model 25 spectrometer. Amount of liberated hemoglobins, or hemolysis, were measured at 530nm using a Coleman absorbance spectrometer Mode 6/20A.

The surface charge of the quartz was determined as a function of zeta potential. The zeta potential of quartz was measured in aqueous suspension using a Zeta Meter (manufactured by Zeta-Meter, Inc., 1920 First Avenue, New York, NY).

The Hemolytic System

The hemolytic system described here is modified after Schnitzer and Punsack (1970), who based their protocol on Macnab and Harington (1967) and Secchi and Rezzonico (1968). The hemolysis experiments were performed using packed red cells which were suspended at approximately a 4% suspension in VBS. A 0.25ml aliquot of the 4% RBC suspension was diluted to 5ml with distilled water. If the absorbance at 530nm was not 0.3 absorbance units (A), the volume (V) was

adjusted using the following relationship:

$$V_f \times A_f = V_i \times A_i$$

where V_f is the final volume, A_f is the final absorbance, V_i is the initial volume, and A_i is the initial absorbance. The A_f should be 0.300 ± 0.010 A, so then it follows that:

$$V_f \times 0.3 = V_i \times A_i$$

It is therefore experimentally desirable to prepare a greater than 4% erythrocyte suspension and then dilute to obtain a standard concentration, thereby avoiding differences in cell number due to packing differences. The stock suspension of erythrocytes contains approximately 3.6×10^8 cells/ml.

The quartz was introduced into glass test tubes from a stock suspension in VBS prepared on the day of the experiment. The volume was then adjusted to 4ml with VBS. The erythrocyte suspension was never added to dry quartz; the hemolysis experiment was always carried out in buffered suspension maintained in 16 x 125mm flint disposable culture tubes. After addition of the quartz and VBS, 4ml of stock RBC suspension was added to the tubes. The addition made the final concentration of 1.8×10^8 cells/ml with final volume 8ml.

The positive control used in the experiment was 4ml of stock erythrocyte suspension added to 4ml of distilled water, which yielded total lysis. The negative control was 4ml of VBS added to 4ml of stock RBC suspension, which gave "background" absorbance, reflecting mechanical lysis or leaking from the cells.

The erythrocyte/quartz suspensions were placed in a temperature bath set at 37°C for a period of two hours. The tubes were inverted every 30 minutes by hand to resuspend the settled cells and quartz. In addition, the suspension was generally maintained as the tubes were constantly moved by gyratory motion. At the end of two hours, the contents of all tubes were centrifuged (800xg), and the absorbance of the clear supernatant, cell and particle free, was determined at 530nm.

The absorbance of the 100% lysate should be ten times the A_f value from the standardization of the erythrocyte suspension. Once the absorbance of the sample (A_s) has been determined, the percentage hemolysis (%H) can be calculated from the relationship:

$$\%H = \frac{A_s}{A_f \times 10} \times 100$$

Hemolysis with Quartz -- A Surface Phenomenon

The hemolytic potency of Min-U-Sil 15 was tested. On the basis of eight data points, the hemolytic concentration at which 50% of the cells were lysed (HC50) was determined to be 2.72mg/ml of suspension (r^2 = 0.98 for the computed best fit regression line). Min-U-Sil 15, like a number of other quartz varieties, is a potent hemolytic agent (Nolan et al., 1985).

The interaction between quartz and red cells may be probed with chemical inhibitors. In this study, inhibitors were used to block the surface functionalities of Min-U-Sil

and the effect of this blocking on the hemolytic potency was measured.

Inhibition Studies

Inhibition of hemolysis by PVPNO. The high molecular weight polymer PVPNO is a powerful hydrogen bonding agent. Therefore, the interaction of the polymer with the quartz silanol groups is very strong. The effects of this is that the quartz surface will bind virtually all of the PVPNO present until the surface is saturated (see Iler [1978] for discussion). This polymer, bound to the surface of quartz, has been shown to inhibit hemolysis markedly (Schlipkoter and Brockhaus, 1961).

The binding of PVPNO to quartz may be followed quantitatively, in that the polymer absorbs strongly in the ultraviolet region at about 260nm. The absorption band varies linearly with the concentration of PVPNO up to 50ug/ml in solution. Different concentrations of quartz were added to a 50ug/ml PVPNO solution in distilled water. The quartz was then spun down and the absorption of the supernatant PVPNO solution at 260nm was measured. In all cases below saturation, a marked decrease in the 260nm peak was noted in the supernatant solution, indicating that PVPNO had been removed from solution and had bound to the surface of the quartz (Figure IV.2).

The amount of PVPNO bound by a given mass of quartz may be calculated from the binding data. Quartz, at a concentration of 1.5mg/ml, may bind up to approximately 4ug/ml of

PVPNO (Figure IV.2). Inhibition of hemolysis by PVPNO over a range of concentrations (0.63ug/ml to 15.63ug/ml) shows a marked increase in activity at approximately 3.2ug/ml (Figure IV.3). At concentrations of 10ug/ml, hemolysis is almost totally blocked. The amount of PVPNO required to antagonize the hemolytic effect is less than 0.25% of the total mass of the quartz, indicating a surface effect. Further evidence is that this value varies with the surface area of the quartz.

As shown spectrophotometrically, very little unbound PVPNO appears in solutions below the concentration at which the quartz surface is saturated. The sudden drop in the percentage hemolysis below the calculated saturation level indicates that the primary site of action of the inhibitor (at these concentrations) is on the surface of the quartz and not on the erythrocyte membrane (or as an osmotic regulator; see Shnaidman, 1974). The sharp linear reduction in %H (percentage hemolysis) with the addition of even a few micrograms of PVPNO indicates the sensitivity of the hemolytic assay system to changes in the character of the quartz surface.

Inhibition of hemolysis by metal salts. Inhibition of quartz hemolysis was measured after mineral interaction with solutions of aluminum chloride, ferric chloride, and zinc chloride. The concentrations of inhibitors were selected on the basis of change in zeta potential measurements. Those concentrations which rendered the quartz isoelectric (3mg/ml of quartz in veronal buffer at pH 7.4) were used.

This isoelectric 3mg/ml suspension of quartz was used as a stock solution for the hemolysis experiments (Figure IV.4).

Zinc chloride was the least effective agent for reducing the surface charge of quartz. The high concentrations of zinc chloride required for the neutralization of the surface charge agglutinated the cells as well. The secondary effect compounded the variable, so that no clear statement could be made about the effects of zinc cations on the quartz surface. The bonding of the iron cations on the surface of quartz, however, markedly reduced hemolysis. No erythrocyte agglutination was observed. Determinations may be followed in Figure IV.4. The inhibition of hemolysis as a function of aluminum chloride concentration, for two periods of time, was also determined (Figure IV.5). It is clear from these data that at extraordinarily low concentrations of aluminum chloride the hemolytic activity of quartz is inhibited far more effectively as compared to iron. The period of incubation of aluminum chloride with the quartz was varied and the hemolytic activity after 150 minutes was observed to be less than the value measured at 30 minutes. This appeared to be related to the quartz surface and not the erythrocyte. In both instances, the erythrocyte/aluminum chloride interaction conditions were identical (Figure IV.5). The sudden decrease in the hemolytic activity occurred over the same concentration range -- where the surface charge (zeta potential) approaches zero. No cell agglutination was noted, even at the highest concentrations.

It was considered important to determine changes in the

surface charge of quartz as a function of aluminum chloride concentration. The results are shown in Figure IV.6. From these data, the relationship between the decrease in hemolytic activity and the decrease in the negative surface charge can be followed. The point of zero surface charge correlates well with the lowest point in hemolytic activity.

It was thought possible that the presence of aluminum or other cation salts on quartz could alter the hydrogen-bonding character of its silanol groups. Excess aluminum chloride was added to varying amounts of quartz in aqueous suspension, along with controls (silica without aluminum chloride). The suspensions were incubated at room temperature for two hours to equilibrate. A stock solution of PVPNO was added to these mixtures. These suspensions were incubated at room temperature for 30 minutes, they were spun down, and the absorbance of the supernatant determined. A plot was made of mg/ml SiO_2 vs. ug/ml PVPNO (Figure IV.7). The presence of the aluminum chloride did not effect the ability of the silica to bind PVPNO. Zeta potential measurements showed that the surface remained positive in the presence of PVPNO, again indicating that both compounds were absorbed on the surface, simultaneously, in a noninterfering manner. Binding of PVPNO and that of Al^{3+} occur independently of each other, indicating that different sites are involved for each compound. The negative centers bind the Al^{3+} and the protons on the silanol group bind the PVPNO.

DISCUSSION AND CONCLUSIONS

In the presence of water, the surface of quartz forms silanol groups which are partially ionized. At a pH 7, the ratio of -SiOH to $-SiO^-$ sites is approximately 30:1. (In 0.1 N NaCl, amorphous silica has been about 0.25 SiO^-/nm^2, yielding a -SiOH to $-SiO^-$ ratio of about 32:1 [R.K. Iler, personal communication]). This high ratio is, in part, responsible for the previous lack of focus on the SiO^- groups in silica activity.

The hydrogen-bonding characters of the quartz surface has been extensively studied and implicated in the pathogenesis of silicosis (see, e.g., Nash et al., 1966; Mehrishi and Seamen, 1966; Stober and Brieger, 1968; Allison, 1968). PVPNO has been shown to inhibit the cytotoxic effect (fibrogenicity) of silica in vitro and in vivo. This polymer possesses two lone pairs of electrons on terminal oxygens resulting in strong hydrogen bonding potential. The use of this compound has been extensive in silicosis research and has been demonstrated to effectively blunt the activity of quartz (see, e.g., Schlipkoter and Brockhaus, 1961; Macnab and Harington, 1967; Schlipkoter, 1968; Klosterkotter, 1968; Schnitzer and Pundsack, 1970).

From our experiments, measurements show that 1.5mg/ml of quartz will bind approximately 4ug/ml of PVPNO. The quartz binds less than 0.25% of its mass in PVPNO, confirming that this interaction occurs with the silanol groups, which exist only at the surface. Therefore,

equivalent masses of quartz which differ in surface area (with varying particle size) will bind different amounts of PVPNO. Binding curves must, therefore, be determined for each individual specimen. The hemolytic activity of quartz, as a function of PVPNO bonding, shows that the %H drops off rapidly after the concentration of PVPNO goes above the point of saturation, and that the quartz remains inactive at higher concentrations. Quartz has a very high affinity for the PVPNO polymer and binds virtually all the polymer present below the saturation points.

It has been suggested that PVPNO might absorb on the erythrocyte surface and thereby act to stabilize the membrane. At the concentration of PVPNO used in this experiment, it appears that the polymer is acting solely on the quartz surface. The %H decreases linearly with increasing PVPNO concentration below the point of saturation. Assuming that the polymer is distributed randomly over the surface of all the quartz particles, these data suggest that the particle requires only a small amount of surface in actual contact with the erythrocyte to induce lysis.

The negative charge from the ionized silanol groups can be reduced and the surface may even become positive at high concentrations of Lewis acids. These Lewis acids, such as aluminum and ferric chloride, ionize in water and the metal cations bind to the negative centers on the surface of quartz. The suitability of these cations for the quartz surface is related to their charge/radius ratio and the

geometrical features of the surface oxygen groups. These cations are frequently encountered in naturally occurring quartz specimens. When they are present in quartz in measurable concentrations the biological activity is blunted. This may be of importance when miners are exposed to silica during hematite (iron) mining and when coal miners are exposed to host rocks which include aluminous shales (see discussion in Langer, 1978). The charge on the surface of naturally occurring quartz is therefore a function of cation concentration, and may be followed by measurement of zeta potential. When the surface charge of quartz is made isoelectric by the addition of aluminum chloride, the hemolytic activity is observed to decrease by 90%. The concentration of aluminum chloride required to produce such a diminution in hemolytic activity is only some 0.3% of the mass of quartz used. The reduction in the absolute value of the negative charge of quartz follows the addition of aluminum chloride; the isoelectric point occurs at approximately the same concentration as that at which the %H becomes minimum.

At higher concentrations of aluminum chloride, the zeta potential becomes positive. Additional aluminum chloride in amounts qreater than the isoelectric point has very little effect on further reducing the %H, and may actually increase hemolysis. This compound is a strong Lewis acid and can reduce the pH. Therefore, the membrane damage is likely related to strong pH shifts. As the amount of aluminum chloride increases in the system beyond the quantities required for maximum inhibition, membrane lysis is induced.

Inhibition of hemolysis can occur by bonding a cationic metal or a hydrogen-bonding polymer to the surface of quartz. The two inhibitors, specific for different functionalities, are independent of each other and noninterfering. The question of which of the blocked functionalities (or both) is responsible for membrane damage remains unanswered. It is possible that the high molecular weight polymer, PVPNO, may physically prevent the quartz particle from interacting with the red cell membrane. Light scattering study has shown that the polymer used in these experiments is a random coil with a radius of gyration of approximately 100-200A (Nolan, Langer, and Oster, unpublished data). This coiled polymer would present a formidable steric obstruction. The negatively charged quartz surface is therefore "buried" several hundred angstroms below the new surface created by the bonding of the polymer. Even when the surface silanol groups are available for bonding, if the net negative surface charge is reduced, hemolytic activity is also markedly reduced. The contribution of the negative surface charge to the hemolytic activity appears to be real, significant, and of a sizable magnitude.

Figure IV.1 -- Micrographs of Min-U-Sil 15, by plane polarized light microscopy.

Figure IV.2 -- Quartz binding of PVPNO in linear binding range. The introduction of varying concentrations of quartz to a stock solution of PVPNO produced binding, measured by a decrease in the ultraviolet intensity at 260nm. (Quartz mg/ml binding of PVPNO (ug/ml), Q:PVPNO = 1.87:5.4; 2.24:5.4; 2.41:6.6; 2.74:7.0; 4.49:12.6; 4.86:11.2; 5.45:14.3; 7.05:18.6).

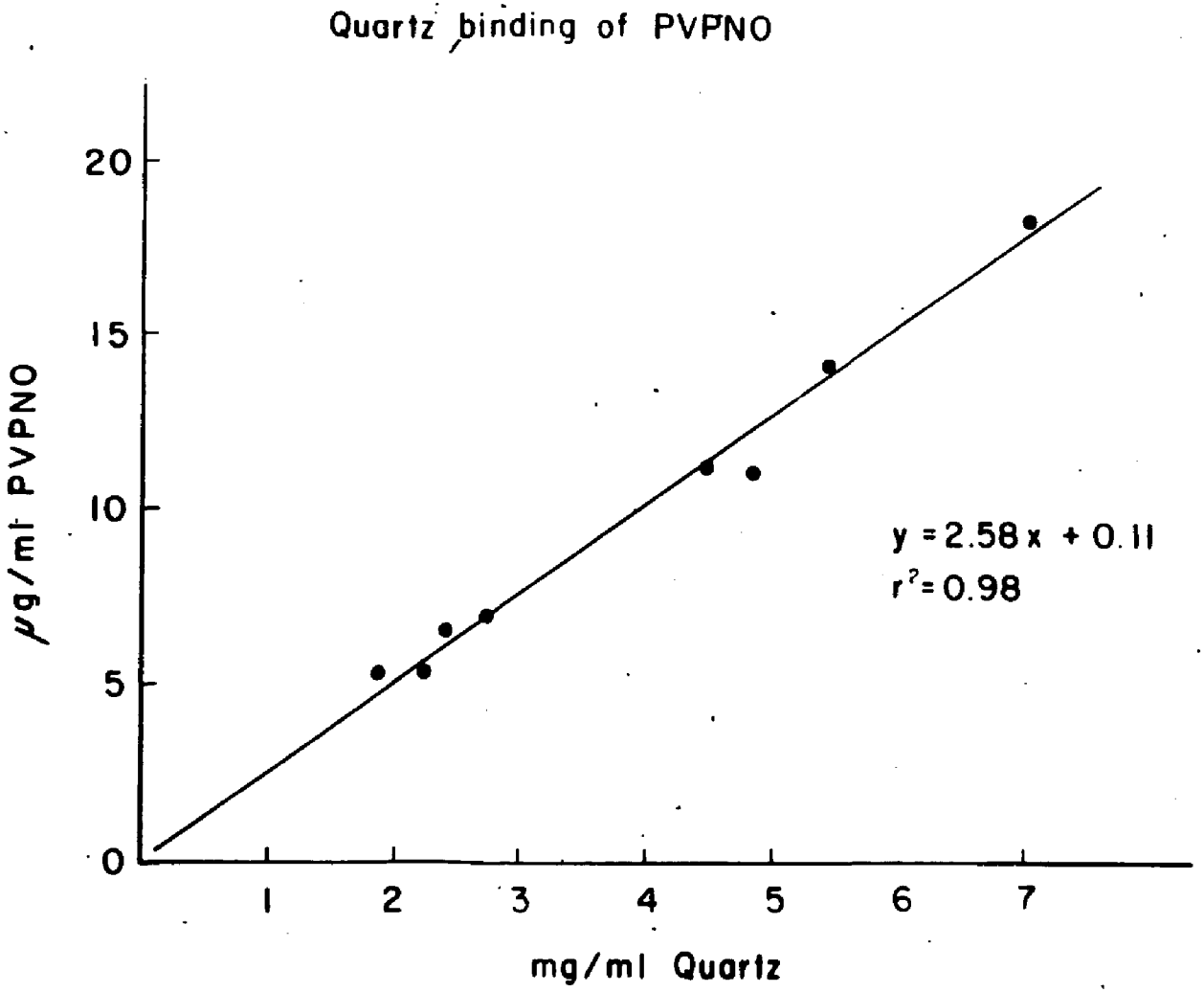
Quartz binding of PVPNO
20
15
10
5
0
μg/ml PVPNO
1
2
3
4
5
6
7
mg/ml Quartz
y = 2.58x + 0.11
r² = 0.98

Figure IV.3 -- Inhibition of quartz hemolysis as a function of PVPNO absorption. In this experiment, 1.5mg/ml quartz induced 27% hemolysis. (In other experiments, 1.52mg/ml quartz produced 28% hemolysis, in good agreement with this data set.) With only 3.4ug/ml of PVPNO, a 75% reduction in hemolytic potency is observed. This reduction appears to continue with a gradual decline in membrane activity until almost 16ug/ml are present. (PVPNO: %H = 0.00:27.37; 0.63:25.84; 1.25:20.71; 3.13:7.44; 6.25:6.01; 9.38:4.22; 15.63:3.41.)

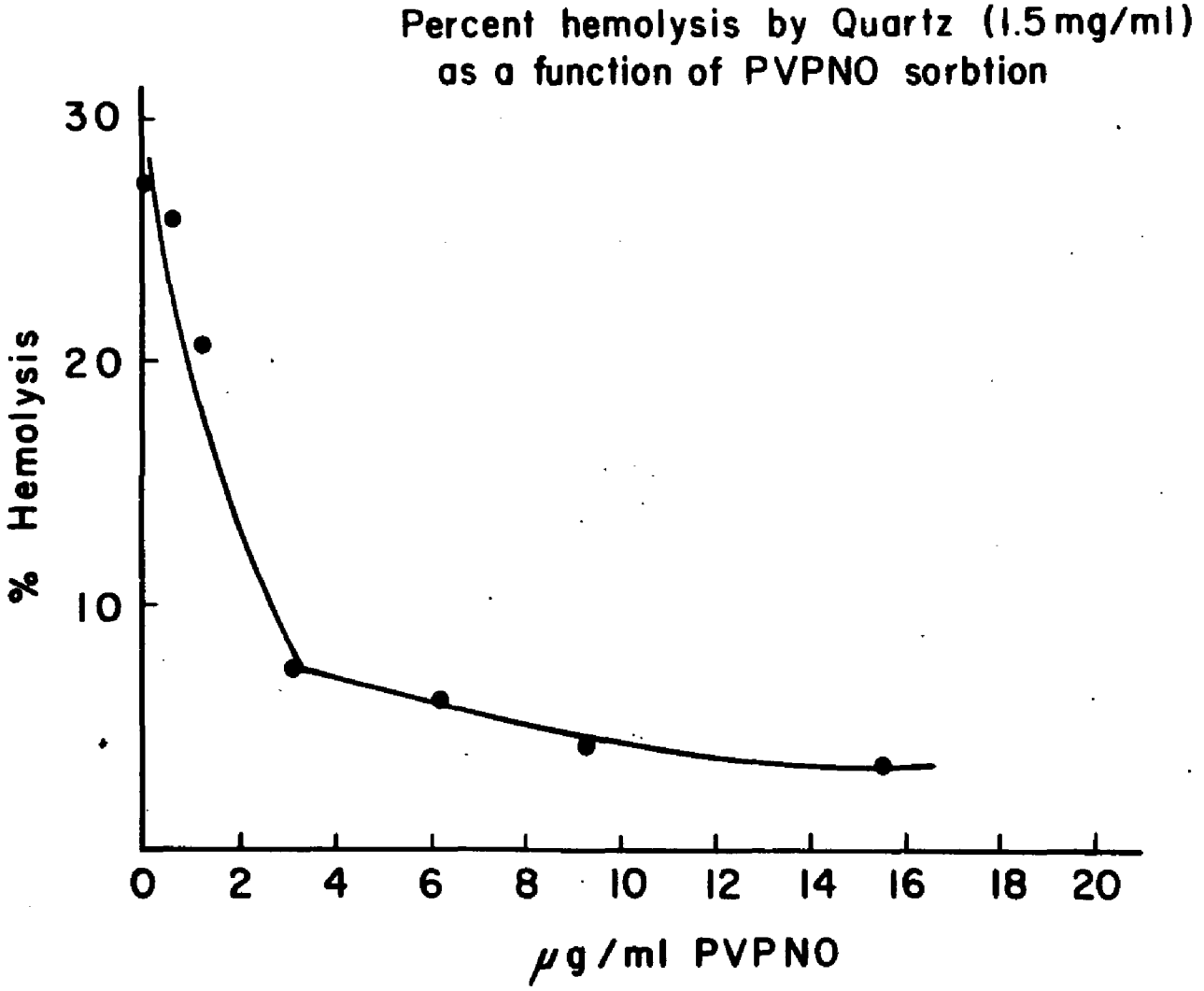
Percent hemolysis by Quartz (1.5 mg/ml)
as a function of PVPNO sorbtion
% Hemolysis
30
20
10
0
2
4
6
8
10
12
14
16
18
20
μg/ml PVPNO

Figure IV.4 -- Inhibition of quartz hemolysis as a function of cationic and PVPNO binding. Aluminum and iron chloride hydrates (Lewis acids) were added to stock suspensions of quartz at concentrations which rendered the quartz isoelectric (zeta potential = 0.00mV). Inhibition was achieved up to 97% for iron chloride and 98% for aluminum chloride. More iron was required for reaction (30ug/ml) as compared to aluminum (10ug/ml). Although not shown, 300ug/ml zinc chloride produced marked antagonism, but also agglutinated RBCs.

Inhibition of Quartz Hemolysis by Lewis acids and PVPNO. The Lewis acids were present at concentrations which made the Quartz isoelectric.

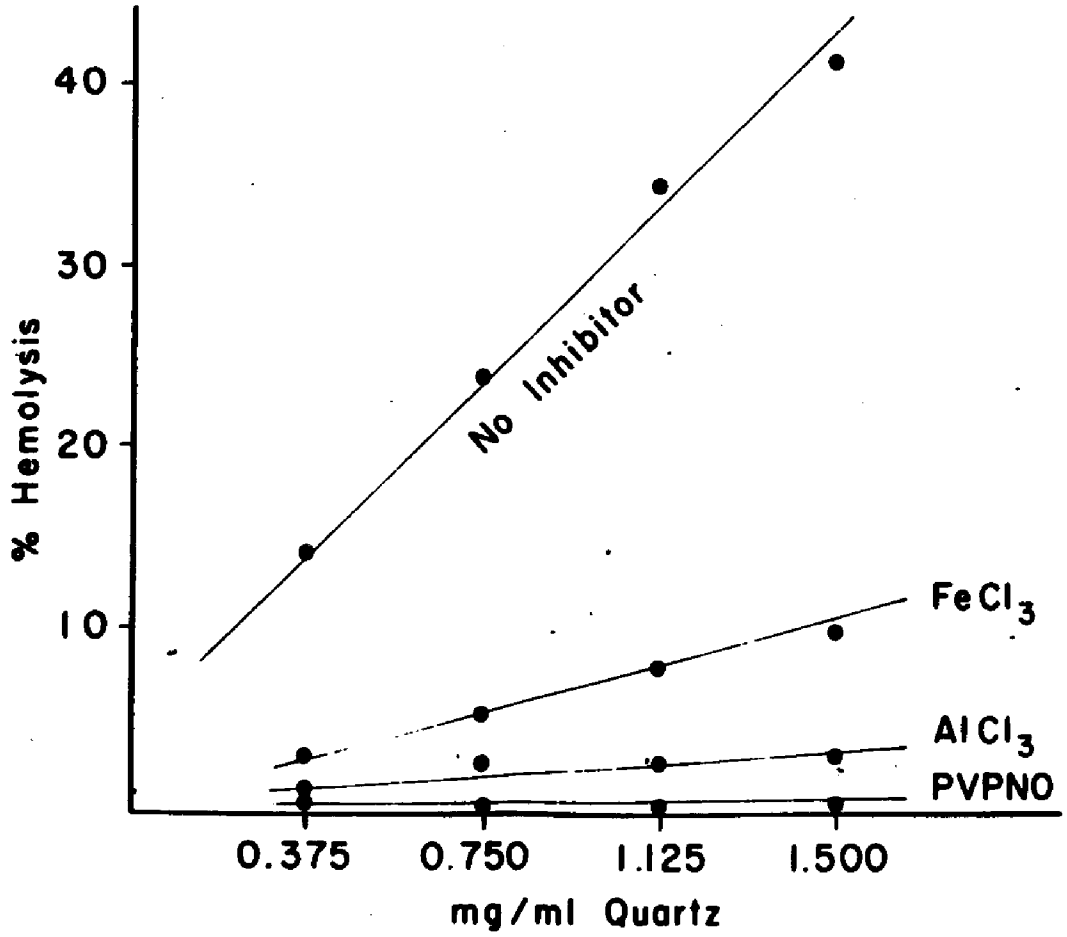

Figure IV.5 -- Inhibition of quartz hemolysis by aluminum chloride as a function of time. Using a stock suspension of quartz, longer time of contact produces more bound cations and more effective antagonism of hemolysis as compared to short contact time. Note that concentrations which produce marked blunting of hemolysis are those which render equivalent masses of quartz isoelectric.

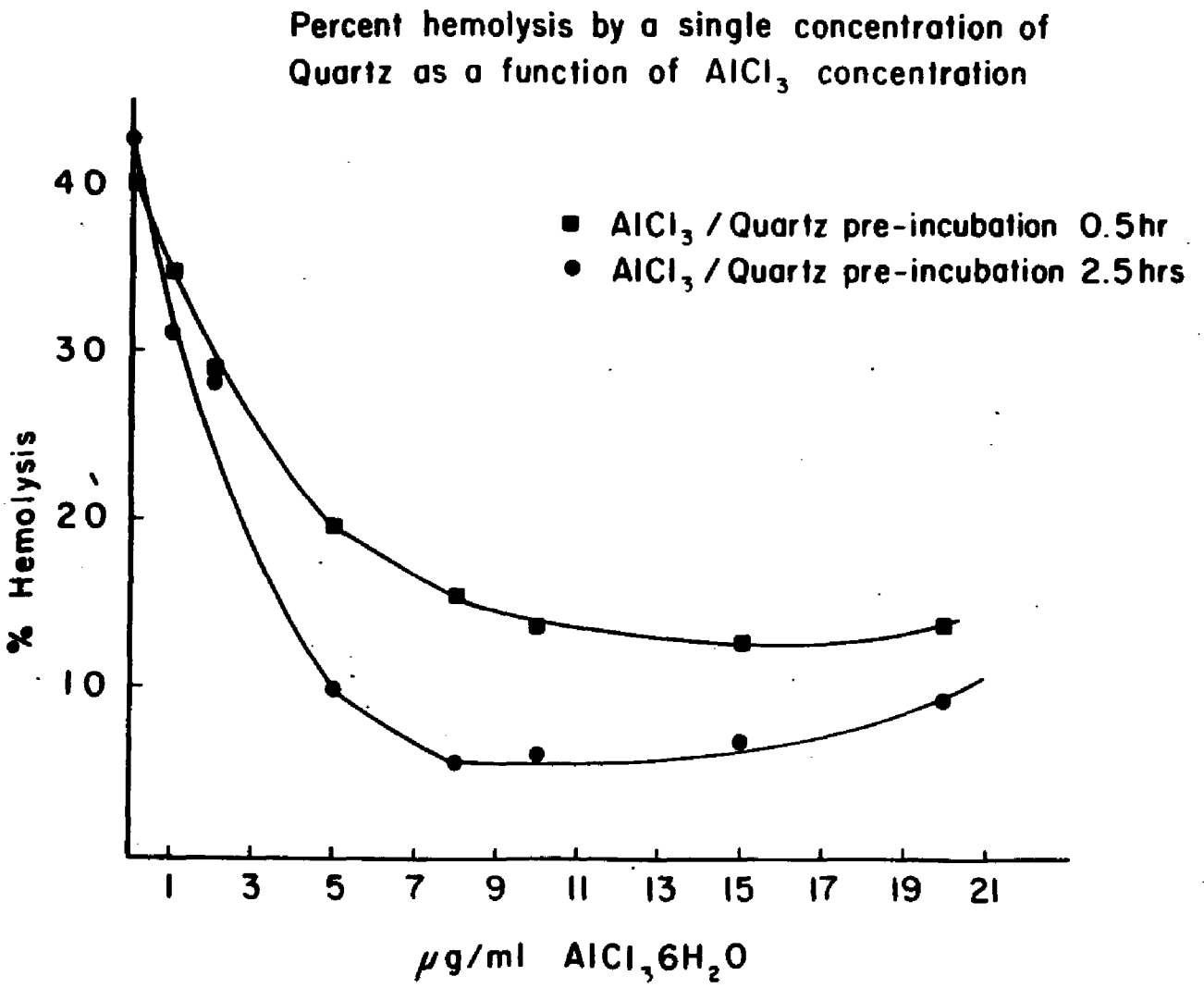
Percent hemolysis by a single concentration of
Quartz as a function of AlCl3 concentration
AlCl3 / Quartz pre-incubation 0.5hr
AlCl3 / Quartz pre-incubation 2.5hrs
% Hemolysis
40
30
20
10
1
3
5
7
9
11
13
15
17
19
21
μg/ml AlCl3 6H2O

Figure IV.6 -- The change in the zeta potential of quartz (HC50 concentration suspension) as a function of $AlCl_3:6H_2O$ concentration in veronal buffer (without saline) at pH 7.4. Note that the first challenge of aluminum into the system causes a measurable negative shift in the surface charge. This effect has been observed in other systems previously and the explanation offered is that "bulk" stress causes a contraction of the double layer giving the particle an enhanced electrophoretic mobility. This effect is reversed at higher cationic concentrations and the shift is then toward the "positive" (Riddick, 1968). The concentration at which $AlCl_3:6H_2O$ establishes an isoelectric particle is that at which hemolysis is most effectively blocked.

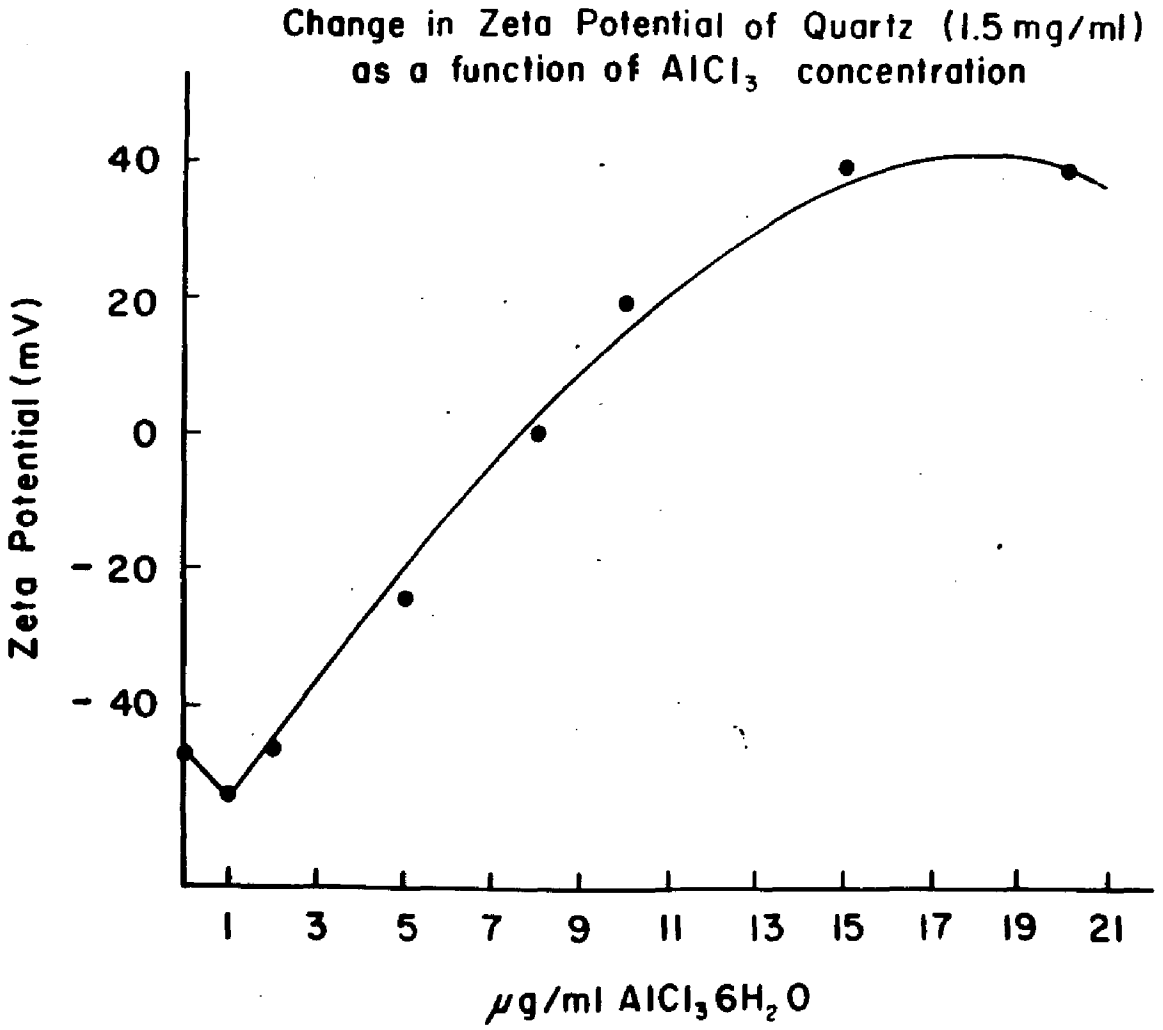
Change in Zeta Potential of Quartz (1.5 mg/ml)
as a function of $AlCl_3$ concentration
Zeta Potential (mV)
40
20
0
- 20
- 40
1
3
5
7
9
11
13
15
17
19
21
$\mu g/ml\ AlCl_3 6H_2O$

Figure IV.7 -- The influence of quartz-bound aluminum on the binding of PVPNO. The generation of two areas of binding PVPNO onto quartz, with and without the presence of aluminum, produced statistically identical binding curves: Q/PVPNO, $Y = 2.01x + 3.58$, $r^2 = 0.99$; Q/PVPNO + Al, $Y = 2.41x + 2.53$, $r^2 = 0.99$; all points, $Y = 2.15x + 3.29$, $r^2 = 0.97$.

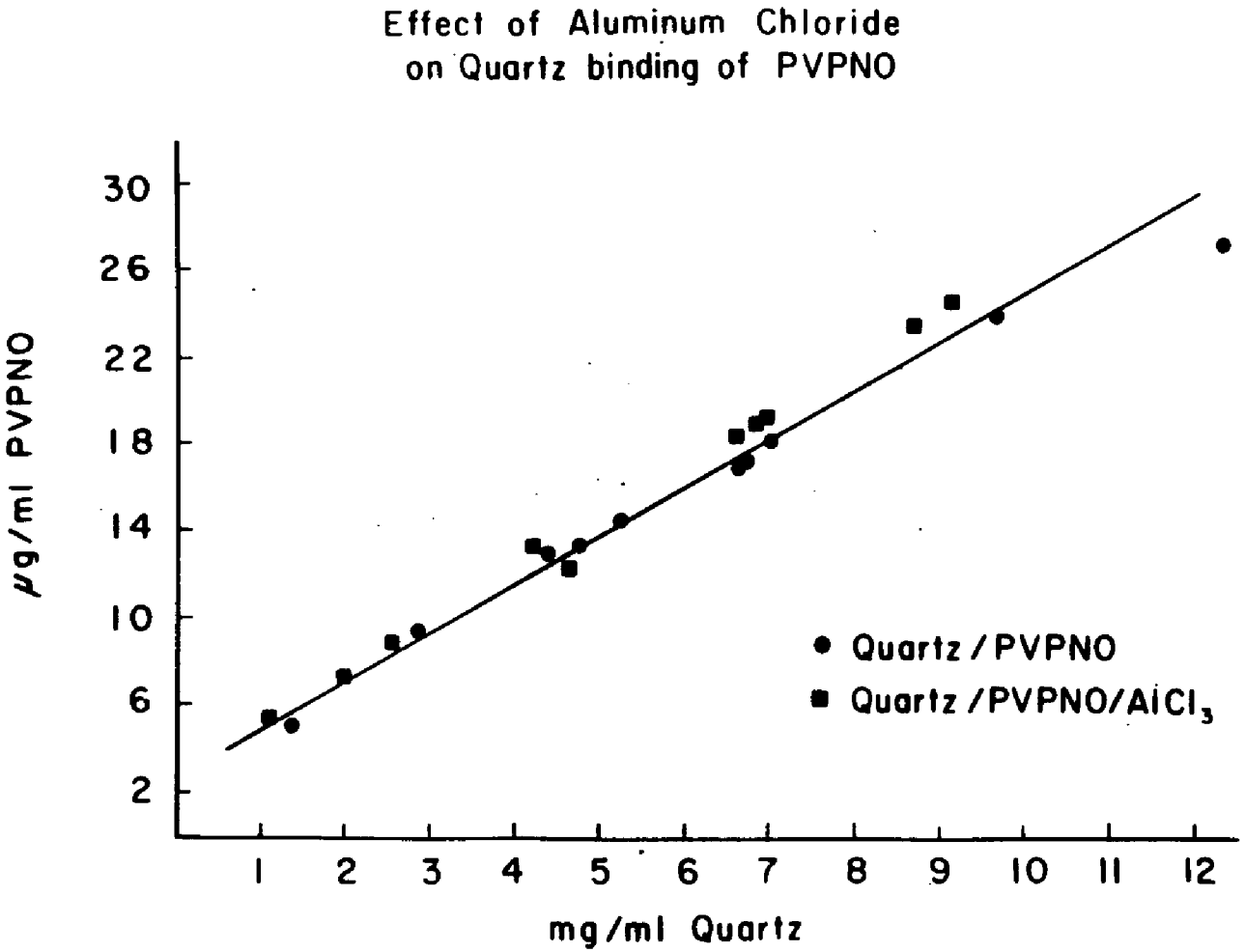
Effect of Aluminum Chloride
on Quartz binding of PVPNO
μg/ml PVPNO
30
26
22
18
14
10
6
2
1
2
3
4
5
6
7
8
9
10
11
12
mg/ml Quartz
Quartz / PVPNO
Quartz /PVPNO/AlCl3

CHAPTER V

Recognition of Quartz by Erythrocyte Membranes

INTRODUCTION

The nature of the membranolytic interaction between the quartz surface and the erythrocyte membrane has been characterized using inhibitors. The inhibitors were first bound to the quartz surface and the specimens then used to challenge erythrocytes. This experimental approach led to the conclusion that the quartz surface was best able to bind hydrogen bonding polymers and that the presence of these polymers inhibited cell lysis (Nash et al, 1966). Quartz membranolytic activity was attributed to the proton-donor characteristics of the surface (Allison, 1978). This concept was further generalized to conclude that most biological macromolecules are hydrogen-acceptors and the few compounds which are hydrogen-donors are toxic.

Of the many hydrogen bonding polymers studied, 2-polyvinylpyridine-N-oxide was found to be the most effective inhibitor. For inhibition, the polymer must be of a molecular weight of 10,000 daltons or greater (Holt, 1968). It was further hypothesized that membrane lysis was caused by the rigidly placed silanol groups on the quartz surface. These are able to form multiple hydrogen bonds with the phosphate ester groups of phospholipids, and probably also with the secondary amide groups of proteins, thereby distorting the membrane and increasing its permeability (Allison, 1973).

The hydrogen-donor hypothesis does not explain the observation that quartz membranolytic activity can be

completely inhibited by blocking the negative charge on the quartz surface (Nolan et al, 1981). The membranolytic activity is reduced in a dose response manner as the surface charge is reduced and the isoelectric quartz particle retains its hydrogen-donor character. The negative surface charge of quartz is attributed to the ionized silanol groups. To further demonstrate the importance of surface charge in quartz membranolytic activity, it would be useful to identify a receptor on the erythrocyte membrane with which the charge could bind. The human erythrocyte contains an extensive anion transport system, the receptor of which would have the appropriate chemistry to bind an anion.

Anion transport in erythrocytes was first described by Hermann Nasse in 1878; he observed that horse erythrocytes were capable of exchanging chloride for bicarbonate. This was nine years before Arrhennis described electrolytic dissociation (see Knauf, 1979 for discussion). The physiological purpose of anion transport was to increase the CO_2-carrying capacity of the blood. The CO_2 rapidly diffuses into the erythrocyte where the intracellar enzyme, carbonic anhydrase, catalyzes the hydration of CO_2 to H_2CO_3, which dissociates to $H^+ + HCO_3^-$. The intracellular bicarbonate anion is then exchanged with extracellular chloride one for one in an electrically silent step. The reduction of the partial pressure of CO_2 and the removal of the bicarbonate anion from the cell increases the overall CO_2-carrying capacity of the blood.

The anion transport system of the erythrocyte has been

extensively studied (see Cabantchik, 1978; Knauf, 1979, for review) and many low molecular weight probes have been identified which inhibit anion transport. To test the hypothesis that the anion transport receptor is the site of attachment for the quartz surface charge, the effect of anion transport inhibitors on quartz membranolytic activity was determined.

MATERIALS AND METHODS

Quartz Specimen

A single quartz specimen obtained as a fine powder was used in this study. It is a commercially available crystalline silica distributed under the trade name Min-U-Sil 15 by Pennsylvania Glass and Sand Company, Pittsburgh, PA. It was shown by continuous scan x-ray diffraction to be a high purity alpha quartz. The size distribution was determined by counting 984 particles by direct measurement on light microscopy photographs: 11% possessed greatest dimension between 5-20um, 20% between 2-4.9um, and 67% at or below 1.9um (see Nolan et al, 1981; Nolan et al, 1985).

Inhibition of Quartz Membranolytic Activity

The effect of the following anion transport inhibitors on quartz hemolysis was determined:

4,4'-diisothiocyanostilbene-2,2'-disulfonic acid disodium salt trihydrate (DIDS) MW 552.5, 4-Acetamido-4'-isothiocyanostibene-2,2'-disulfonic acid (SITS) MW 498, and

N-(4-Azido-2-nitrophenyl)-2-aminoethylsulfonate (NAP-taurine) MW 345.23, all of which were obtained from Pierce Chemical Company, Rockford, IL.

Pyridoxal 5'-Phosphate (P5P) MW 247.2, phloridzin MW 436.4, and Phloretin MW 274.26 were obtained from Sigma Chemical Company, St. Louis, MO.

Hemolytic Model

The ability of each of the anion transport inhibitors listed above to inhibit quartz from altering the permeability of the human erythrocyte to hemoglobin was determined. The erythrocytes were obtained from peripheral blood (50ml) taken by venipuncture in a plastic syringe containing 15U/ml preservative-free heparin. Ficoll-Hypaque gradient centrifugation was used to separate the peripheral blood lymphocytes and plasma proteins from the erythrocytes. Fifty milliliters of blood was diluted with an equal volume of saline, overlaid onto a 25ml Ficoll-Hypaque gradient, and centrifuged at F~800g at 20^{o}C for 45 minutes. The lymphocytes and plasma proteins were removed and the erythrocytes were stored at 4^{o}C and used within a week.

Before the stored erythrocytes were used, approximately 5ml of packed human erythrocytes were diluted to 50ml with pH 7.4 Veronal Buffered Saline (VBS, 24mM sodium barbital and 145mM sodium chloride) in a plastic centrifuge tube and spun at F~800g, at room temperature, for 30 minutes. The erythrocyte wash was repeated twice. Using optical spectroscopy, the washed human erythrocytes were made into a

standard suspension which contained approximately 3.6×10^8 cells/ml (Nolan et al, 1981).

For the experiments in which the inhibitors were studied under conditions of irreversible binding, a single stock suspension of Min-U-Sil 15 was made in VBS. The quartz suspension was diluted to four concentrations in duplicate. Each of the four different dilutions were adjusted to 4ml and then 4ml of the standard erythrocyte suspension was added. The final volume at each concentration was therefore 8ml and the erythrocyte concentration was 1.8×10^8 cells/ml. The quartz and the erythrocytes were incubated at $37^{\circ}C$ for 120 minutes and shaken continuously with a gyratory motion. The plot of mg/ml of mineral vs %H is generally linear up to about 40% hemolysis, below which all of the measurements reported here fell. The duplicate determinations were averaged and the values are shown with variance. Linear regression analysis was made for each set of eight points and the equation of the line calculated. This equation was used to compute the HC50, the concentration of quartz (in mg/ml) required to lyse half of the erythrocytes in the suspension.

In the experiments where the concentration of inhibitor is varied, the quartz concentration is held constant at 1.5mg/ml SiO_2. A stock solution of the inhibitor is made up such that when 1ml is diluted to 8ml, this is the highest final concentration used. Various concentrations of inhibitor were diluted to 1ml, to which 4ml of the standard erythrocyte suspension is added and the 5ml suspension is

allowed to incubate. During this period, the inhibitor is allowed to interact with the membrane. Then 3ml of a 4mg/ml SiO_2 stock suspension is added, making the final volume 8ml. The inhibitor concentrations shown are the final concentrations when the erythrocytes are at a concentration of $1.8x10^8$ cells/ml.

EXPERIMENTAL RESULTS

Bimodal Class of Anion Transport Inhibition

Bimodal inhibitors are able to bind both reversibly and irreversibly to the cell membrane. The reversible bonding is electrostatic via negatively charged groups, i.e., sulfate or phosphate, while the irreversible binding involves a covalent bond.

Disulfonic Acid Stilbene

The sulfonic acid stilbenes are one of the most effective classes of anion transport inhibitors so far identified (Knauf, 1979). DIDS and SITS were studied to determine their effect on quartz membranolytic activity. The reversible binding is considered to be electrostatic via the charged sulfate groups while the irreversible binding is covalent involving a functional group reaction with the isothiocyano groups and an amine on the erythrocyte membrane (Cabantchik and Rothstein, 1972, 1974a,b). The criterion used to differentiate the two types of binding is washing the inhibitor treated cells with bovine serum albumin. It

is assumed that any inhibitor not covalently bound would be removed by binding to albumin. Albumin is known to bind anions and can undergo a functional group reaction with the isothiocyano group(s). It has been demonstrated using radioactively labeled albumin that the protein does not bind to the erythrocyte membrane (Cabantchik and Rothstein, 1974a).

Both DIDS and SITS were inhibitors of quartz membranolytic activity. At concentrations of 1uM DIDS inhibited over 50% of the membranolytic activity while SITS at a concentration of 95uM gave 35% inhibition (Figures V.1 and V.2). At higher concentrations, DIDS inhibited the activity of quartz almost completely (Table V.1). DIDS, irreversibly bound to the erythrocyte, increased the HC50 by almost 2.5 times (Table V.2) and SITS also showed inhibitory activity under irreversible conditions (Figure V.3). The same erythrocyte suspensions used in the experiment shown in Figure V.3 were challenged with UICC Canadian chrysotile and no inhibition was observed (see Table V.3).

Pyridoxal 5'-Phosphate

Pyridoxal 5'-phosphate has been used as a probe to explore the "sidedness" of membrane proteins (Cabantchik et al, 1973). The salient features of the probe as regards to its chemical reactivity and labeling characteristics of intact erythrocytes are the following: 1) P5P reacts with amino groups with a high degree of specificity by forming a Schiff base which can be reduced by sodium borohydride.

This probe is of the bimodal class due to the fact that it can bind reversibly via a Schiff base and an electostatic bond from the phosphate group. The probe is irreversibly bound when the double bond of the Schiff base is reduced by sodium borohydride; 2) P5P interacts with intact erythrocyte membranes and can label all the protein bands seen by staining with SDS-polyacrylamide gel electrophoresis and hemoglobin under conditions of maximum uptake: low pH (approximately pH 6), prolonged incubaton, increased P5P concentration, and elevated temperatures. Under a different set of conditions, uptake of the probe into the cell can be minimized which results in specific labeling of band 3, a 95,000 dalton transmembrane protein associated with anion transport and three glycoprotein (Cabantchik et al, 1975). This rapid probe binding is favored by lower temperatures, high pH (approximately pH 8), and shorter incubation times. The lower temperature reduces transport and the high pH is thought to enhance the formation of the Schiff base, possibly by allowing the probe to displace a proton from the charged amino group more easily and/or catalyzing the dehydration. The "rapid binding" of the P5P to the erythrocyte membrane is considerably reduced by DIDS, a specific inhibitor of anion transport. The DIDS also blocks the slow component labeling of the cell, implying that the probe enters the cell through the anion transport system.

Inhibition of quartz membranolytic activity by P5P under conditions of reversible binding is shown in Figure V.4. The P5P inhibition of quartz membranolytic activity

occurs at high inhibitor concentration, i.e., in the millimolar range. To determine if the effect is non-specific and related to ionic strength or the presence of anions, the inhibitor activity of both sodium chloride and disodium phosphate were determined in similar concentration ranges. Only P5P had inhibitory activity (Figure V.5).

NAP-Taurine

The photoaffinity label, NAP-taurine, was found to be an effective inhibitor of quartz membranolytic activity (see Figure V.6). The vermillion-colored NAP-taurine is photo-activated to a highly reactive group called a nitrene (Staros and Richards, 1974). The nitrene group is reactive enough to displace a hydrogen from a carbon-hydrogen bond (Knowles, 1972). Arylnitrenes have a range of lifetimes from 0.1 to 1.0msec in hydrolytic solvents (Reiser et al, 1968). The photoactivated nitrene can form covalent bonds with proteins, lipids, and carbohydrates, although the predominant stable products are probably secondary amines produced by insertion into a carbon-hydrogen bond (Smith, 1970).

At 0°C, the NAP-taurine does not enter the erythrocytes to any significant extent (Staros and Richards, 1975). It was also found that the probe had a high affinity for band 3 (see Fairbanks et al, 1971 and Steck, 1974, for discussion of nomenclature). At 37°C, the NAP-taurine enters the erythrocyte via a pathway inhibited by DIDS (Cabantchik et al, 1976). The earlier observation that NAP-taurine has a

high affinity for band 3 was confirmed by this study.

The NAP-taurine probe can inhibit anion transport bound to either side of the membrane. If two erythrocyte suspensions were exposed to NAP-taurine, one at 37°C and the other at 0°C, and then photolyzed to make the bonding covalent, the labeling would be different. The erythrocytes exposed at 37°C and photolyzed have the label internally bound while the erythrocytes exposed at 0°C and photolyzed have the probe bound externally. Data obtained on the transport of chloride and sulfate in these cells showed marked differences depending on how the cells were labeled. The probe was 15 times more effective as an anion transport inhibitor when bound externally than internally (Knauf et al, 1978a). The position of the probe was further characterized by using radioactively labeled probes and then enzymatically cleaving the erythrocyte membrane proteins. The fragments are then separated using SDS-polyacrylamide gel electrophoresis to determine which fragment contains the label (Knauf et al, 1978b).

Non-Covalent Inhibitors of Anion Transport

Phloretin and its derivatives were studied to determine their inhibitory effect on quartz membranolytic activity. Phloretin, also known as 2',4',6'-trihydroxyl-3-(p-hydroxylphenyl) propiophenone, is almost insoluble in water. Phloridzin, sometimes called phlorizin, differs from phloretin in that it has a glucose in the 2' position of the aromatic ring alpha to the ketone that makes phloridzin much

more water-soluble. Only the more soluble phloridzin had an inhibitory effect (Figure V.8).

Phloretin is an effective inhibitor of anion transport in the micromolar range (Knauf et al, 1979). It is an effective inhibitor of monosaccharide transport from either side of the erythrocyte membrane (Benes et al, 1972). Phloretin has been shown to effect the interfacial dipole fields of thin lipid membranes (Andersen et al, 1978). Structure activity studies of the effect of phloretin on chloride permeability support this observation (Cousin and Motais, 1978). Phloretin has been shown to be a competitive inhibitor with the anion transport inhibitor, 4,4'-dibenzamido-2,2'-disulfonic acid stilbene (DBDS) (Forman et al, 1982). DBDS is a fluorescent analog of DIDS. Phloretin has a high affinity for band 3 and at higher concentrations it can interact with the lipid bilayer.

Phloridzin is a less effective inhibitor of anion transport than phloretin. It is effective in the millimolar range (Knauf et al, 1979). This molecule has a low dipole moment (Andersen et al, 1976) and does not effect the binding of 1-fluoro-2,4-dinitrobenzene or H_2DIDS to band 3 (Passow, 1977). As an inhibitor of sulfate, chloride, and iodide exchange, phloridzin is effective only externally (Lepke and Passow, 1973; Schnell et al, 1973).

DISCUSSION AND CONCLUSIONS

Quartz membranolytic activity can be inhibited by the

presence of anion transport inhibitors. DIDS and SITS, the two inhibitors shown to bind to the anion transport receptor, were the most effective inhibitors of quartz membranolytic activity. On the other hand, phloretin, thought to be a non-competitive inhibitor of anion transport, had no effect on quartz membranolysis (Knauf, 1979). DIDS is a more effective inhibitor of anion transport than SITS. The same was found to be true for their relative inhibition of quartz membranolytic activity.

By binding radioactively labeled DIDS to the erythrocyte membrane under the conditions shown in Figure V.1 and then isolating the membranes and then separating their constitutive proteins using SDS-polyacrylamide gel electrophoresis, 95% of the label is found associated with band 3 (Cabantchik and Rothstein, 1974a). Maximum inhibition of quartz membranolytic activity at low DIDS concentration occurs at 1.13uM DIDS. There are 1.2×10^{6} copies of band 3 per erythrocyte and 1.8×10^{8} erythrocytes per milliliter in the standard erythrocyte suspension (Branton, 1983). This means there are 2.16×10^{14} band 3 proteins per milliliter of erythrocyte suspension. At a concentration of 1uM DIDS, about 10^{14} DIDS molecules per milliliter are present. The high affinity inhibition becomes a maximum at approximately one DIDS molecule/band 3 protein.

Under the conditions described above, the DIDS molecules are thought to bind to the receptor site of anion transport (Knauf, 1979). These data support the hypothesis

that quartz surface charge can damage the erythrocyte membrane by interacting with the anion transport receptor on band 3. The possibility that the unbound DIDS is interacting with the quartz surface is small considering that the inhibition is the same when DIDS is bound irreversibly (very little unbound DIDS is present to interact with the quartz surface under conditions of irreversible binding).

Pyridoxal 5'-phosphate was also found to be an effective inhibitor of quartz activity. The probe at a higher concentration than DIDS or SITS was very effective and it has a high selectivity for proteins (Cabantchik et al, 1975). Virtually all of the activity can be inhibited by P5P and this strongly suggests that quartz membranolytic activity is a protein-mediated process. It has previously been speculated that a quartz/lipid interaction is important in lysis (Weissmann and Rita, 1972; Dakorosy and Tabuch, 1973).

The NAP-taurine inhibited quartz activity although it is thought to bind to a modifier site and not the anion transport receptor (Knauf et al, 1978a, b). The probe is known to reduce the binding of DIDS and it may act as a steric hindrance to SiO^-/erythrocyte interaction.

Phloridzin was an effective hemolytic inhibitor while phloretin was not. This is unexpected because phloretin is a more efective anion transport inhibitor than phloridzin (Knauf, 1979). Although phloretin and phloridzin are structural analogs and both inhibit anion transport non-

competitively, the mechanism of action is thought to differ. Phloretin has been shown experimentally to have a strong interaction with lipids (because of its high dipole moment), but this is not true for phloridzin (Andersen et al, 1978). The observation that one probe inhibits quartz membranolytic activity while the other does not further supports the idea of different mechanisms. It is not the inhibition of anion transport which is important, then, it is specifically blocking the anion transport receptor which is critical for inhibition of quartz membranolytic activity.

Table V.1 -- Effect of DIDS at high concentrations on quartz membranolytic activity. The erythrocytes, from a single donor, were washed and standardized in VBS containing various concentrations of DIDS. The DIDS and the erythrocytes were allowed to stand for 10 minutes at room temperature before the addition of quartz. The quartz and DIDS treated erythrocytes were then incubated at 37°C for 120 minutes.

SiO_2 mg/ml	Control %H	10^{-7}M DIDS %H	10^{-6}M DIDS %H	10^{-5}M DIDS %H	10^{-4}M DIDS %H
---	1.4	1.5	1.7	1.2	2.6
0.375	10.7	7.5	6.5	6.1	3.0
0.750	18.8	12.6	11.4	9.9	3.2
1.125	24.9	17.0	14.6	13.1	5.0
1.50	29.8	19.6	17.2	15.8	6.0

Control $\%H = 17.04X + 4.97$, $r^2 = 0.99$, HC50 = 2.64mg/ml

10^{-7}M DIDS $\%H = 10.89X + 3.96$, $r^2 = 0.98$, HC50 = 4.23mg/ml

10^{-6}M DIDS $\%H = 9.41X + 3.60$, $r^2 = 0.98$, HC50 = 4.93mg/ml

10^{-5}M DIDS $\%H = 8.66X + 3.12$, $r^2 = 0.99$, HC50 = 5.41mg/ml

10^{-4}M DIDS $\%H = 2.90X + 1.61$, $r^2 = 0.92$, HC50 = 16.69mg/ml

Table V.2 -- Effect of DIDS on quartz membranolytic activity under conditions of irreversible binding. Seven milliliters of packed erythrocytes were added to 50ml of VBS which contained 70uM DIDS and the suspension was allowed to stand for 36 hours at 4°C. The control was the same concentration of erythrocytes suspended in 50ml of VBS without DIDS. After 36 hours, the cells were spun down and the unbound DIDS removed by washing three times with 50ml of VBS. The standard erythrocyte suspensions were made and then challenged with quartz.

SiO_2 mg/ml	Control %H	DIDS Modified %H
---	0.9±0.3	0.8±0.0
0.439	4.0±0.2	3.9±0.1
0.875	16.6±2.6	8.2±0.2
1.313	25.8±2.2	11.8±0.8
1.750	34.0±1.4	14.9±0.3

Control %H = 22.7X -4.73, r^2 = 0.99, HC50 = 2.41mg/ml

DIDS Modified %H = 8.37X + 0.54, r^2 = 0.99, HC50 = 5.91mg/ml

Table V.3 -- UICC Canadian chrysotile was not inhibited by DIDS or SITS under conditions of irreversible binding.* The chrysotile was suspended at 2mg/ml and sonicated at 50 Watts for 5 minutes to disperse the fibers.

UICC Chrysotile ug/ml	Control %H	50uM DIDS %H	75uM SITS %H	150uM SITS %H
---	1.1	1.8	1.1	1.1
2.5	3.1	3.8	4.0	3.9
5.0	5.8	6.6	8.7	7.2
10.0	11.2	13.0	18.6	14.7
20.0	22.2	25.9	29.7	26.3

*The erythrocytes were modified with DIDS and SITS as described in Figure V.3

Figure V.1 -- Inhibition of quartz membranolytic activity by DIDS. The standard erythrocyte suspension was modified with various concentrations of SITS and allowed to stand for 30 minutes at room temperature before the addition of quartz. The quartz was then added to the DIDS-modified erythrocytes and incubated at 37^{o}C for 120 minutes. The concentration of quartz was held constant at 1.5mg/ml.

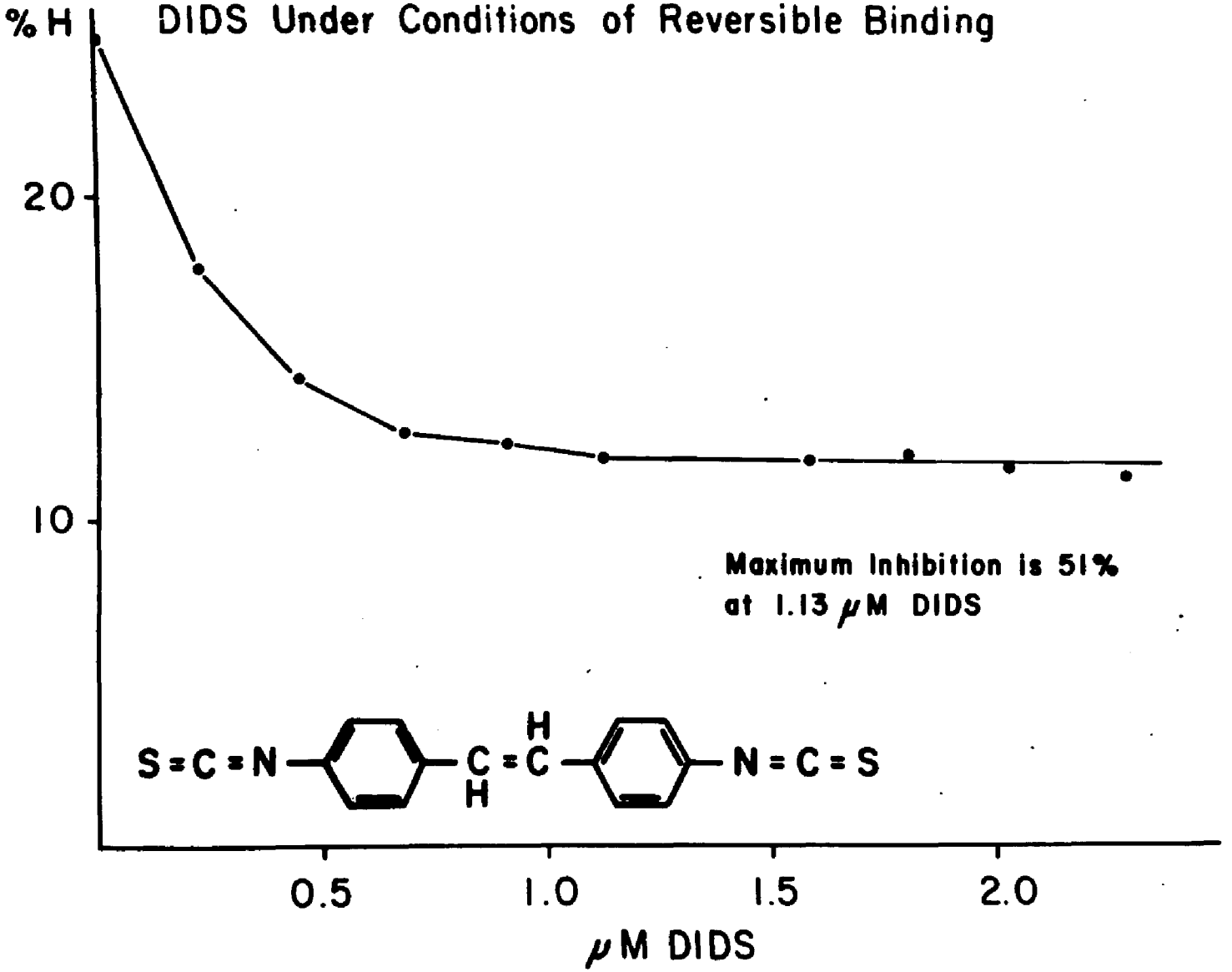
% H
DIDS Under Conditions of Reversible Binding
20
10
Maximum Inhibition is 51%
at 1.13 μM DIDS
S=C=N
C
H
H
C=C
N=C=S
0.5
1.0
1.5
2.0
μM DIDS

Figure V.2 -- Inhibition of quartz membranolytic activity by SITS. The standard erythrocyte suspension was modified with various concentrations of SITS and allowed to stand for 135 minutes at room temperature before the addition of quartz. The quartz was then added to the SITS-treated erythrocytes and incubated at 37^{o}C for 120 minutes. The concentration of quartz was held constant at 1.5mg/ml.

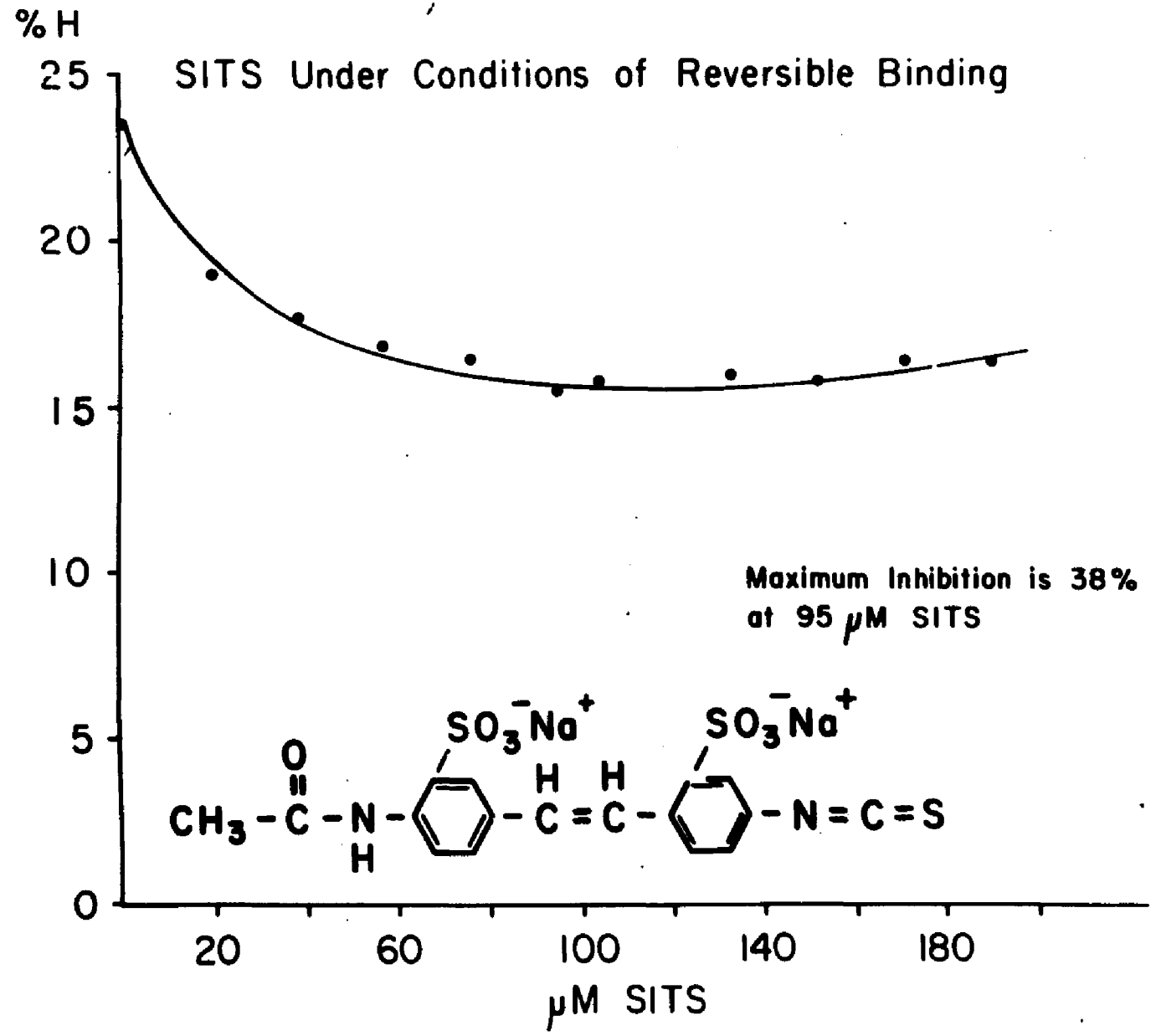
%H
SITS Under Conditions of Reversible Binding
25
20
15
10
5
0
Maximum Inhibition is 38%
at 95 μM SITS
SO3⁻Na⁺
SO3⁻Na⁺
O
CH3-C-N-
H
H H
-C=C-
-N=C=S
20
60
100
140
180
μM SITS

Figure V.3 -- Inhibition of quartz membranolytic activity by irreversibly bound DIDS and SITS. The erythrocytes were washed three times with VBS. Then 2ml of the washed packed erythrocytes were brought to 50ml with each of the following solutions: a) 50uM DIDS in VBS; b) 150uM SITS in VBS; and c) VBS without any inhibitor as a control. All three suspensions were stored at $4^{o}C$ for 72 hours. The three suspensions were then standardized and challenged with quartz. The erythrocytes and quartz were incubated at $37^{o}C$ for 120 minutes.

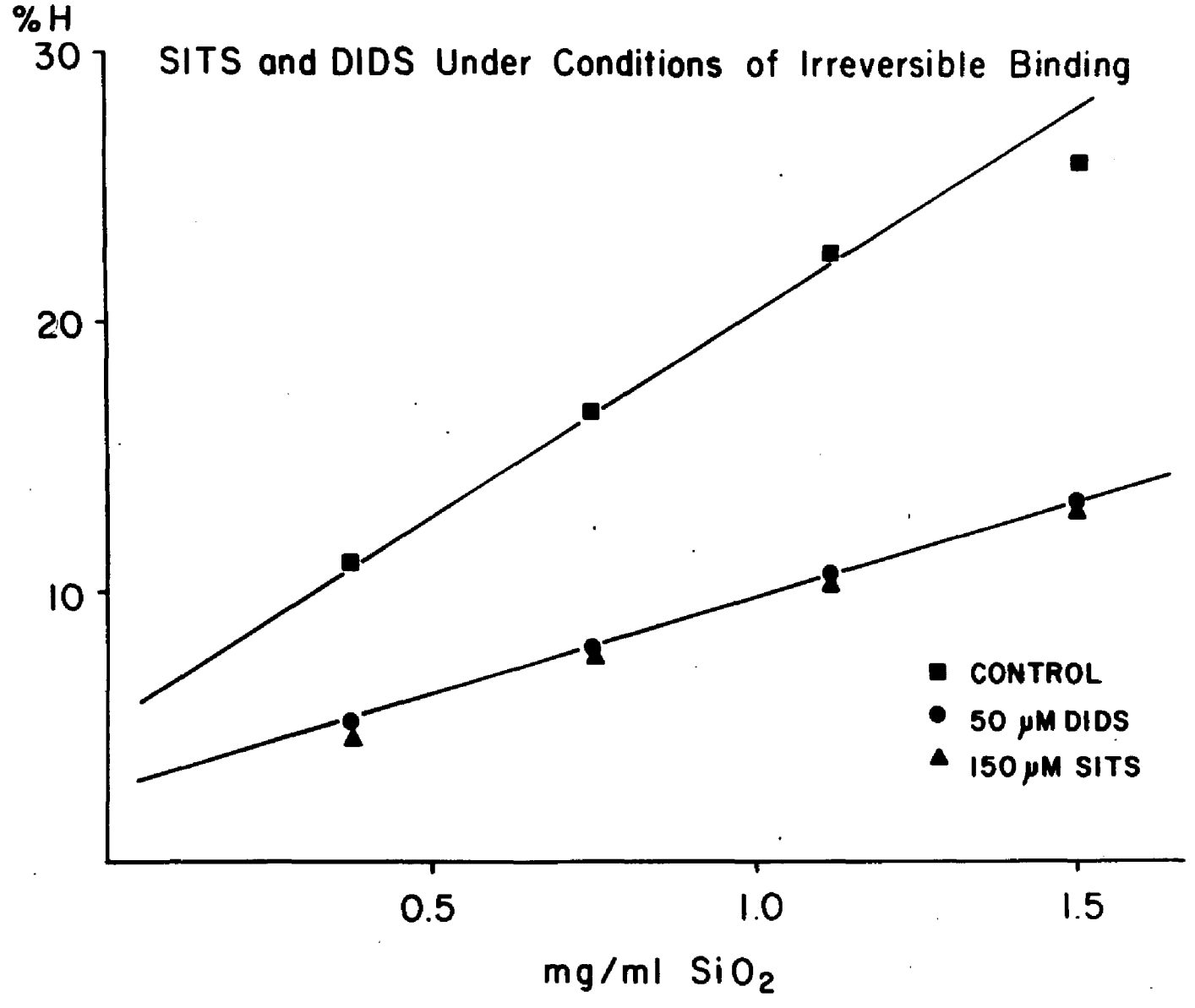
%H
30
20
10
SITS and DIDS Under Conditions of Irreversible Binding
CONTROL
50 μM DIDS
150 μM SITS
0.5
1.0
1.5
mg/ml SiO_2

Figure V.4 -- Inhibition of quartz membranolytic activity by pyridoxal 5'-phosphate. The erythrocytes and the probe were incubated at room temperature for 30 minutes before the addition of quartz. The quartz was then added to the pyridoxal 5'-phosphate-modified erythrocytes and incubated at 37^{o}C for 120 minutes. The concentration of quartz was held constant at 1.5mg/ml.

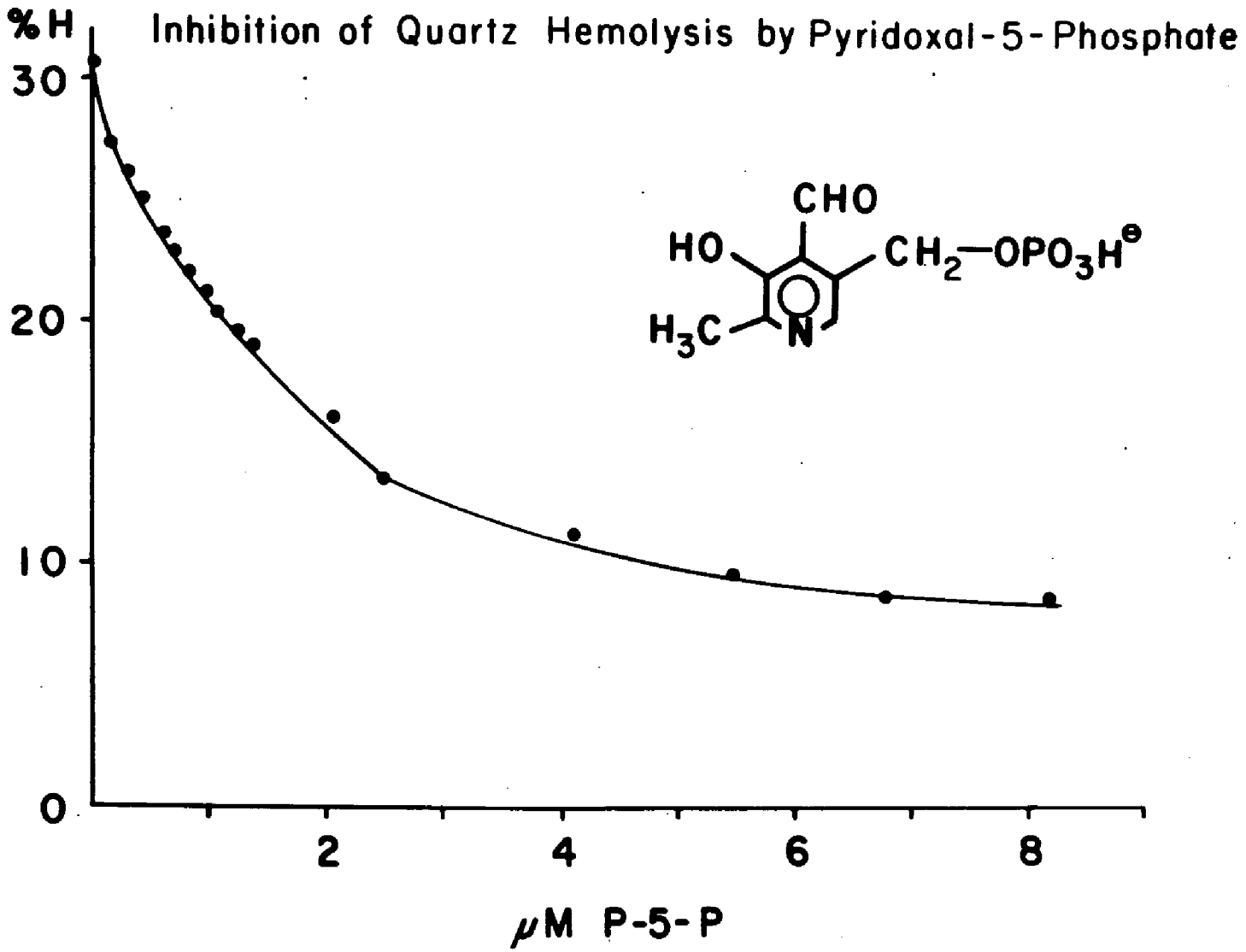
%H
Inhibition of Quartz Hemolysis by Pyridoxal-5-Phosphate
30
20
10
0
2
4
6
8
μM P-5-P
CHO
HO
CH2—OPO3H⊖
H3C
N

Figure V.5 -- Effect of pyridoxal 5'-phosphate, sodium chloride, and disodium phosphate on quartz membranolytic activity. The compounds were incubated with erythrocyte suspensions at room temperature for 30 minutes before the addition of quartz. The quartz and the modified erythrocyte suspensions were incubated at 37^{o}C for 60 minutes.

Figure V.6 -- Inhibition of quartz membranolytic activity by NAP-taurine. The standard erythrocyte suspension was modified with various concentrations of NAP-taurine and allowed to stand at ice temperatures for 170 minutes in the dark. The NAP-taurine-modified cells were then challenged with quartz and incubated at 37^{o}C for 120 minutes.

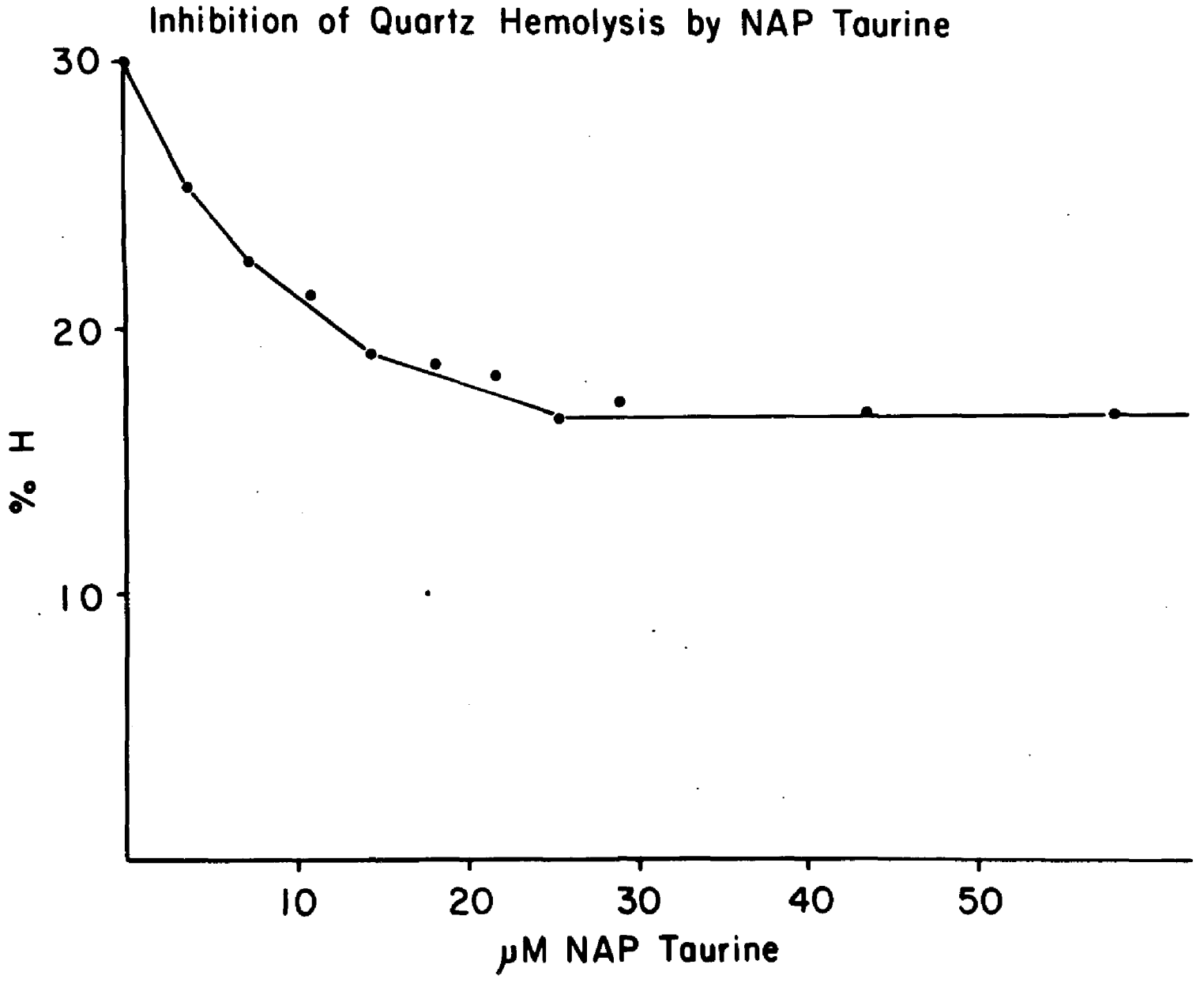
Inhibition of Quartz Hemolysis by NAP Taurine
30
20
10
% H
10
20
30
40
50
μM NAP Taurine

Figure V.7 -- Effect of phloretin and phloridzin on quartz membranolytic activity. The standard erythrocyte suspension was modified with various concentrations of phloretin or phloridzin and allowed to stand at room temperature for one hour. The quartz was then added to the modified erythrocytes and incubated at $37^{\circ}C$ for 120 minutes.

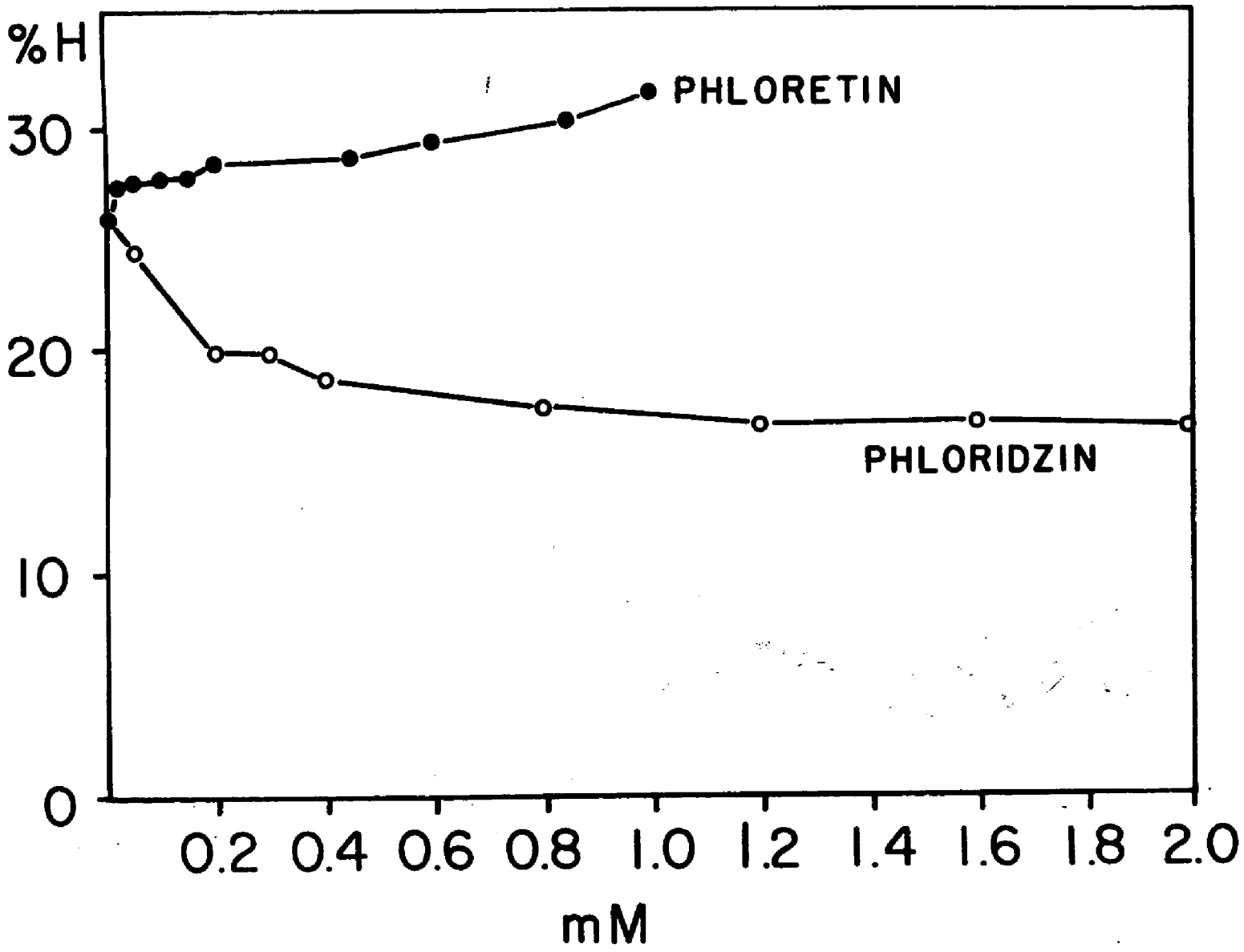
%H
30
20
10
0
PHLORETIN
PHLORIDZIN
0.2 0.4 0.6 0.8 1.0 1.2 1.4 1.6 1.8 2.0
mM

CHAPTER VI

Membranolytic Activity of Rutile and Anatase -- Two Titanium Dioxide Polymorphs

INTRODUCTION

The occurrence of interstitial fibrosis, bronchiolo-alveolar adenomas and squamous cell carcinomas in rats exposed to high concentrations of synthetic rutile by inhalation has recently been reported (Lee et al, 1985a, b). Previously, very low biological activity was attributed to both of these titanium dioxide polymorphs. To underscore how inert rutile and anatase have been considered, these materials were often used as control or "sham" dusts against which the activity of other mineral particulates were compared (Ferin and Oberdorster, 1985; Richards et al, 1985). In support of these observations, a few studies of workers engaged in the synthesis of titanium dioxide have failed to demonstrate health effects attributed specifically to inhalation of titanium dioxide dust (Uragado and Pinto, 1972; Daum et al, 1977). Although both of the titanium dioxide polymorphs have occasionally been found to have *in vitro* properties consistent with a biologically active particulate (Harington et al, 1971; Zitting and Skytta, 1979), they are today generally considered inert.

Both rutile and anatase are important materials in a number of consumer products, e.g., as pigment in paints, food items, cosmetics, etc. (Verbonic, 1985). Titanium dioxide production in the United States for the year 1985 is expected to exceed 800,000 tons (Table VI.1). Virtually all of the synthetically produced titanium dioxide is in the respirable-size range. The widespread use of these

materials and its ubiquitous presence in the environment raises several important issues: What is the biological activity which may be attributed to the titanium dioxide polymorphs, in all the forms in which it can exist, and, were the results of the most recent inhalation study valid (Lee et al, 1985a, b)?

The interstitial fibrosis and lung tumors caused by synthetic rutile upon inhalation (Lee et al, 1985b) cannot be readily compared to previous reports in the literature for the following reasons: 1) often, the specific titanium dioxide polymorph used experimentally in these studies was not properly identified (Lee et al, 1985b); 2) no data on particle size distribution were given for the materials used; and 3) important surface characteristics of the particle, i.e., the ability to bind specific polymers, or the biological activity in one of the in vitro assays commonly used in pneumoconiosis research for the assessment of the toxicity of inorganic matter, were not determined (Leyko and Gendek, 1985). It would also have been useful if the source of the material had been reported. The use of minerals in some experiments often reflects the presence or absence of specific trace metals, e.g., iron, which has been shown to lessen the activity of other oxide minerals, i.e., quartz (Langer, 1978; Engelbrecht and Thiart, 1972).

The only identification frequently given for materials tested is titanium dioxide (Lee et al, 1985a). However, often the characterization may be incomplete or misleading. As examples, Aldrich Chemical Company's titanium oxide-

anatase is a mixture of rutile and anatase; Fisher Scientific Company's titanic oxide is pure anatase; the British MRC Pneumoconiosis Research Units' "respirable TiO_2" used as a control dust, is a mixture of rutile and anatase (Table VI.3). The conflicting reports concerning the biological activity of titanium dioxide found in the literature may in part be related to inadequate characterization of the mineral.

The following section provides a brief description of some important mineralogical differences between the titanium dioxide polymorphs which facilitate interpretation of the data presented.

Naturally Occurring Titanium Dioxide Polymorphs

Three titanium dioxide polymorphs have been identified in nature: rutile, anatase, and brookite (Deer et al, 1972). Brookite is unimportant in terms of human exposure and is included in the data comparison (Table VI.2) only for completeness. Rutile and anatase are formed under a wide range of physico-chemical conditions and are present throughout a number of geological provenances. Although common in nature, industrially used titanium dioxide is mostly the product of chemical synthesis.

Crystal Structure of the Titanium Dioxide Polymorphs

The three crystal structures of TiO_2 are made of titanium octahedrally coordinated with oxygen atoms. They display a six-fold coordination of oxygen about a titanium

atom, with each of the oxygens occupying the corners of a regular octahedron. In turn, every oxygen atom is coordinated with three titanium atoms which occupy the approximate corners of an equilateral triangle. This structure has been referred to as a 6:3 coordination and is referred to by crystallographers as the "rutile structure" (Table VI.2) (Bragg et al, 1965; Bunn, 1961). Though this coordination is constant, the octahedra bond angles and distances differ between the polymorphs so that the sharing of edges of the octahedrons increase from two in rutile to three in brookite to four in anatase. For the two most commercially important polymorphs, rutile and anatase, the position of the octahedra in the lattice and the number of octahedra in the unit cell differ. Anatase contains four TiO_2 molecules per unit cell while rutile contains two. As edges and faces of the octahedra are increasingly shared, the titanium distances decrease setting up cation-repulsive forces. This decreases the stability of the mineral structure and is reflected in such basic features as hardness and solubility. Rutile, the most stable, is the hardest and least soluble polymorph (Pauling, 1961).

Crystal Structure and Surface of Titanium Dioxide Polymorphs

The small variations in the structure of rutile and anatase lead to different cleavage and twin planes along which separation tends to occur. Therefore, one would assume that the density of surface titanols and their isoelectric point for anatase and rutile would be different

regardless of whether the crystals were grown to a certain size or reduced in size from larger particles (Table VI.2) (Furlong and Parfitt, 1978).

Chemistry of the Titanium Dioxide Polymorphs

The bulk chemistry for the titanium dioxide polymorphs has the empirical formula TiO_2. However, the natural titanium dioxide specimens contain substantial quantities of trace or minor metals and even discrete mineral impurities (Table VI.3). Although the naturally occurring titanium dioxides possess very high light dispersion capacity, natural minerals cannot be used as a pigment because of the trace metal content which imparts dark color and occasionally even opacity (Kitel, 1967). It has been noted that iron substitution not only effects the optical properties of rutile but alters its density as well.

The hydration of anatase gives rise to two different titanol groups, each with a different reactivity (Kennedy, 1979). Comparing the hydrated surface of anatase with rutile, it is observed that the titanol vibrations occur at $3717cm^{-1}$ and $3676cm^{-1}$ in anatase. The doublet is produced by the two titanol groups on the (001) plane. The single titanol vibration of rutile occurs at $3780cm^{-1}$. The chemical reactivity of these protonated surfaces differs markedly (Kennedy, 1979).

It has been noted that the titanol vibration at $3676cm^{-1}$ on anatase disappears at $150^{o}C$, whereas the rutile may be heated to temperatures in excess of $200^{o}C$ with

preserved titanol vibration. At higher temperatures, up to 450°C, a titanol vibration has been resolved at 3740cm^{-1}. The rutile surface still has scattered titanols at 610°C. The importance of temperature-stable titanols with regard to biological activity is discussed later.

Preparation of Synthetic Titanium Dioxide for Pigment

Two commercial processes, sulfate and chloride, are used to produce synthetic rutile and anatase. The sulfate process is the older of the two and the bulk of the world TiO_2 pigment product is made by this process. The starting material for the sulfate process is ilmenite ore ($FeTiO_3$), which is converted to $TiOSO_4$ after reaction with concentrated sulfuric acid at 150-180°C:

$$TiO_2FeO + H_2SO_4 \rightarrow TiOSO_4 + FeSO_4 + H_2O$$

This solution is then cooled, filtered, and concentrated by evaporation under reduced pressure to crystallize the ferrous sulfate. The crystalline $FeSO_4$ is separated. The titanium sulfate solution is then hydrolyzed by heating to 90°C to form insoluble titanyl hydroxide:

$$TiOSO_4 + 2H_2O \rightarrow TiO(OH)_2 + H_2SO_4$$

The titanyl hydroxide precipitate is then separated from the solution by filtration and washed extensively to remove all traces of discoloring elements (Fe, Cr, V, and Mn). The hydrated precipitate is then modified to produce the characteristics desired in a pigment. If the solution is seeded with rutile prior to hydrolysis, then rutile is formed. In the absence of seed crystals, the product will

be anatase. The modified precipitate is calcined at 800-1000°C (see Figure VI.1).

The chloride process was commercially developed in the 1950s and requires an enriched titanium dioxide ore. The ilmenite may be beneficiated or natural rutile used. The high grade titanium dioxide ore (70-85% TiO_2) is chlorinated in a fluidized bed reactor with coke at 925-1010°C:

$$TiO_2 + C + 2Cl_2 \rightarrow 2CO + TiCl_4$$

The volatile titanium tetrachloride is then separated from the unreacted solids and non-volatile chlorides by double distillation. Impurities can alter the brightness and color of the pigment. The $TiCl_4$ is then reacted with O_2 in a flame reaction at 925°C. This reaction produces fine particle TiO_2 and liberates Cl_2 gas, which is recycled (see Figure VI.2):

$$TiCl_4 + O_2 \rightarrow TiO_2 + Cl_2$$

The low temperature sulfate process can be used to produce either 100% rutile or 100% anatase, while the high temperature chloride process cannot be used to produce a 100% anatase product and is generally used to produce rutile (see Singer, 1982; Knittel, 1982; and Whitehead, 1982).

MATERIALS AND METHODS

Sixteen specimens of rutile and anatase were studied experimentally:

I. Naturally-Occurring Titanium Dioxide:

Rutile, Muiane Altoligoha, Mozambique, Africa --

obtained as two single crystals, together weighing approximately 4gm, from the Department of Mineral Sciences, Catalogue #27404, The American Museum of Natural History, Central Park West at 79th Street, New York, NY, 10024.

Rutile Sand, Myrtle Beach, South Carolina -- obtained as a coarse powder from Ward's Natural Science Establishment, Inc., Rochester, NY.

Rutile, Graves Mountain, Georgia -- obtained as a large euhedral crystal weighing approximately 25gm, from Ward's Natural Science Establishment, Inc., Rochester, NY.

Rutile, Champion Mine, White Mountains, Mono County, California -- obtained as a large euhedral crystal weighing approximately 25gm, from Ward's Natural Science Establishment, Inc., Rochester, NY.

Anatase, Minas Girais, Brazil -- obtained as a collection of pellets from Ward's Natural Science Establishment, Inc., Rochester, NY.

The above five specimens were ground dry by hand in a carborundum mortar until the particle size was fine enough to pass through a 45um mesh screen.

II. Synthetic Titanium Dioxide: The following specimens were obtained as fine industrial powders:

Titanium Dioxide #10082 -- obtained from N.

Wotherspoon, Mount Sinai School of Medicine (reportedly a rutile made by Dupont).

Titanium Dioxide, Rutile -- Central Research and Development Department, E.I. Dupont de Nemours & Co., Inc., Haskell Laboratory for Toxicology & Industrial Medicine, Haskell #11,564, P.O. Box 50, Elkton Road, Newark, Deleware, 19714.

Titanic Oxide Anhydrous -- Fisher Scientific Company, Fairlawn, NJ (chemical reagent grade).

Titanium (IV) Oxide Anatase -- Aldrich Chemical Company, Inc., Milwaukee, WI (chemical reagent grade).

III. Titanium Dioxide Specimen Used in Penumoconiosis Laboratories as Controls. The following specimens were obtained from Pneumoconiosis Laboratories and have been used as inert control dusts experimentally.

Respirable TiO_2 PRU No. 159 (Hexhlet Collected) obtained from R. Davies, MCR Pneumoconiosis Unit, Llandough Hospital, Penath S. Glamorgan, U.K.

Titanium Dioxide -- obtained as two separate specimens called IOM-1 and IOM-2 from K. Donaldson, Institute of Occupational Medicine, Roxburgh Place, Edinburgh, U.K.

Titanox AWO -- obtained from R.J. Schnitzer, Mount Sinai School of Medicine.

IV. Anatase Specimens. The following specimens were

obtained from K. Towe, Smithsonian Institution, Washington, DC.

Calcined anatase -- origin through industrial processing; synthetic.

Milled anatase -- origin through industrial processing; synthetic.

Precipitated $TiO_2:xH_2O$ -- origin through industrial processing; synthetic.

The following quartz specimens were obtained as fine industrial powders from Pennsylvania Glass and Sand Company and were used as positive controls in the hemolytic test systems.

Min-U-Sil 5 and Min-U-Sil 15 -- Both specimens were obtained as fine industrial quartz powders. The 5 and 15 denotes that 98% of the particles are less than 5 and 15um in size, respectively. The 1 and 2um Stokes' diameter of each specimen was separated by sedimentation techniques (Nolan and Langer, 1983). Min-U-Sil 15 was used as a positive control (Nolan et al, 1981).

Binding studies, for determination of the hydrogen bonding character of the mineral surface, were carried out with:

2-poly(vinylpyridine-N-Oxide) obtained from Polyscience, Inc., Warrington, PA. The weight-average molecular weight of the 2-PVPNO polymer, as determined by light scattering, was ~276,000 (Nolan and Langer, unpublished data).

Characterization of Specimens

The examination of these specimens by polarized light microscopy and continuous scan x-ray diffraction was carried out for: determination of the presence or absence of crystalline impurities; ascertainment of gross size distribution; identification of specific polymorphic phase.

Polarized light microscopy. Approximately 0.1mg of powder was withdrawn from each specimen and placed on a glass slide. The powder was covered with an immersion oil (n = 1.52) and dispersed by sliding another glass slide across the preparation surface. Virtually every specimen smeared to yield a uniform homogeneous distribution. The natural specimens produced a yellow-brown opaque suspension in natural light, whereas the synthetic specimens produced an opaque white suspension. The smear was further "wetted" with an additional drop of immersion oil and then a cover slip placed on its surface. The preparations were examined by polarized light microscopy, both in plane polarized light and between crossed Nicols, at magnification ranging from 35X-500X magnification.

The natural minerals are composed of large-sized, yellow-brown fragments. Some particles are 100um in greatest dimension, but the numerically preponderant size is about 3-5um. Single rutile particles show twin-plane lamellae, as well as some mineral intergrowths. These latter impurities are clearly evident when specimens are viewed between crossed Nicols. Quartz, other silicates, e.g., micas and clays, and brown opaques (limonite

minerals?) are observable in several specimens and are not restricted to any single polymorphic species.

In contrast, the synthetic preparations are all fine-grained with particles <1um in size, and with no visible mineral impurity. The impressive features of the synthetic materials are their small and uniform particle sizes, purity, and opacity.

Continuous scan x-ray diffraction. Two hundred milligrams of powder were withdrawn from each specimen, tamped into a 1x2cm area in an aluminum specimen holder, and subjected to continuous scan x-ray diffraction analysis. The experimental conditions are identical to those used for the analysis of silica specimens (Nolan et al., 1981). The x-ray diffraction tracings were converted to d-spacings and these were compared with standard diffraction data for rutile (ASTM 21-1276), anatase (ASTM 21-1272) and other minerals. The results are given in Table VI.3.

Size Distribution Measurements

Each titanium dioxide specimen and the 1 and 2um Stokes' diameter fractionated by sedimentation from Min-U-Sil 5 and Min-U-Sil 15 were photographed by transmission electron microscopy at 2000x direct magnification, and were photographically enlarged 2.5x to yield a final enlargement of 5000x (Nolan and Langer, 1983). The longest dimensional aspect was measured as particle diameter. The results are, therefore, skewed toward larger particle-size values. The particle size distribution of the titanium dioxide specimens

studied and the five quartz specimens used as controls are given in Table VI.4.

Hemolytic Model

The ability of each of the titanium dioxide and quartz specimens to alter the permeability of the human erythrocyte was determined quantitatively. The erythrocytes were obtained from peripheral blood (50ml) taken by venipuncture in a plastic syringe containing 15U/ml preservative-free heparin. Ficoll-Hypaque gradient centrifugation was used to separate the peripheral blood lymphocytes and plasma proteins from the erythrocytes. Fifty ml of blood was diluted with an equal volume of saline, overlaid onto a 25ml Ficoll-Hypaque gradient and centrifuged at F~850g at 20^{o}C for 45 minutes. The lymphocytes and plasma proteins were removed and the erythrocytes were stored at 4^{o}C and used within a week (Nolan et al, 1981).

Before the stored erythrocytes were used, approximately 5ml of packed human erythrocytes were diluted to 50ml with pH 7.4 veronal buffered saline (VBS, 2.4mM sodium barbital and 145mM sodium chloride) in a plastic centrifuge tube and spun at F~800 g at room temperature for 30 minutes. The erythrocyte wash was repeated twice. Using optical spectroscopy, the washed human erythrocytes were made into a standard suspension which contained approximately 3.6 x 10^{8} cell/ml (Nolan et al, 1981).

A single stock suspension of each specimen was also made in VBS. To disperse the suspensions, each was

sonicated using a Sonifier Cell Disrupter (Heat Systems - Ultrasonics Inc.) at 50 watts power for several minutes until the suspension was visibly homogeneous. Each of the stock mineral suspensions were diluted to four concentrations (mg/ml) in duplicate. Each of the four different dilutions were adjusted to 4ml, and the 4ml of the standard erythrocyte suspension was added. The final volume at each concentration was 8ml, and the erythrocyte concentration was 1.8×10^8 cells/ml. The powder and erythrocytes were incubated at $37^{\circ}C$ for 120 minutes and shaken continuously with a gyratory motion. The plot of mg/ml of mineral vs. %H is generally linear up to about 40% hemolysis, below which value all measurements fell. The duplicate determinations were averaged, and the values are shown with their variance. Linear regression analysis was made for each set of eight points and the equation of the line calculated. This equation is used to compute the HC50, the concentration of powder (in mg/ml) required to lyse half of the erythrocytes in the suspensions.

Determination of 2-poly(vinylpyridine-N-Oxide) Binding

The amount of 2-PVPNO that bound to selected titanium dioxide and quartz specimens was determined quantitatively. Various amounts of the mineral powders were weighed out into glass centrifuge tubes and to each was added 30ml of 50ug/ml 2-PVPNO in distilled water. The tubes were allowed to stand at room temperature for 30 minutes. The tubes were then centrifuged at F~8000g at room temperature for 40 minutes,

which pelletized the powder at the bottom of the tubes. The amount of polymer able to bind to each concentration of powder is thereby removed from the supernatant. The 2-PVPNO polymer has an absorbance peak in the ultraviolet at 260nm, and a molar absorptivity (a) of 5631, calculated using the molecular weight of the monomer (MW 121.1). The absorbance of the supernatant was then measured at 260nm and the concentration of 2-PVPNO removed from the supernatant was assumed to be bound to the powder surface. The data was plotted graphically as mineral powder (mg/ml) vs. 2-PVPNO (ug/ml).

Positive Controls

Unfractionated Min-U-Sil 15 was included in each experiment as a positive control. The Min-U-Sil HC50 value and any variation in this value indicates the extent of difference among the erythrocyte suspensions which may exist, e.g., due to donor, etc.

EXPERIMENTAL RESULTS

Membranolytic Activity of the Titanium Dioxide Specimens

Of the five naturally occurring rutile and anatase specimens studied, none were found to have significant membranolytic activity (Table VI.5). Of the 11 titanium dioxide specimens obtained as fine industrial powders, only two were found to be membranolytically active (Table VI.6, Figures VI.3 and VI.4). These, the Dupont rutile and TiO_2

#10082, were markedly hemolytic. The membranolytic activity of Dupont rutile was compared to four fine particle size quartz specimens and two titanium dioxide specimens used as an inert control in experimental pneumoconoisis (Figure VI.4 and VI.5). The precipitated $TiO_2:xH_2O$, when suspended in VBS, was found to lower the pH to 3 but was adjusted back to pH 7.4 with 1N sodium hydroxide.

Comparison of the Bonding Ability of the Titanium Dioxide Specimens and Quartz With 2-poly(vinylpyridine-N-oxide)

The biological activity of quartz, a potent fibrogenic mineral, has been shown to be related to the ability of that mineral to bind 2-PVPNO (Nash et al, 1966). The current binding studies were carried out to determine if the different membrane behavior observed for the titanium dioxide specimens could be distinguished on the basis of their differential 2-PVPNO binding abilities. If a titanium dioxide specimen could bind the polymer, would it act as an inhibitor of membrane activity, as happens with quartz?

The ability of two membranolytically active rutile specimens to bind 2-PVPNO was quantitatively compared to two fine sized quartz specimens and several of the non-membrane active titanium dioxide specimens. The Dupont rutile and TiO_2 #10082 have hydrogen bonding ability comparable with the 1 and 2um Stokes' diameter fractions of Min-U-Sil 15 (Figures VI.6 and VI.7). The two membranolytically active TiO_2 specimens are of a smaller particle size and thus greater surface area than the two fine particle size quartz

specimens.

The titanic oxide from Fisher did not have the appropriate surface chemistry to hydrogen bond the polymer while the rutile from White Mountain, California, bound relatively high amounts of 2-PVPNO. The amount of 2-PVPNO bound by the California rutile is even more significant considering it is of a much coarser particle size than the Fisher specimen and therefore has much less surface area (Figures VI.6 and VI.7). The concentration of TiO_2 used in the experiment (in Figure VI.6), 5-40mg/ml were on the plateau of the adsorption isotherm (Adamson, 1982). The polymer binding experiment was repeated at lower concentrations of TiO_2 so that an increase in binding could be shown as a function of TiO_2 concentration (Figure VI.5). The titanium (IV) oxide and rutile IOM-1 bound significantly less 2-PVPNO than the two membranolytically active TiO_2 specimens.

The TiO_2 #10082 was found to be the most hemolytic of all the titanium dioxide specimens studied. The concentration of TiO_2 #10082 was held constant at 2.25mg/ml and the amount of 2-PVPNO per tube was varied from 0-25ug/ml. The TiO_2/2-PVPNO tubes were allowed to stand for 30 minutes at room temperature and then challenged with standard erythrocyte suspension as described in Materials and Methods. Almost 88% of the membranolytic activity was inhibited at the highest concentration of 2-PVPNO (Figure VI.8). The polymer binding on the titanium dioxide specimens and its subsequent antagonism of membrane activity

parallels 2-PVPNO effect on quartz.

DISCUSSION AND CONCLUSIONS

The biological potential of the titanium dioxide polymorphs, rutile and anatase, are incompletely understood. Although both of these polymorphs commonly exist in the environment, experimental studies regarding their activities have rarely specified which was studied.

The surface properties of the two polymorphs vary depending on whether they are naturally occurring or synthetically made. The surface properties of synthetic rutile vary greatly depending on the conditions of the synthetic process. Membrane activity probably depends on the conditions of synthesis which control surface chemistry, e.g., titanol formation. The difference in surfaces makes it more difficult to define the biological potential of synthetic rutile and anatase.

The naturally occurring specimens of rutile and anatase used in this study contained a few large, colored particles: the Brazilian anatase fragments were up to 100um in size and were cream colored; all the other natural rutiles also contained large, brownish fragments. These colors suggest the presence of trace metal and mineral impurities. Both of these factors have been linked to reduced membrane activity (Langer, 1978).

Synthetic rutile or anatase form white homogeneously fine powders. Several of the synthetic preparations were

mixtures of both polymorphs (Table VI.3). The synthetic polymorphs differ in composition, color, and particle size as compared to the natural minerals. Virtually every particle within these specimens exists in a size ≤1.0um (see Tables VI.4 and 7). It should be noted that the synthetic materials also differ from the naturally occurring materials in particle shape, tending to be oval-to-rounded, with less straight edges.

Only two of the sixteen specimens tested were found to be membranolytically active in a human erythrocyte model. All the anatase specimens and all the naturally occurring rutiles were found to be inactive (Tables VI.5 and 6). Of the five synthetic rutiles studied, only the Dupont rutile and TiO_2 #10082, were found to be active (Figure VI.3). Other investigators have observed synthetic anatase to be active and rutile inert (Zitting and Skytta, 1979).

The membranolytic activity of the Dupont rutile and TiO_2 #10082 were compared to four fine particle size quartz specimens. Computation of the surface area (SA) for the mineral dusts shows the Min-U-Sil 15 to possess an expressed SA of ~$4.5m^2/gm$ as compared to the Dupont and #10082 rutile's ~$15.7m^2/gm$. These values are based on an average particle size of 0.5um for quartz, and a size of 0.1um for the rutile specimens. The activity of rutile is, therefore, less than quartz on a single particle basis (Table VI.7). Although the synthetic anatase specimens have very small size distributions and possess surface areas as high as those calculated for the active rutiles, they are inactive.

Thus, the importance of the nature of the particle surface is underscored.

The ability of several of the titanium dioxide specimens to bind 2-PVPNO was compared to 1 and 2um Stokes' diameter Min-U-Sil 15. The two active rutiles had the appropriate surface chemistry to hydrogen bond the polymer as did the naturally occurring rutile from White Mountain, California (Figures VI.6 and VI.7). The 2-PVPNO was found to inhibit hemolysis by the TiO_2 #10082. The maximum inhibition for #10082 (Figure VI.8) occurred at about the same concentration of 2-PVPNO as the maximum polymer binding for that TiO_2 at that specific mineral concentration (Figure VI.6). Two other synthetic rutiles and one anatase, all inactive, were unable to bind the polymer. As a point of comparison, much experimental data indicate that the biological activity of quartz is related to the mineral's ability to hydrogen bond 2-PVPNO (Langer and Nolan, 1985). This latter paper highlighted the importance of the SiOH functionality for mineral-cell attachment, claiming it to be required as the initial step in membrane lysis.

The PRU titanium dioxide, the two IOM specimens, and the Dupont specimen have been shown by x-ray diffractometry to be rutile. The PRU rutile has been shown to be weakly cytotoxic to macrophages (Davies et al, 1984). Electron microscopic studies show them all to be of similar particle-size and therefore to have comparable surface area. However, the surface properties of the active rutile are clearly different from that of the other three specimens.

These chemical differences are recognized by the erythrocyte membrane.

A single mineral species may possess a range of biological activities depending on the nature of the chemical functionalities at the particle surface and its particle size distribution and trace metal content. Anatase and rutile appear to have a range of biological activity.

Table VI.1: Production of synthetic titanium dioxide in the United States -- 1985

Producer	Location	Production in Tons/Year Sulfate*	Chloride*
Dupont de Nemours	Antioch, CA	.....	35,000
	DeLisle, MS	.....	150,000
	Edge Moor, DE	.....	110,000
	New Johnsonville, TN	.....	228,000
Kenira Oy (Finnish)	Savannah, GA	66,000	.....
Kerr-McGee	Hamilton, MS	.....	64,000
SCM Corporation	Ashtabula, OH	.....	42,000
	Baltimore, MD	66,000	43,000

NL Industries no longer operates U.S. plants. St. Louis, MO, plant was closed in 1980, as was Sayerville, NJ, plant. Most sulfate plants closed because of stringent EPA pollution codes.

*Sulfate process produces anatase; chloride process produces rutile.

Foreign produced titanium dioxide now constitutes about 20% of U.S. consumption: sources from Canada, Norway, Belgium, West Germany.

Based on data from the U.S. Minerals Yearbook, 1981, chapter on titanium by Lynd and Hough, and on data reported in an article by C. Verbonic, Chemical Business, August, 1985.

Table VI.2: Comparison of the physical and chemical properties of the titanium dioxide polymorphs

Property	TITANIUM DIOXIDE POLYMORPH		
	Rutile	Anatase[1]	Brookite
X-ray data ASTM SPDF*	21-1276	21-1272	16-617
Crystal system	Tetragonal	Tetragonal	Orthorhombic
Space group	$P4_2/m\ nm(136)$	$14_1/a\ md\ (141)$	P cab (61)
Unit cell x-axis	4.5933(4.59)	3.7852(3.78)	9.1819(9.14)
y-axis	.....	.....	5.4559(5.44)
z-axis	2.9592(2.96)	9.5139(9.50)	5.1429(5.15)
Z-cell	2	4	8
Density[2]	4.250(4.18-4.25)	3.893(3.82-3.95)	4.119(3.87-4.12)
Packing coordination	6:3 HCP	6:3 CCP	6:3
Bulk chemistry	TiO_2	TiO_2	TiO_2
Trace metals	Cr,V,Fe,Al,Sn, Mn,H_2O,Ta,Nb	V,Ve,Al,Sn,Ca	Fe,Mg,Many Tr metals reported
Trace minerals	Quartz,ilmenite, biotite,others	Many minerals reported	Many minerals reported
Planes of Failure			
Twinning	e(101) common v(301) rare (011) glide	(112) rare	(230) possible
Cleavage	a(100) moderate m(110) good s(111) traces	c(001) perfect p(011) perfect	m(120) poor c(100) v.poor
Parting	Along glide planes		
Fracture	Uneven, subconchoidal	Uneven, subconchoidal	Uneven, subconchoidal

*ASTM-SPDF = American Society of Testing Materials -- Standard Powder Diffraction File

Table VI.2: Comparison of the physical and chemical properties of the titanium dioxide polymorphs (cont)

Property	TITANIUM DIOXIDE POLYMORPH		
	Rutile	Anatase[1]	Brookite
Stability - T,pH	Highest 2 shared edges	Least 3 shared edges	Intermediate 4 shared edges 1 shared face
Color[3]	R,B,Br,V,Y,G	Br,Y,G,B,Bl	R,Br,B,V
Dispersion	Very strong	Strong	Strong,variable
Refractive Index	W 2.605-2.613 E 2.899-2.901 J 0.286-0.296	E 2.488 W 2.501 J 0.073	

[1]Anatase is also referred to as octahedrite in older mineralogical literature.

[2]Density appears to vary according to iron content which may occur as a "minor" element rather than as a "trace" element (some %). The density of anatase changes dramatically after heating (d = 4.16).

[3]Colors are R=red, B=blue, Br=brown, V=violet, Y=yellow, G=green, Bl=black. Synthetic rutile tends to be white. Titania in pulmonary tissues tends to be greenish-white.

Table VI.3 -- X-ray diffraction characterization of titanium dioxide specimens used experimentally

Specimen Name	Source	% Rutile	% Anatase	Other Phases
I. Natural Minerals				
Rutile	Mozambique, Africa	≥ 99	0	Tr quartz, clay minerals.
Rutile sand	Myrtle Beach, S. Carolina	≥ 98	0	Up to 2% ilmenite, silicates.
Rutile	Graves Mountain, Georgia	≥ 99	0	Tr-1% ilmenite.
Rutile	White Mountain, California	≥ 97	Tr-1	Tr-2% silicates, clay minerals.
Anatase	Brazil	Tr-1	≥ 99	Tr-1% silicates, clay minerals.
II. Synthetic Titanium Dioxide--Industrial Powders				
TiO_2 #10082	N. Wotherspoon, MSSM, CUNY	100	0	None detected.
Rutile	Dupont Haskell Labs	100	0	Tr phase, unidentified.
Titanic oxide	Fisher Scientific	0	100	None detected.
Titanium (IV)	Aldrich Chemical	~5	~95	None detected.
III. Polymorphs Used in Pneumoconiosis Laboratories				
Rutile	PRU #159 Wales, U.K.	≥ 99	Tr-1	None detected.
Rutile	IOM-1 Scotland	≥ 99	Tr-1	None detected.
Rutile	IOM-2 Scotland	100	0	None detected.
Titanox AWO	R.J. Schnitzer	Tr-1	≥ 99	None detected.

Table VI.3 -- X-ray diffraction characterization of titanium dioxide specimens used experimentally (cont)

Specimen Name	Source	% Rutile	% Anatase	Other Phases
IV. Anatase Specimens--Smithsonian Institution				
Calcined anatase	K. Towe Smithsonian	~2	~98	None detected.
Milled anatase	K. Towe Smithsonian	0	100	None detected.
TiO_2 X H_2O	K. Towe Smithsonian	0	100	None detected.

The clay minerals include the alteration product leucoxene; the silicate most frequently encountered appears to be a feldspar phase.

The PRU is the Pneumoconiosis Research Unit of the British MRC.

The IOM is the Institute of Occupational Medicine, Edinburgh.

Table VI.4 -- Size distribution of titanium dioxide and quartz specimens

I. Natural Titanium Dioxide Minerals

Specimen	Phase*	(N)	Percent Within Each Size Class ≦0.50um	0.51-1.00um	1.01-2.00um	2.01-5.00um	5.01-10.00um	≧10.1um
Mozambique	R	597	51.6%	16.2%	20.8%	8.6%	2.8%	0.0%
Myrtle Beach	R	767	48.9%	21.6%	17.9%	9.0%	2.1%	0.5%
Graves Mtn.	R	783	41.4%	26.0%	22.0%	8.4%	1.8%	0.4%
White Mtn.	R	735	60.7%	22.9%	11.5%	4.9%	0.0%	0.0%
Brazil	A	783	61.4%	23.0%	12.0%	3.2%	0.4%	0.0%

II. Industrial Powders (Synthetics)

Specimen	Phase	(N)	≦0.25um	0.26-0.50um	0.51-1.00um	≧1.01um
#10082	R	309	66.4%	33.3%	0.3%	0.0%
Dupont	R	376	62.2%	37.3%	0.5%	0.0%
Fisher	A	376	88.1%	9.8%	2.2%	0.0%
Aldrich	A	332	86.1%	13.0%	0.9%	0.0%

III. Titanium Dioxide Used in Pneumoconiosis Laboratories as Control Dusts

Specimen	Phase	(N)	≦0.25um	0.26-0.50um	0.51-1.00um	≧1.01um
PRU #159	R	320	48.8%	51.2%	0.0%	0.0%
IOM-1	R	344	46.0%	51.7%	2.3%	0.0%
IOM-2	R	200	43.5%	49.5%	7.0%	0.0%
Titanox AWO	A	219	92.2%	7.8%	0.0%	0.0%

Table VI.4 -- Size distribution of titanium dioxide and quartz specimens (cont)

			Percent Within Each Size Class			
IV. Anatase Specimens--Smithsonian Institution						
Specimen	Phase	(N)	≤0.25um	0.26-0.50um	0.51-1.00um	≥1.01um
Calcined	A	345	76.5%	22.6%	0.9%	0.0%
Milled	A	376	96.8%	3.2%	0.0%	0.0%
Precipitated	A	-	100.0%	-	-	-
V. Min-U-Sil (Quartz) Controls						
Specimen	Phase	(N)	≤0.50um	0.51-1.00um	1.01-2.00um	2.01-5.00um	≥5.01um
MUS 5 1 um	Q	380	17.6%	26.3%	33.4%	21.9%	0.8%
MUS 5 2 um	Q	387	18.1%	19.4%	13.4%	30.3%	18.8%
MUS 15 1 um	Q	443	24.6%	32.1%	26.6%	16.2%	0.5%
MUS 15 2 um	Q	307	12.7%	14.7%	7.5%	43.6%	21.5%

*R, A, and Q denote rutile, anatase, and quartz, respectively.

Table VI.5 -- Membranolytic activity of the naturally occurring titanium dioxide polymorphs: Rutile and anatase

TiO_2 mg/ml	Anatase Brazil %H	Rutile Sand S. Carolina %H	Rutile California %H	Rutile Georgia %H	Rutile Africa %H	Min-U-Sil mg/ml	%H
0.625	1.3±0.1	1.0±0.0	1.2±0.0	1.1±0.0	1.2±0.0	0.375	5.2±0.0
1.250	1.8±0.0	1.1±0.0	1.8±0.2	1.2±0.1	1.5±0.0	0.750	11.4±0.0
1.875	2.2±0.0	1.3±0.1	2.5±0.4	1.5±0.0	1.8±0.1	1.125	16.7±0.0
2.500	2.5±0.3	1.5±0.0	3.7±0.2	1.9±0.0	1.8±0.1	1.500	21.6±0.1

Table VI.6 -- Membranolytic activity of titanium dioxide specimens obtained as fine industrial powders (synthetics)

TiO_2 mg/ml	Dupont %H	TiO_2 #10082 %H	TiO_2 mg/ml	Calcined Anatase %H	Milled Anatase %H	$TiO_2 \times H_2O$ %H
0.313	5.1±0.3	6.4±0.3	0.50	1.2±0.1	1.2±0.1	1.5±0.1
0.625	14.3±0.8	16.4±2.2	1.00	1.2±0.1	1.4±0.1	2.0±0.1
0.938	27.6±3.1	30.7±1.2	1.50	1.1±0.1	1.5±0.1	2.7±0.0
1.250	38.0±4.5	37.5±2.2	2.00	1.0±0.1	1.7±0.1	3.4±0.3

TiO_2 mg/ml	Anatase Titanox %H	Anatase Aldrich %H	Titanic Acid Fisher %H	Min-U-Sil 15 mg/ml	Min-U-Sil 15 %H	Sonicated %H
0.625	3.0±0.1	2.1±0.2	1.9±0.1	0.375	7.7±0.2	11.8±0.1
1.250	3.8±0.3	2.9±0.1	2.3±0.1	0.750	15.3±0.4	25.7±0.3
1.875	4.8±0.1	4.0±0.1	4.2±0.1	1.125	21.8±0.4	35.3±0.5
2.500	5.9±0.0	5.3±0.1	4.4±0.2	1.500	27.6±0.6	44.1±0.1

Table VI.7 -- Relationship between particle size and surface area with constant shape for quartz, anatase and rutile

Particle Size um	No. of particles/mg			Surface Area (um^2)/particle	Surface Area (um^2)/mg		
	Quartz	Anatase	Rutile		Quartz	Anatase	Rutile
0.5	3.02×10^9	2.05×10^9	1.88×10^9	1.5	4.5×10^8	3.0×10^8	2.8×10^8
1.0	3.77×10^7	2.57×10^8	2.35×10^8	6.0	2.2×10^8	1.5×10^8	1.4×10^8
2.0	4.72×10^7	3.21×10^7	2.94×10^7	24.0	1.1×10^8	7.7×10^8	0.7×10^8
5.0	3.02×10^6	2.05×10^6	1.88×10^6	150.0	4.5×10^8	3.1×10^8	2.8×10^8
10.0	3.77×10^5	2.57×10^5	2.35×10^5	600.0	2.3×10^8	1.5×10^8	1.4×10^8
20.0	4.72×10^4	3.21×10^4	2.94×10^4	2400.0	0.9×10^8	0.8×10^8	0.7×10^8

Density of Quartz ≅ 2.656 g/cc # 5-0490 (SPDF)
Density of Anatase ≅ 3.893 g/cc #21-1272 (SPDF)
Density of Rutile ≅ 4.250 g/cc #21-1276 (SPDF)

Figure VI.1 -- Flow diagram for the synthesis of titanium dioxide via the sulfate process.

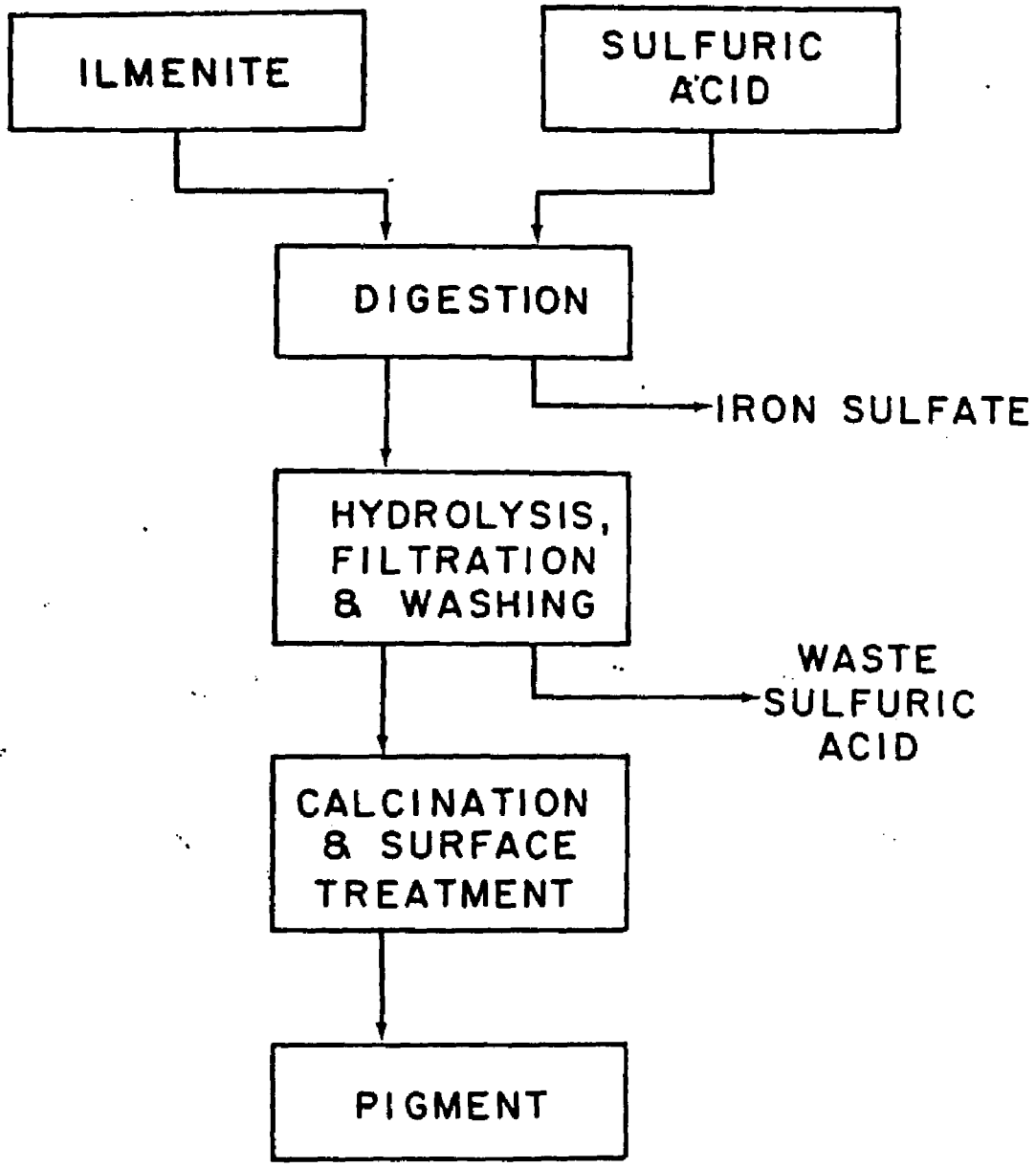
ILMENITE
SULFURIC ACID
DIGESTION
IRON SULFATE
HYDROLYSIS, FILTRATION & WASHING
WASTE SULFURIC ACID
CALCINATION & SURFACE TREATMENT
PIGMENT

Figure VI.2 -- Flow diagram for the synthesis of titanium dioxide via the chloride process.

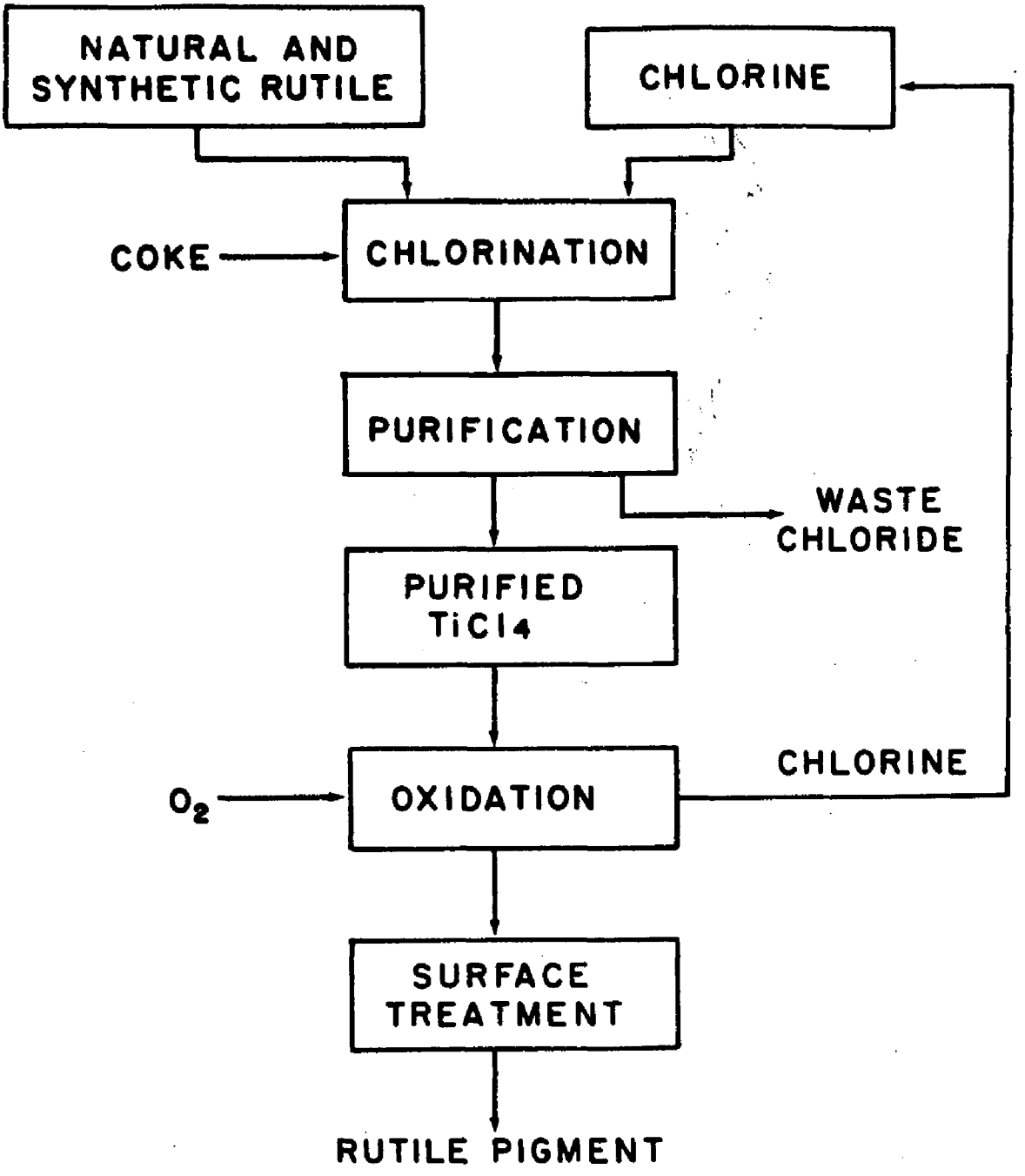
NATURAL AND SYNTHETIC RUTILE
CHLORINE
COKE
CHLORINATION
PURIFICATION
WASTE CHLORIDE
PURIFIED TiCl4
CHLORINE
O2
OXIDATION
SURFACE TREATMENT
RUTILE PIGMENT

Figure VI.3 -- Comparison of the membranolytic activity of six synthetic titanium dioxide specimens and quartz.

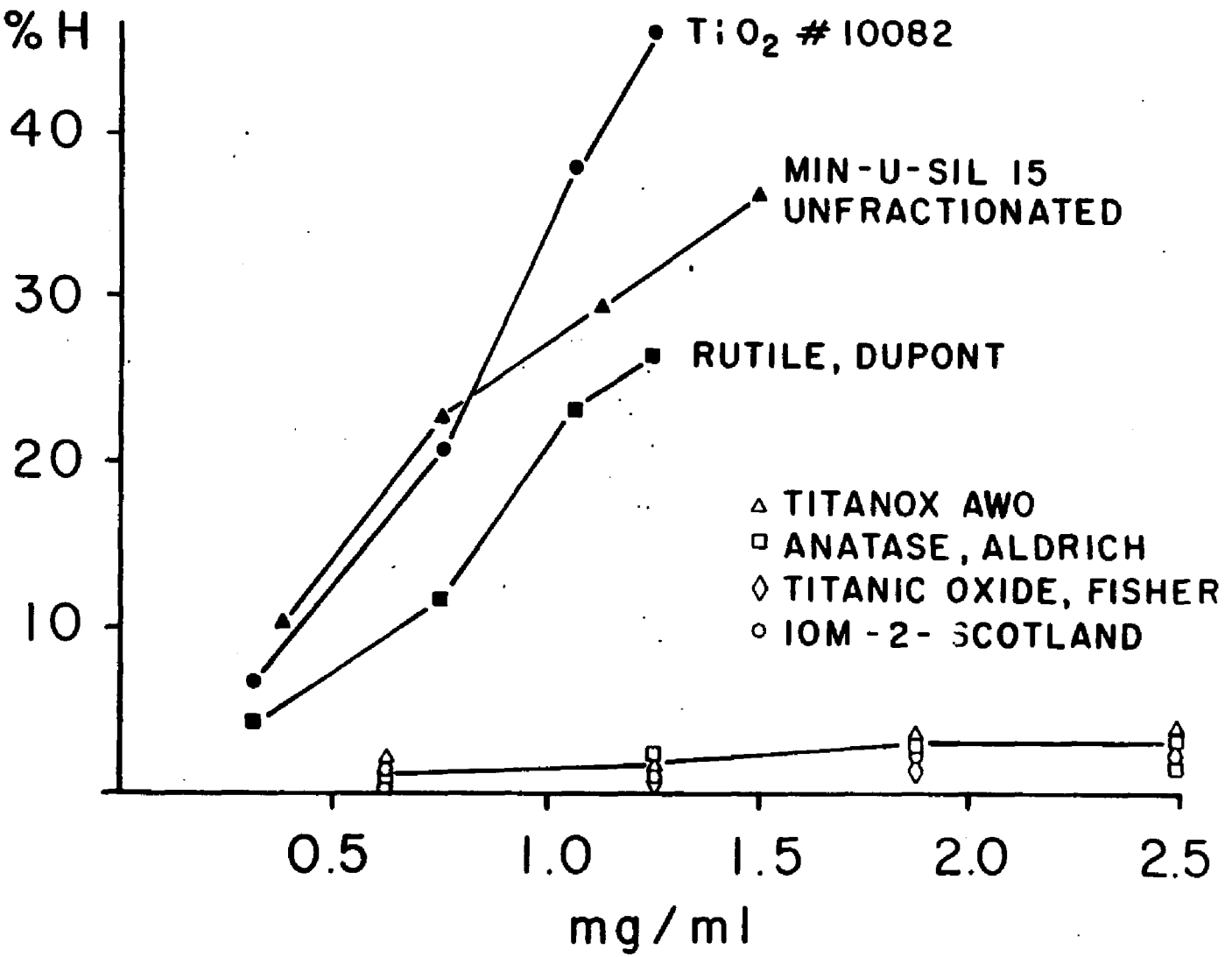
%H
40
30
20
10
TiO_2 #10082
MIN-U-SIL 15
UNFRACTIONATED
RUTILE, DUPONT
△ TITANOX AWO
□ ANATASE, ALDRICH
◇ TITANIC OXIDE, FISHER
○ IOM-2- SCOTLAND
0.5
1.0
1.5
2.0
2.5
mg/ml

Figure VI.4 -- Comparison of the membranolytically active rutile (Dupont) with two fine particle size quartz specimens and two titanium dioxide specimens used in pneumoconiosis research as inert controls.

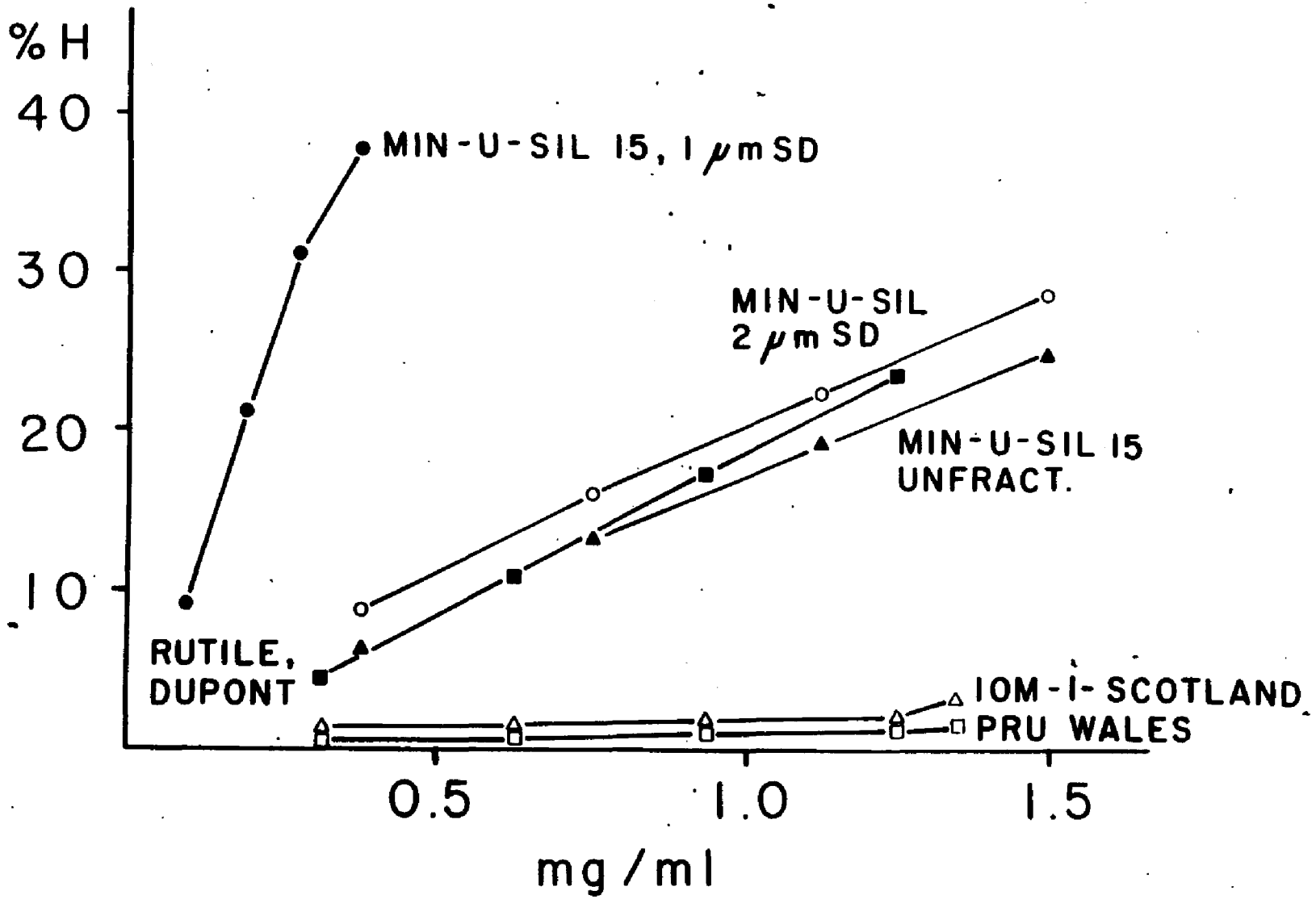
%H
40
30
20
10
MIN-U-SIL 15, 1 μm SD
MIN-U-SIL
2 μm SD
MIN-U-SIL 15
UNFRACT.
RUTILE,
DUPONT
IOM-I-SCOTLAND
PRU WALES
0.5
1.0
1.5
mg/ml

Figure VI.5 -- Comparison of the membranolytic activity of two fine particle size quartz specimens and two synthetic rutile specimens.

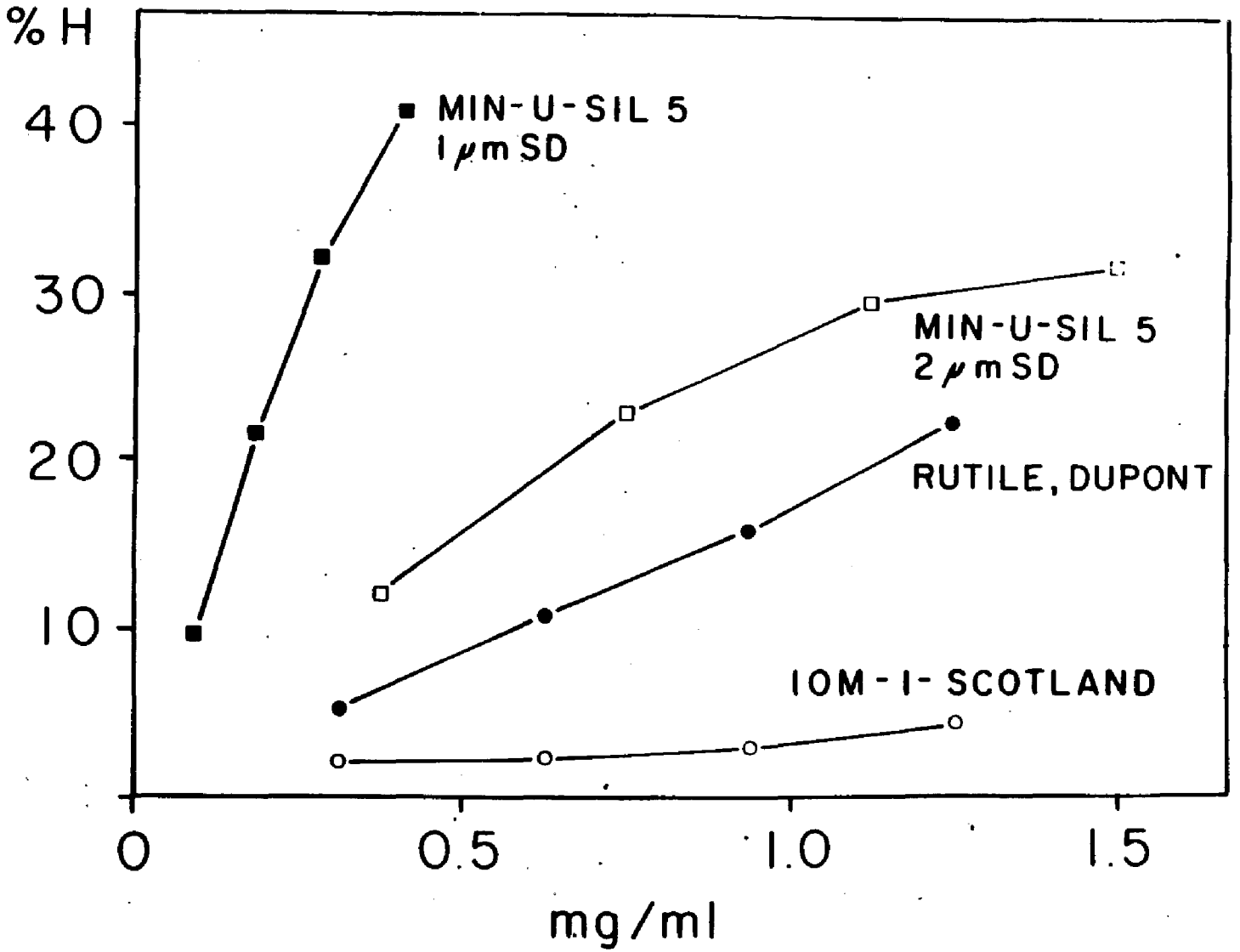
%H
40
30
20
10
0
0.5
1.0
1.5
mg/ml
MIN-U-SIL 5
1 μm SD
MIN-U-SIL 5
2 μm SD
RUTILE, DUPONT
10M-I-SCOTLAND

Figure VI.6 -- The hydrogen bonding ability of two fine particle size quartz specimens was compared to four titanium dioxide specimens.

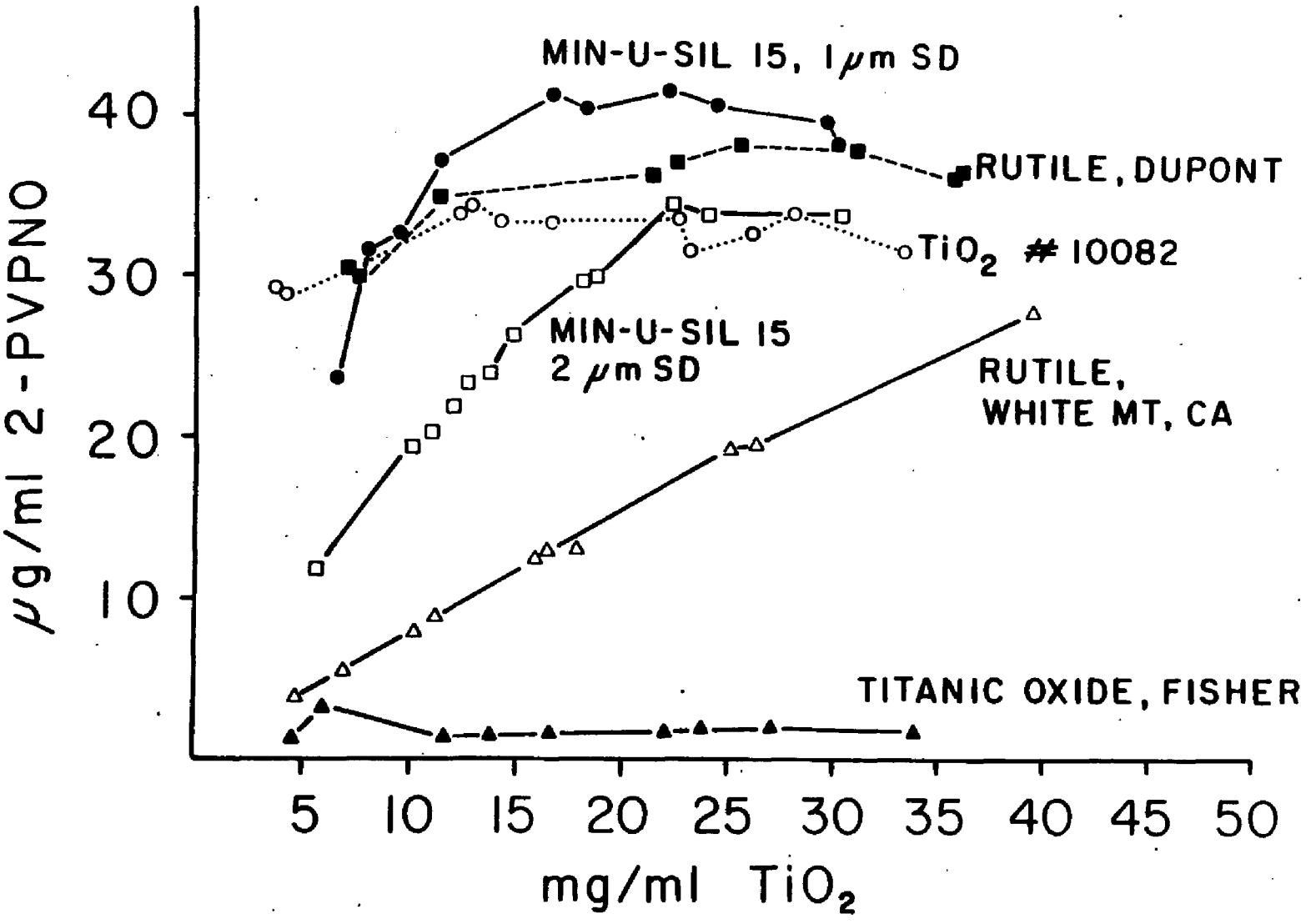
MIN-U-SIL 15, 1 μm SD
RUTILE, DUPONT
TiO2 # 10082
MIN-U-SIL 15
2 μm SD
RUTILE,
WHITE MT, CA
TITANIC OXIDE, FISHER
μg/ml 2-PVPNO
40
30
20
10
5
10
15
20
25
30
35
40
45
50
mg/ml TiO2

Figure VI.7 -- The ability of four synthetic rutiles to hydrogen bond with the polymer, 2-PVPNO, was determined.

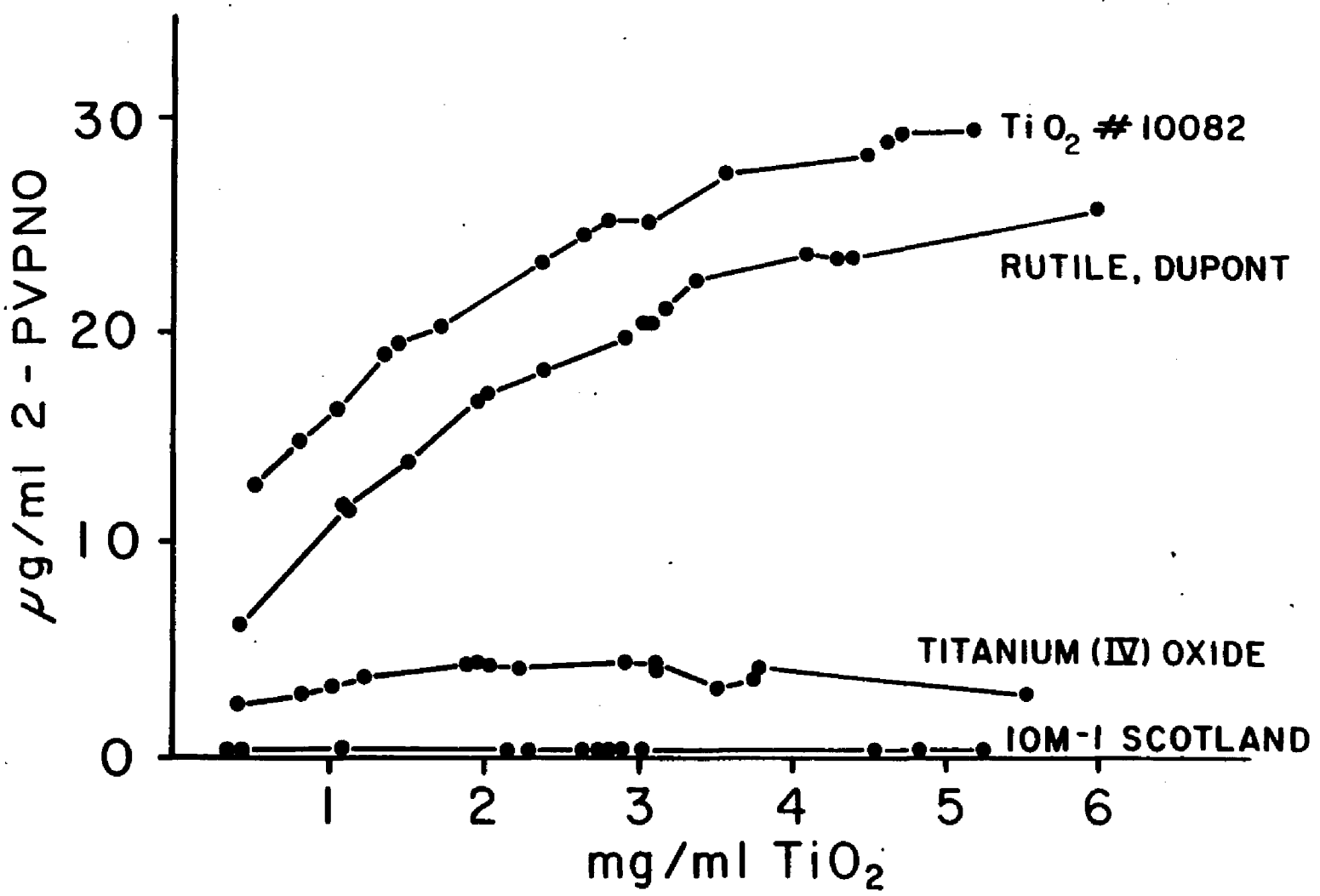
30
20
10
0
μg/ml 2-PVPNO
1
2
3
4
5
6
mg/ml TiO2
TiO2 #10082
RUTILE, DUPONT
TITANIUM (IV) OXIDE
IOM-1 SCOTLAND

Figure VI.8 -- Inhibition of titanium dioxide #10082 membranolytic activity with 2-PVPNO.

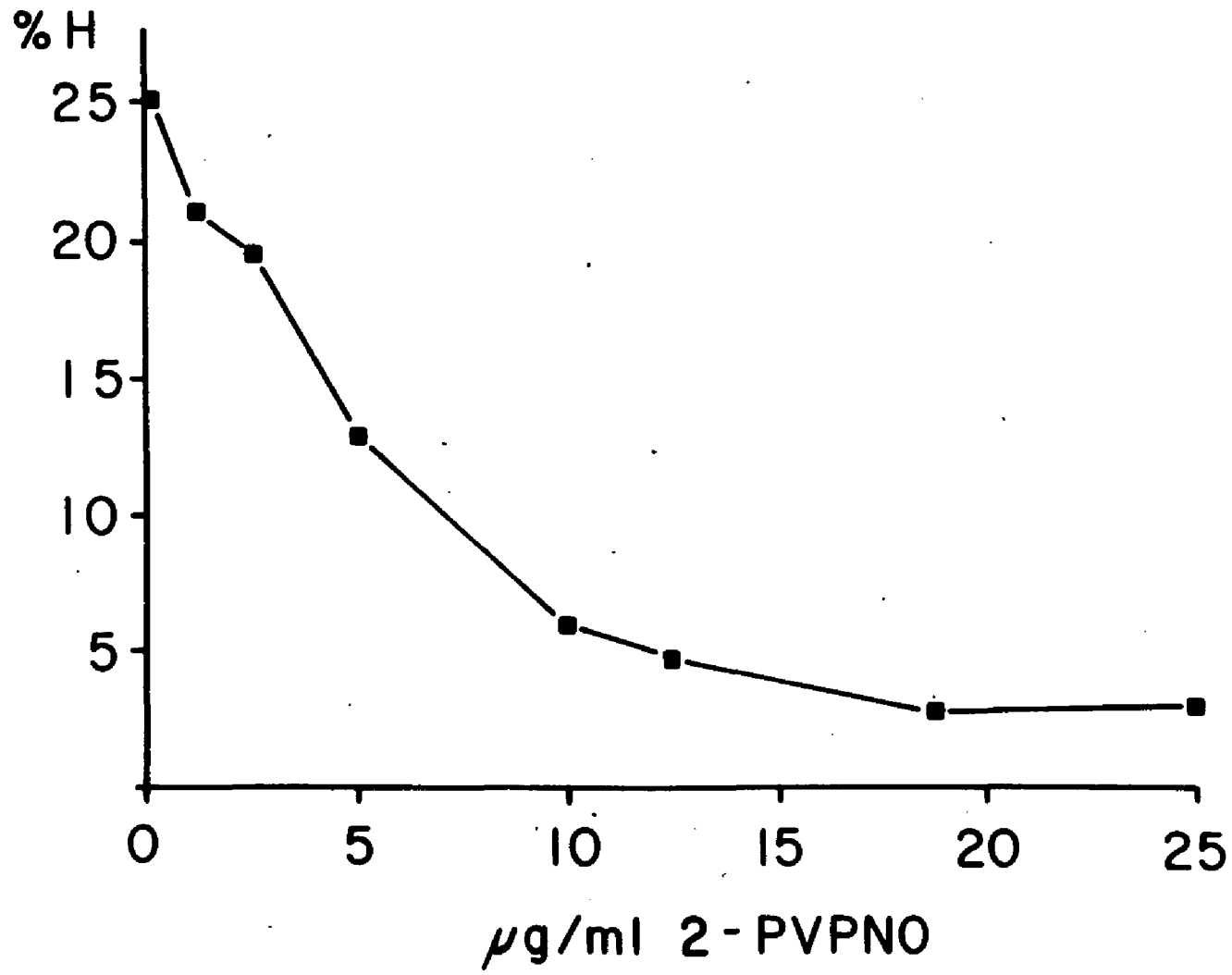
%H
25
20
15
10
5
0
5
10
15
20
25
μg/ml 2-PVPNO

REFERENCES

REFERENCES

Adamson AW (1982). "Physical Chemistry of Surfaces". New York; Wiley - Interscience.

Allison AC (1968). Silicon compounds in biological systems. Proc R Soc London Ser B 171:19-30.

Allison AC (1971). Lysosomes and the toxicity of particulate pollutants. Arch Intern Med 128:131-139.

Allison AC (1973). Experimental methods - cell and tissue culture: effect of asbestos particles on macrophages, mesothelial cells and fibroblasts. In "Biological Effects of Asbestos" (Bogovski P, Gilson JC, Timbrell V and Wagner JC, Eds), International Agency for Research on Cancer, Lyon, France, pp.89-93.

Allison AC (1978). Interactions of silica and asbestos with macrophages. In "Biochemistry of Silicon and Related Problems" (G Bendz and I Lindqvist, Eds), pp. 337-355. Plenum, New York.

Allison AC, Harington JS, and Birbeck M (1966). An examination of the cytotoxic effects of silica on macrophages. J Exp Med 24:141-153.

Andersen OS, Finkelstein A, Katz I and Cass A (1976). Effect of phlocetin on the permeability of thin lipid membranes. J Gen Physiol 67:749-771.

Beck EG, Holusa R, Jirakova D, Kysela B, Robock K, and Skoda V (1973). Uber die unterschiedlich Wirkung von zwei Quartzen in Tier und zellversuch and ihre physikalische Halbleitereigenschaften. Staub-Reinhalt Luft 33:3-7.

Bergman I and Langrish B (1972). Silica powders of respirable size: The effect of methods of comminution and pretreatment of electrophoretic mobility in solution of varying ionic strength, acidity and metal-iron content. J Electroanal Chem Interfacial Electrochem 34:203-210.

Bragg L, Claringbull GF, and Taylor WH (1965). Crystal structures of minerals: The crystalline state. Vol. 4. London: G. Bell and Son, Ltd., pp. 409.

Branton D (1983). Erythrocyte membrane protein associations and erythrocyte shape. In "The Harvey Lectures." Academic Press, New York, pp. 23-42.

Bretscher MS (1973). Membrane structure: Some general principles. Science 181:622-629.

Brown EA (1957). The adsorption of lipids from the erythrocyte surface by silica and alumina. J Cell Comp Physiol 50:49-56.

Bunn CW (1961). "Chemical Crysallography. An Introduction to Optical and X-Ray Methods." 2nd Edition. Oxford: Clarendon Press, p. 509.

Cabantchik ZI, Balshin M, Breuer W and Rothstein A (1975). Pyridoxal phosphate an anionic probe for protein amino groups exposed on the outer and inner surfaces of intact human red blood cells. J Biol Chem 250:5130-6.

Cabantchik ZI, Knauf PA, Ostwald T, Markus H, Davidson L, Breuer W and Rothstein A (1976). The interaction of an anionic photo-reactive probe with the anion transport system of the human red blood cell. Biochemica et Biophysica Acta 455:526-37.

Cabantchik ZI, Knauf PA and Rothstein A (1978). The anion transport system of the red blood cell. The role of membrane protein evaluated by the use of probes. Biochemica Biophysica Acta (Biomembr Rev) 515:239-302.

Cabantchik ZI and Rothstein A (1972). The nature of the membrane sites controlling anion permeability of human red blood cells as determined by studies of disulfonic stilbene derivatives. J Membrane Biol 10:311-30.

Cabantchik ZI and Rothstein A (1974a). Membrane proteins related to anion permeability of human red blood cells. I. Localization of disulfonic stilbene binding sites in proteins involved in permeation. J Membrane Biol 15:207-26.

Cabantchik ZI and Rothstein A (1974b). Membrane proteins related to anion permeability of human red blood cells. II. Effects of proteolytic enzymes on disulfonic stilbene sites of surface protein. J Membrane Biol 15:227-48.

Chvapil M (1974). Pharmacology of fibrosis and tissue injury. Environ Health Perspect 9:283-294.

Chvapil M (1977). Cellular mechanisms of lung fibrosis. In "Biochemical Effects of Environmental Pollutants" (SD Lee, Ed), pp. 315-324. Ann Arbor Science Pub., Ann Arbor, Mich.

Chvapil M and Peng YM (1975). Oxygen and lung fibrosis. Arch Environ Health 30:528-532.

Chvapil M, Stankova L, and Malshet V (1976). Lipid peroxidation as one of the mechanisms of silica fibrogenicity. Environ Res 11:78-88.

Cousin JL and Motais R (1978). Effect of phloretin on chloride permeability: A structure-activity study. Biochimica Biophysica Acta 507:531-8.

Daum SM, Anderson HA, Lilis R, et al (1977). Pulmonary changes among titanium workers. Proc R Soc Med 70:31-32.

Davies R, Griffiths DM, Johnson NF, et al (1984). The cytotoxicity of kaolin toward macrophages in vitro. Br J Exp Pathol 65:453-466.

DeKorosy F and Tabuch MF (1973). Effects of colloidal silica acid on lecithin bilayers. Biochem Biophys Acta 291:608-611.

Deer WA, Howie RA, and Zussman J (1972). Rock forming minerals. Non-silicates. Longman, London 5:34-47.

Depasse J (1978). Influence of the sialic acid content of membranes on their sensitivity to silica and aluminate-modified silica. Environ Res 16:88-91.

Desai R, Hext P, and Richards RJ (1975). The prevention of asbestos-induced hemolysis. Life Sci 16:1931-1938.

Desai R and Richards RJ (1978). The adsorption of biological macromolecules by mineral dusts. Environ Res 16:447-464.

Dognon A and Simonot YL (1951). L'hemolyse par particles. C R Soc Biol 145:1615-1617.

Engelbrecht FM and Thiart BF (1972). The effect of small amounts of aluminum, carbon and carborundum on the development of silicosis and asbestos. S Afr Med J 46:462-464.

Fairbanks G, Steck TL and Wallach DFH (1971). Electrophoretic analysis of the major polypeptides of the human erythrocyte membrane. Biochem 10:2606-17.

Ferin J and Oberdorster G (1985). Biological effects and toxicity assessment of titanium dioxides: Anatase and rutile. Am Ind Hyg Assoc J 46(2):69-72.

Forman SA, Verkman AS, Dix JA and Solomon AK (1982). Interaction of phloretin with the anion transport proteins of the red blood cell membrane. Biochimica Biophysica Acta 689:531-8.

Frondel C (1962). System of Mineralogy, Vol. III. Silica Minerals, Wiley, New York.

Furlong DN and Parfitt GD (1978). Electrokinetics of titanium dioxide. J Colloid Interface Sci 65:548-554.

Gabor S and Anca Z (1974). Effect of silica on lipid peroxidation in the red cells. Int Arch Arbeitsmed 32:327-332.

Goldie H (1938). "Hemolytic" action of silicic acid. C R Soc Biol 129:1090-1093.

Harington JS (1974). Fibrogenesis. Environ Health Perspect 9:271-279.

Harington JS, Allison AC, and Badami DV (1975). Mineral fibers: Chemical, physiochemical and biological properties. Advan Pharmacol Chemother 12:291-402.

Harington JS, Macnab GM, Miller K, and King PC (1971a). Enhancement of haemolytic activity of asbestos by heat-labile factors in fresh serum. Med Lavoro 62:171-176.

Harington JS, Miller K, and Macnab G (1971b). Hemolysis by asbestos. Environ Res 4:95-117.

Harington JS, Ritchie M, King PC and Miller K (1973). The in vitro effects of silica-treated hamster macrophages on collagen production by hamster fibroblasts. J Pathol 109:21-37.

Harley JD and Margolis J (1961). Hemolytic activity of colloidal silica. Nature (London) 189:1010-1011.

Heppleston AG (1978). Cellular reactions with silica. In "Biochemistry of Silicon and Related Problems" (G Bendz and J Lindqvist, Eds), pp. 357-379. Plenum, New York.

Heppleston AG and Styles JA (1967). Activity of a macrophage factor on collagen formation by silica. Nature 214:521-522.

Hobza P and Hurych J (1978). Quantum chemical study of properties and reactivity of quartz dust. Environ Res 15:432-442.

Holt PF (1957). "Pneumoconiosis Industrial Diseases of the Lung Caused by Dust." Arnold, London.

Holt PF (1968). The interaction of poly-2-vinylpyridine 1-oxide and poly-4-vinylpyridine 1-oxide. J Chem Soc B:233-237.

Iler RK (1978). Hydrogen bonded complexes of silica with organic compounds. In "Biochemistry of Silicon and Related Problems" (G Bendz and I Lindqvist, Eds), pp. 53-76. Plenum, New York.

Iler RK (1979). "The Chemistry of Silica." Wiley, New York.

Kennedy JF (1979). Transition-metal oxide chelates of carbohydrate-directed macromolecules. Chem Soc Reviews 8:221-257.

Kessel R, Monaco L and Marchisio MA (1963). The specificity of the cytotoxic action of silica -- A study in vitro. Brit J Exp Pathol 44:351-364.

Kilroe-Smith TA (1974). Peroxidative action of quartz in relation to membrane lysis. Environ Res 7:110-116.

Kitel C (1967). "Introduction to Solid State Physics." New York: Wiley, p. 648.

Kleinerman J (1974). Industrial pulmonary diseases: Silicosis, asbestosis and talc pneumoconoisis. In "Textbook of Pulmonary Diseases" (GG Baum, Ed), pp. 489-507. Little, Brown, Boston.

Klosterkotter W (1968). Experimental studies on the significance of fiber length in asbestos fibrosis and studies on the impairment of fibrosis by polyvinyl pyridine-N-oxide. In "Proceedings, International Conference on Biological Effects of Asbestos, Dresden, DDR" (Anspach, Ed), pp 47-52.

Knauf PA, Ship S, Breuer W, McCullouch and Rothstein A (1978a). Asymmetry of the red cell anion exchange system. J Gen Physiol 72:607-30.

Knauf PA, Breuer W, McCulloch and Rothstein A (1978b). N-(4-azido-2-nitrophenyl-2-aminoethylsulfonate (NAP-taurine) as a photoaffinity probe for identifying membrane components containing the modifier site of the human red blood cell anion exchange system. J Gen Physiol 72:631-49.

Knauf PA (1979). Erythrocyte anion exchange and the band 3 protein: Transport kinetic and molecular structure. Current Topics in Membranes and Transport 12:249-363.

Knittel, D (1982). Titanium and titanium alloys. In "Kirk-Othmer Encyclopedia of Chemical Technology." Vol. 23, pp. 131-176. Wiley-Interscience, New York.

Knowles JR (1972). Photogenerated reagents for biological receptor-site labelling. Acc Chem Res 5:155-60.

Koshi K, Hayashi H and Sakabe H (1968). Cell toxicity and hemolytic action of asbestos dusts. Ind Health 6:69-79.

Kriegreis W, Biederbick R, Boese J, Robock K and Scharmann A (1976). Investigations into the determination of the cytotoxicity of quartz dust by physical methods. In "Proceedings, Inhaled Particles and Vapours. IV. BOHS Edinburgh" (Walton, Ed), pp. 345-359. Oxford Univ. Press, London.

Langer AM (1978). Crystal faces and cleavage planes in quartz as templates in biological processes. Q Rev Biophys 11:543-575.

Langer AM (1980). Mineralogy of dust diseases. In "Maxcy-Rosenau Public Health and Preventive Medicine," 11th ed, pp. 637-641. Appleton-Century-Crofts, New York.

Langer AM, Nolan RP (1985). Physicochemical properties of quartz controlling biological activity. In "Silica, Silicosis and Cancer: Controversy in Occupational Medicine." Goldsmith DF, Winn DM, Shy CM (Eds), Praeger Publishers, New York, pp. 125-135.

Lee KP Trochimowicz HJ and Reinhardt CF (1985). Pulmonary response of rats exposed to titanium dioxide (TiO_2) by inhalation for two years. Toxicol Appl Pharmacol 79:179-192.

Lee KP, Trochimowicz HJ and Reinhardt CF (1985). Transmigration of titanium dioxide (TiO_2) particles in rats after inhalation exposure. Experiment Molec Pathol 42:331-343.

Lepke S and Passow H (1973). Asymmetric inhibition by phlorizin of sulfate movement across the red blood cell membrane. Biochimica Biophysica Acta 298:529-33.

Leyko W and Gendek E (1985). A spin label study of the effect of asbestos, quartz and titanium dioxide dust on the bovine erythrocyte membrane. Br J Ind Med 42:281-284.

Macnab G and Harington JS (1967). Hemolytic activity of asbestos and other mineral dusts. Nature (London) 214:522-523.

Marasas LW and Harington JS (1960). Some oxidative and hydroxylative actions of quartz: Their possible relationship to the development of silicosis. Nature (London) 189(No. 4757):1173-1174.

Mehrishi JN and Seaman GVF (1966). Temperature dependence of the electrophoretic mobility of cells and quartz particles. Biochim Biophys Acta 112:154-159.

Miller K (1979). Alterations in the surface-related phenomena of alveolar macrophages following inhalation of crocidolite asbestos and quartz dusts: An overview. Environ Res 20:162-182.

Miller K, Calverley A and Kagan E (1980). Evidence of a quartz-induces chemotactic factor for guinea pig alveolar macrophages. Environ Res 22:31-39.

Miller K and Harington JS (1972). Some biochemical effects of asbestos on macrophages. Brit J Exp Pathol 53:397-405.

Nash T, Allison AC and Harington JS (1966). Physio-chemical properties of silica in relation to its toxicity. Nature (London) 210:259-261.

Nolan RP and Langer AM, (1983). Quartz and hemolysis: Physico-chemical factors controlling membrane activity. For "Health Issues Related to Mining and Minerals (Wagner W, Merchant J and Rom W (Eds.). Michigan; Ann Arbor Press, pp. 63-81.

Nolan RP, Langer AM, and Foster KW (1985). Particle size and chemically induced variability in the membrolytic activity of quartz: Preliminary observations. In "In Vitro Effects of Mineral Dusts (Beck EG and Bignon, Eds). Third Internal Workshop, Springer-Verlag, Berlin, pp. 39-50.

Nolan RP, Langer AM, Harington JS, et al (1981). Quartz hemolysis as related to its surface functionalities. Environ Res 26:503-520.

Passow H (1977). Passive anion transport. Proc Int Union Physio Sci Paris 12:86-7.

Pauling L (1961) "The Nature of the Chemical Bond and the Structure of Molecules and Crystals." 3rd Ed., Cornell University Press.

Policard A, Letort M, Charbonnier J, Daniel-Moussard H, Martin JC and LeBouffant L (1971). Recherches experimentales concernant l'inhibition de l'action cytotoxique du quartz au moyen du substances mineralse, notamment de composes de l'aluminum. Beitr Silikose-Forsch 23:3-57.

Reiser A, Willets FW, Terry GC, Williams V and Hanley R (1968). Photolysis of aromatic azides. Trans Faraday Soc 64:3265-75.

Richards RJ, White LR and Eik-Nes KB (1985). Biological reactivity of different crystalline forms of titanium dioxide in vitro and in vivo. Scand J Work Environ Health 11:317-320.

Riddick TM (1968). "Control of Stability through Zeta Potential," Creative Press, New York.

Robock K and Klosterkotter W (1975). Untersuchung uber die zytotoxizitat von SiO_2-Stauben. Ergeb Unters Geb Staub-Silikosebekaupf Steinkohlenbergbeau 10:159-162.

Scheel LD (1955). Study of surface properties of quartz dust. AMA Arch Ind Health 12:262-265.

Scheel LD, Smith B, Van Piper J and Fleischer E (1964). Toxicity of silica. Arch Ind Hyg Occup Med 9:29.

Schepers GW (1960). Theories of the causes of silicosis. Ind Med Surg 291:326-333, 359-369, 434-439.

Schlipkoter HW (1968). Animal experiments and in vivo studies of asbestos dusts. In "Proceedings, International Conference on Biological Effects of Asbestos, Dresden, DDR" (Anspach, Ed), pp. 67-74.

Schlipkoter HW and Brockhaus A (1961). Die hemmung der experimentellen silikose durch subcutane verabreichung von polyvinyl pyridin-N-oxide. Klin Wochenschr 39:1182-1189.

Schnell KF, Gerhardt S, Lepke S and Passow H (1973). Asymmetric inhibition by phlorizin of halide movement across the red blood cell membrane. Biochimica Biophysica Acta 318:474-7.

Schnitzer RJ and Pundsack FL (1970). Asbestos hemolysis. Env Res 3:1-13.

Secchi GC, and Rezzonico A (1968). Hemolytic activity of asbestos dusts. Med Lav 59:1-5.

Shnaidman IM (1974). Mechanims underlying the protective action of polyvinyl pyridine-N-oxide. Gg Tr Prof Zabol 1:19-23.

Singer, JJ (1982). Pigments. In "Kirk-Othmer Encyclopedia of Chemical Technology." Vol. 17, pp. 788-889. Wiley-Interscience, New York.

Smith PAS (1970). In "Nitrenes." Lwowski W (ed). Wiley, New York.

Stalder K and Stober W (1965). Hemolytic activity of suspensions of different silica modification and inert dusts. Nature (London) 206:874-875.

Staros JV and Richards FM (1975). Photochemical labeling of the cytoplasmic surface of the membrane of intact human erythrocytes. J Biol Chem 250:8174-8.

Steck TL (1974). The organization of proteins in the human red blood cell membrane. J Cell Biol 62:1-19.

Stober W and Brieger H (1968). On the theory of silicosis. Arch Environ Health 16:706-708.

Summerton J, Hoenig S, Butler C and Chvapil M (1977). The mechanism of hemolysis by silica and its bearing on silicosis. Exp Mol Pathol 26:113-128.

Uragado CG and Pinto MRM (1972). An investigation into the health of workers in an ilmenite extracting plant. Med J Aust 1:167-169.

Verbonic C (1985). Titanium dioxide: Will its dazzle dim? Chem Bus August:10-14.

Vigliani EC and Pernis B (1963). Immunological aspects of silicosis. Advan Tuberc Res 12:230.

Weiss Z, Kysela B and Skoda V (1973). The disturbances of SiO_2 lattice and the fibrogenic reaction of lung tissue. In "Proceedings, Second International Symposium on Experimental Silicosis" Velke Karlovice pp. 56-73. Dum techniky CVTS, Ostrava.

Weissmann G and Rita GA (1972). Molecular basis of gouty inflammation: Interaction of monosodium urate crystals with lysosomes and liposomes. Nature New Biol 240:167-172.

Whitehead J (1982). Titanium compound (Inorganic). In "Kirk-Othmer Encyclopedia of Chemical Technology." Vol. 23, pp. 98-130. Wiley-Interscience, New York.

Zaidi SH (1969). "Experimental Pneumoconiosis" Johns Hopkins Press, Baltimore.

Zitting A and Skytta E (1979). Biological activity of titanium dioxide. Int Arch Occup Environ Health 43:93-97.

Ziskind M, Jones RN and Weill H (1976). Silicosis (State-of-the-Art). Amer Rev Respir Dis 115:643-665.